

**A Study on Fluvial Flood Hazard and Risk Assessment of Arial Khan River
Floodplain under Future Climate Change Scenarios**

A Thesis Submitted

by

Binata Roy
1015162003P

In partial fulfillment of the requirements for the Degree of
MASTER OF SCIENCE IN WATER RESOURCES ENGINEERING



Department of Water Resources Engineering

BANGLADESH UNIVERSITY OF ENGINEERING & TECHNOLOGY (BUET)

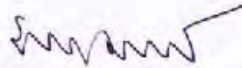
DHAKA-1000

January 2019

**DEPARTMENT OF WATER RESOURCES ENGINEERING
BANGLADESH UNIVERSITY OF ENGINEERING AND TECHNOLOGY**

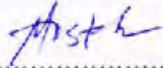
The thesis titled 'A Study on Fluvial Flood Hazard and Risk Assessment of Arial Khan River Floodplain under Future Climate Change Scenarios' submitted by Binata Roy, Roll No. 1015162003P, Session October, 2015, has been accepted as satisfactory in partial fulfillment of the requirement for the degree of M. Sc. in Water Resources Engineering on 14 January, 2019.

BOARD OF EXAMINERS



.....
Dr. Md. Sabbir Mostafa Khan
Professor
Department of Water Resources Engineering
Bangladesh University of Engineering and Technology, Dhaka

Chairman
(Supervisor)



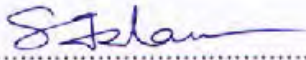
.....
Dr. Md. Mostafa Ali
Professor and Head
Department of Water Resources Engineering
Bangladesh University of Engineering and Technology, Dhaka

Member
(Ex-Officio)



.....
Dr. Umme Kulsum Navera
Professor
Department of Water Resources Engineering
Bangladesh University of Engineering and Technology, Dhaka

Member

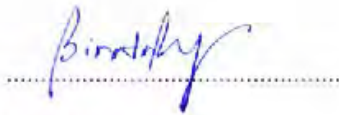


.....
Dr. A. K. M. Saiful Islam
Professor
Institute of Water and Flood Management
Bangladesh University of Engineering and Technology, Dhaka

Member
(External)

CANDIDATE'S DECLARATION

This is to certify that this thesis entitled '**A Study on Fluvial Flood Hazard and Risk Assessment of Arial Khan River Floodplain under Future Climate Change Scenarios**' has been done by me under the supervision of Dr. Md. Sabbir Mostafa Khan, Professor, Department of Water Resources Engineering, Bangladesh University of Engineering and Technology, Dhaka. I do hereby declare that this thesis or any part of it has not been submitted elsewhere for the award of any degree or diploma from any other institution.



Binata Roy

Dedicated to

My Beloved Parents, the source of all inspirations in my life

ACKNOWLEDGMENT

The author is grateful to the Almighty for the successful completion of this thesis work. The author would like to express her sincere gratitude to her supervisor Dr. Md. Sabbir Mostafa Khan, Professor, Department of Water Resources Engineering, Bangladesh University of Engineering and Technology, without whose constant supervision and support this research work would probably reach nowhere. His constant guidance, invaluable suggestions, motivation under challenging times and affectionate encouragement were extremely helpful in accomplishing this study.

The author expresses her sincere appreciation to Dr. A.K.M. Saiful Islam, Professor, Institute of Water and Flood Management, Bangladesh University of Engineering and Technology, and Dr. Mashfiqus Salehin, Professor, Institute of Water and Flood Management, Bangladesh University of Engineering and Technology for their enormous guidance. The expresses her profound gratitude to Mr. Md. Khaled, Ph.D. student, Universite de Sherbrooke, Canada, and Md. Jamal Uddin Khan, Ph.D. Student, Universite Toulouse III - Paul Sabatier, France for their enormous help in data collection.

The author thanks Dr. Md. Mostafa Ali, Professor and Head, Department of Water Resources Engineering, Bangladesh University of Engineering and Technology, Dr. Umme Kulsum Navera, Professor, Department of Water Resources Engineering, Bangladesh University of Engineering and Technology and Dr. A.K.M. Saiful Islam, Professor, Institute of Water and Flood Management, Bangladesh University of Engineering and Technology, for their kind review and suggestions, without these suggestions the successful completion of the thesis was quite impossible.

The author would like to express her gratitude to her parents, spouse, brother, friends, and colleagues for their continuous support, sacrifice and inspiration during the period of this study.

ABSTRACT

Bangladesh is highly susceptible to flood due to its location at the confluence of the world's three major basins– Ganges-Brahmaputra-Meghna (GBM) and hydro-meteorological and topographical characteristics of the basins. Increase in temperature and precipitation due to climate change will significantly increase the monsoon flow of the GBM rivers which may lead to more intense and frequent floods in Bangladesh in upcoming decades. In this study, the fluvial flood hazard and risk of Arial Khan River floodplain have been assessed for the predicted climate change scenarios of RCP 2.6 and RCP 8.5.

A calibrated and validated SWAT model of GBM basins has been used to project the future flow magnitudes at Bahadurabad Transit (Brahmaputra River) and Hardinge Bridge (Ganges River) for RCP 2.6 and 8.5 scenarios. Using the flow magnitude of these stations as the upstream boundaries, a 1D HEC-RAS model has been set up for the Brahmaputra-Ganges-Padma River for generating future flow magnitude at Mawa of Padma River. Later, the discharge at the offtake of Arial Khan has been calculated establishing a linear regression equation between the Arial Khan and Padma River. Finally, a 1D-2D coupled model of Arial Khan River floodplain has been set up in HEC-RAS. This coupled model is calibrated and validated for Manning's roughness coefficient 'n' = 0.015-0.02 for the year of 2015 and 2017 respectively. After calibration and validation, the model is simulated for different periods of RCP 2.6 and RCP 8.5 scenarios: baseline (1976-2005), 2020s (2006-2035), 2050s (2036-2065) and 2080s (2066-2095).

The model result shows that the total flood affected area is nearly 15% at the base condition which is increased to 30% and 47% approximately for the 2080s of RCP 2.6 and RCP 8.5 respectively. The hazard assessment reveals that at the base condition, 48%, 34% and 18% area are in the very low, low and high hazard zone respectively. It is increased to manifolds such as 21%, 27%, 34% and 18% in the very low, low, medium and very hazard zone respectively for the 2080s of RCP 2.6 and it became 22%, 26%, 34% and 18% in the low, medium, high and very high hazard zone respectively for the 2080s of RCP 8.5. Similar to hazard, risk assessment also shows that the very low and low risk zone will decrease and high and very high risk zone will increase significantly by the end of 21st century compared to the base period. Incorporation of vulnerability and exposure gives a complete different horizon to the overall assessment. It is found that some medium hazard zones have a high risk of flood damage due to its high exposure and vulnerability to flood while some high hazard zone falls into the low risk zone because of its low exposure and vulnerability. The overall flood assessment for different projections of RCP 2.6 and RCP 8.5 show that there is an increasing trend of the flood from baseline to 2080s, both for RCP 2.6 and RCP 8.5. From baseline to 2050s, the difference between RCP 2.6 and RCP 8.5 is slight. However, this variation becomes very drastic after the 2050s. The inundation pattern, hazard and risk extent increase manifolds in the 2080s of RCP 8.5 than those of RCP 2.6. So future climate change is going to have a terrible effect on the flood situation of Arial Khan River floodplain. The results found in this study provide useful information on projected changes of flood hazard and risk in the Arial Khan River floodplain over the next decades to a century. Additionally, this study will act as a guideline regarding how to incorporate the globalize climate change scenarios of a large basin to a small local river and its floodplain and find out localized flood hazard and risk maps under climate change scenarios.

TABLE OF CONTENTS

ACKNOWLEDGEMENT	I
ABSTRACT	II
TABLE OF CONTENTS	II
LIST OF FIGURES	VI
LIST OF TABLES	IX
LIST OF ABBREVIATION	X
CHAPTER 1 INTRODUCTION	1
1.1 Background of the Study	1
1.2 Objectives of the Study	3
1.3 Organization of the Thesis	3
CHAPTER 2 LITERATURE REVIEW	5
2.1 Rivers of Bangladesh	5
2.2 Arial Khan River	6
2.3 Hydro-Morphological Status of Arial Khan River	7
2.3.1 Hydrology	7
2.3.2 Morphology	9
2.3.3 Instability/ Erosion	9
2.4 Floods of Bangladesh	10
2.4.1 Floods and types of floods	10
2.4.2 Causes of Floods in Bangladesh	11
2.4.3 Conventional Flood Mitigation Strategies	13
2.4.4 Flood Statistics in Bangladesh	16
2.4.5 Flood History in the Study Area	19
2.5 Impact of Climate Change on Flood Situation of Bangladesh	20
2.6 Concepts of Hazard, Exposure, Vulnerability & Risk	23
2.6.1 General Concept of Vulnerability and Risk	23
2.6.2 IPCC conceptualization of Vulnerability and Risk	23
2.7 Previous Studies	25
2.7.1 Studies on Flood Hazard and Risk Assessment around the World	25
2.7.2 Studies on Flood Hazard and Risk Assessment of Bangladesh	26
2.7.3 Studies on Arial Khan River	27

2.7.4	Application of HEC-RAS in Floodplain Inundation Modelling	28
2.8	Summary	29
	CHAPTER 3 SALIENT FEATURES OF THE MODELS	31
3.1	General	31
3.2	HEC-RAS	31
3.2.1	Theoretical Basis for Hydrodynamic Calculation in HEC-RAS	31
3.2.2	Capabilities of HEC-RAS	37
3.3	ArcGIS	41
3.3.1	Data Model	42
3.4	HEC-GeoRAS	43
3.4.1	Software Requirements	43
3.4.2	Data Requirements	43
3.4.3	HEC-GeoRAS Menus	43
	CHAPTER 4 METHODOLOGY	45
4.1	General	45
4.2	Study Area	45
4.3	Data Collection	46
4.3.1	Bathymetry	48
4.3.2	Discharge Data	48
4.3.3	Water Level Data	48
4.3.4	DEM	49
4.3.5	Satellite Image	49
4.4	Generation of Future Flow Hydrograph	49
4.4.1	Selection of RCP Scenarios	49
4.4.2	Hydrological Model SWAT	51
4.4.3	Generation of Future Flow Hydrograph	52
4.4.4	Statistical Relation between the Padma and Arial Khan River	55
4.5	HEC-RAS 1D Model Set Up	56
4.5.1	Processing in HEC-RAS	56
4.5.2	Boundary Condition	57
4.6	HEC-RAS 1D-2D Coupled Model Set up	59
4.6.1	Datum Correction of Digital Elevation Model (DEM)	59
4.6.2	Clipping of the Study Area from DEM	60

4.6.3	Generation of Triangulated Irregular Network (TIN)	61
4.6.4	Pre-processing in HEC-GeoRAS	61
4.6.5	Processing on HEC-RAS	65
4.6.6	Model Performance Evaluation	71
4.7	Preparation of Flood Inundation, Hazard and Risk Maps	72
4.7.1	Flood Inundation Classification	72
4.7.2	Selection of Indicators	73
4.7.3	Normalization of the Indicators	75
4.7.4	Risk Assessment	75
	CHAPTER 5 RESULTS AND DISCUSSIONS	77
5.1	Calibration and Validation of the Ganges-Brahmaputra-Padma 1D model	77
5.1.1	Calibration	77
5.1.2	Validation	78
5.2	Calibration and Validation of Arial Khan 1D-2D coupled Model	79
5.2.1	Calibration & Validation of 1D Model	79
5.2.2	Comparison of 2D Flood Inundation	81
5.3	Analysis of Historical Flood Events of Arial Khan River	83
5.3.1	Flood Inundation Maps of Historical Flood Events	83
5.4	Flood Hazard and Risk Assessment of Arial Khan River under Climate Change Scenarios	87
5.4.1	Flood Inundation Assessment for RCP 2.6 & RCP 8.5 Scenario	87
5.4.2	Flood Hazard Assessment for RCP 2.6 and RCP 8.5 Scenario	92
5.4.3	Flood Exposure and Vulnerability Assessment	98
5.4.4	Flood Risk Assessment for RCP 2.6 and RCP 8.5 Scenario	103
5.5	Discussions	110
	CHAPTER 6 CONCLUSIONS AND RECOMMENDATIONS	114
6.1	Conclusions	114
6.2	Recommendations for Future Studies	117
	REFERENCES	118

LIST OF FIGURES

Figure 2.1: Ganges, Brahmaputra and Meghna Basins (<i>Source: Banglapedia</i>)	5
Figure 2.2: Yearly peak inflows in the Arial Khan River from the Padma River (<i>source: Mamun, 2008</i>)	7
Figure 2.3: Annual stream flow of the Arial Khan River (1965-2007) (<i>source: Akter, et al., 2013</i>)	8
Figure 2.4: Annual maximum and minimum water levels (<i>Source: Akter, et al., 2013</i>)	8
Figure 2.5: Yearly variation of bed material load (<i>source: Akter, et al., 2013</i>)	9
Figure 2.6: Percentage of Flooded, Non Flooded, Flood Protected Areas in 2003 (<i>source: WMO, 2003</i>)	14
Figure 2.7: Comparison of flood hydrographs at Madaripur station of Arial Khan River	19
Figure 2.8: Changes in temperature and precipitation from the baseline by the end of the 21st Century for RCP 2.6 and RCP 8.5 (<i>source: Stocker, et al., 2013</i>)	21
Figure 2.9: IPCC AR5 concept of risk (<i>source: IPCC, 2014</i>)	24
Figure 3.1 Representation of terms in the energy equation	33
Figure 3.2 Application of the momentum principle	34
Figure 4.1: Summary of steps of methodology in the flow chart	45
Figure 4.2: Arial Khan River and its floodplain	46
Figure 4.3: All forcing agents' atmospheric CO ₂ -equivalent concentrations (ppmv) according to four RCPs (<i>Source: IPCC, 2014</i>)	50
Figure 4.4: GBM basins (<i>Source: Mohammed, et al., 2018</i>)	51
Figure 4.5: Flow hydrographs at Bahadurabad Transit (SW 46.9L) of Brahmaputra for RCP 2.6 & RCP 8.5 scenario	53
Figure 4.6: Flow hydrographs at Hardinge Bridge (SW 90) of Ganges for RCP 2.6 & RCP 8.5 scenario	53
Figure 4.7: 90th Percentile daily flow hydrograph plots for the base period, 2020s, 2050s, 2080s of RCP 2.6 of a) the Brahmaputra and b) the Ganges	55
Figure 4.8: 90th Percentile daily flow hydrograph plots for the base period, 2020s, 2050s, 2080s of RCP 8.5 of a) the Brahmaputra and b) the Ganges	55
Figure 4.9: Statistical Relation between Arial Khan River and the Padma River	56
Figure 4.10: Cross-sections of Brahmaputra, Ganges and Padma River in HEC-RAS	57

Figure 4.11: Boundary Q and WL for the Brahmaputra-Ganges-Padma Model for Calibration 2015	58
Figure 4.12: Boundary Q and WL for the Brahmaputra-Ganges-Padma Model for validation 2017	58
Figure 4.13 Digital Elevation Model (DEM) modification a) before modification b) after modification	59
Figure 4.14: Clipped DEM of the study area	60
Figure 4.15: TIN of the study area	61
Figure 4.16: Processing in HEC-GeoRAS a) River Centerline b) Bank line c) Flow paths d) Cross-sections Cutlines of Arial Khan River	63
Figure 4.17: Arial Khan cross-section in HEC-RAS	65
Figure 4.18: Interpolated Cross-sections of Arial Khan River	66
Figure 4.19: Incorporation of the Terrain of the study area in RAS-Mapper	66
Figure 4.20: 2D flow area computational mesh	67
Figure 4.21: Incorporation of Lateral Structures	68
Figure 4.22: Elevation of 1 of the 8 lateral structures	68
Figure 4.23: Boundary Q and WL for Arial Khan River for Calibration 2015	69
Figure 4.24: Boundary Q and WL for Arial Khan River for Validation 2015	69
Figure 4.25: Incorporation of upper and lower boundary condition for 2D flow area	70
Figure 5.1: Calibration of the Ganges-Brahmaputra-Padma 1D model	77
Figure 5.2: Validation of the the Ganges-Brahmaputra-Padma 1D model	78
Figure 5.3: Calibration of the Arial Khan 1D model	79
Figure 5.4: Validation of the Arial Khan 1D model	80
Figure 5.5: Qualitative comparison between a) MODIS derived inundation Map and b) model generated inundation map (before the flood)	81
Figure 5.6: Qualitative comparison between a) MODIS derived inundation Map and b) model generated inundation map (during the flood)	82
Figure 5.7: Flood inundation map of 1988 based on maximum flood depth	84
Figure 5.8: Flood inundation map of 1998 based on maximum flood depth	84
Figure 5.9: Flood inundation map of 2004 based on maximum flood depth	85
Figure 5.10: Flood inundation map of 2007 based on maximum flood depth	85
Figure 5.11: Flood inundation map of 2010 based on maximum flood depth	86
Figure 5.12: Flood inundation map for baseline	88

Figure 5.13: Flood inundation map for the 2020s of RCP 2.6	88
Figure 5.14: Flood inundation map for the 2050s of RCP 2.6	89
Figure 5.15: Flood inundation map for the 2080s of RCP 2.6	89
Figure 5.16: Flood inundation map for the 2020s of RCP 8.5	90
Figure 5.17: Flood inundation map for the 2050s of RCP 8.5	90
Figure 5.18: Flood inundation map for the 2080s of RCP 8.5	91
Figure 5.19: Flood hazard map for baseline	94
Figure 5.20: Flood hazard map for the 2020s of RCP 2.6	95
Figure 5.21: Flood hazard map for the 2050s of RCP 2.6	95
Figure 5.22: Flood hazard map for the 2080s of RCP 2.6	96
Figure 5.23: Flood hazard map for the 2020s of RCP 8.5	96
Figure 5.24: Flood hazard map for the 2050s of RCP 8.5	97
Figure 5.25: Flood hazard map for the 2080s of RCP 8.5	97
Figure 5.26: Relative contribution of exposure indicators in the study area	101
Figure 5.27: Relative contribution of vulnerability indicators (+ve dependency) in the study area	101
Figure 5.28: Relative contribution of vulnerability Indicators (-ve dependency) in the study area	101
Figure 5.29: Exposure Map of the Study Area	102
Figure 5.30: Vulnerability Map of the Study Area	102
Figure 5.31: Flood risk map for the baseline	105
Figure 5.32: Flood risk map for the 2020s of RCP 2.6	106
Figure 5.33: Flood risk map for the 2050s of RCP 2.6	106
Figure 5.34: Flood risk map for the 2080s of RCP 2.6	107
Figure 5.35: Flood risk map for the 2020s of RCP 8.5	107
Figure 5.36: Flood risk map for the 2050s of RCP 8.5	108
Figure 5.37: Flood risk map for the 2080s of RCP 8.5	108

LIST OF TABLES

Table 2.1: Salient features of Arial Khan River (<i>Source: BWDB, 2011</i>)	6
Table 2.2: Structural measures taken in Bangladesh for Flood Mitigation	14
Table 2.3: Year-wise Flood affected area in Bangladesh (<i>source: FFWC, 2017</i>)	17
Table 2.4: Hydrological characteristics of Floods of 2004 and 2007 (<i>Source: Islam, et al. (2010)</i>)	18
Table 2.5: Mean GBM Flows m ³ /s under 3 SSPs and 3 Climate Realisations (<i>Whitehead, et al., 2015</i>)	21
Table 2.6: Percentage changes in ensemble-mean of flood flows at different time slices compared to the baseline period (<i>Source: Mohammed, et al., 2019</i>)	22
Table 4.1: Summary of the Data Types	47
Table 4.2: List of Indicators used in this study	74
Table 5.1: Flood Affected Areas on the flood of 1998, 1998, 2004, 2007 and 2010	86
Table 5.2: Upazilla-wise flood affected area for historical flood events	87
Table 5.3: Upazilla-wise flood affected area (km ²) for RCP 2.6 and RCP 8.5 Scenarios	92
Table 5.4: Upazilla-wise mean flood depth (m) for RCP 2.6 and RCP 8.5 Scenarios	93
Table 5.5: Upazilla-wise normalized flood depth for RCP 2.6 and RCP 8.5 Scenarios	93
Table 5.6: Percentage of Area under different hazard zones for different projections RCP 2.6 and RCP 8.5	98
Table 5.7: Magnitude of Exposure and Vulnerability Indicators (<i>Source: Population Census 2011 & Agricultural Census 2008</i>)	99
Table 5.8: Normalised Values of Exposure and Vulnerability Indicators	100
Table 5.9: Upazilla-wise Risk for RCP 2.6 and RCP 8.5	104
Table 5.10: Upazilla-wise normalized Risk for RCP 2.6 and RCP 8.5	104
Table 5.11: Percentage of area under different risk zones for different projections of RCP 2.6 and RCP 8.5	109

LIST OF ABBREVIATION

ACRONYM	DEFINITION
2020s	2006-2035
2050s	2036-2065
2080s	2066-2095
ArcGIS	Arc Geographic Information System
Baseline	1976-2005
BBS	Bangladesh Bureau of Statistics
BRB	Brahmaputra River Basin
BTM	Bangladesh Transverse Mercator
BWDB	Bangladesh Water Development Board
CORDEX	Coordinated Regional Climate Downscaling Experiment
DEM	Digital Elevation Model
EC-EARTH	European Community Earth-System Model
FAO	Food and Agriculture Organization
GBM	Ganges Brahmaputra Meghna
GCM	General Circulation Model
HEC-RAS	Hydrologic Engineering Center River Analysis System
IPCC	Intergovernmental Panel on Climate Change
m ³ /s	Cubic meter per second
NASA	National Aeronautics and Space Administration
PWD	Public Works Department
RCM	Regional Climate Model
RCP	Representative Concentration Pathways
SWAT	Soil Water Assessment Tool
TIN	Triangular Irregular Networks
USGS	U.S. Geological Survey
WARPO	Water Resources Planning Organisation
WMO	World Meteorological Organization

CHAPTER 1

INTRODUCTION

1.1 Background of the Study

Bangladesh is highly susceptible to flood due to its location at the confluence of the world's three major basins – Ganges-Brahmaputra-Meghna (GBM) and hydro-meteorological and topographical characteristics of the basins (Shaw, et al., 2013). About 92.5 percent of the combined basin area of the three rivers lies outside of the country. Furthermore, about 80 percent of the annual rainfall occurs in the monsoon (June to September) across the river basins. Therefore, Bangladesh is forced to drain out huge cross-border monsoon runoff together with its runoff through a network of rivers. Most of the time, the volume of generated runoff exceeds the capacity of the drainage channels and this makes it one of the most flood vulnerable countries in the world.

On average, annual floods inundate 20 percent area of the country and this can reach as high as about 70 percent during an extreme flood event (Mirza, 2002). Future climate change along with economic development, increase in population, change in landuse, globalization, and urbanization may worsen this situation manifolds (Shaw, et al., 2013). As per the fifth assessment report (AR5) of IPCC (International Panel on Climate Change), the global mean surface temperature may increase between 0.3°C to 4.8°C for low (RCP 2.6) to high (RCP 8.5) emission scenarios from its baseline (1985-2005) by the end of 21st century (Stocker, et al., 2013). At the same time, the high latitude and equatorial Pacific are likely to experience an increase in annual mean precipitation under the RCP 8.5 scenario (Stocker, et al., 2013). Increase in temperature and precipitation will significantly affect the hydrological cycle of the GBM rivers which may lead to more intense and frequent floods in Bangladesh in upcoming decades (Whitehead, et al., 2015; Masood, et al., 2015; Mirza, et al., 2003; Mohammed, et al., 2018). Firstly, the glacier melting in the upper HKH (Hindu-Kush Himalayan) region in summer will increase the flow of the main rivers of Bangladesh, enhancing the risk of monsoon flood. Simultaneously, the monsoon regime will increase the precipitation in some of the places in Bangladesh. As a result, the frequency and intensity of flood will increase significantly in the future. To cope with future flood situation and minimize potential flood losses and damages, a sustainable flood management plan is a necessity of the day.

For flood management, there are various options which have been long practiced in Bangladesh. Among these, structural measures such as flood embankment, dredging, river training, polders are the principal strategy for the mitigation of flood loss and damage. However, with the experience over the last few decades, it is observed that the structural measures do not bring only blessings. They also have adverse effects such as the rise in bed levels and obstruction to drainage etc. (Islam, et al., 2010). Additionally, the recent concept of flood management is considered from different angles such as improvement of the quality of life, impact on the physical environment, socio-economic condition and eco-system preservation. Hence, the policymakers are now more inclined to focus on non-structural flood measures like flood forecasting and warning system and development of flood hazard and risk maps for the major flood prone rivers of Bangladesh (Hossain, 2015; Nishat, 1998).

In recent times, flood hazard, vulnerability, and integrated risk assessment have been recognized as an essential input for the formulation of plans and policies aiming at flood risk management at national, regional and local levels (ISRBC, 2014). Delineation of flood plain and development of hazard and risk map may help the planners and policy makers in identifying the priority areas for planning any future flood management strategies to reduce the future probable loss and damages. Hence, preparation of flood hazard and risk maps for the important flood-prone rivers of Bangladesh has become essential. Besides, future climate impact should be incorporated in these studies to make this plan more effective, economical and sustainable.

Arial Khan is one of the major rivers of the southwest region of Bangladesh, the upper reach of which is subjected to flood, bringing tremendous sufferings to the people dwelling on its floodplain (Tingsanchali & Karim, 2005). Many studies have been conducted so far on potential flood hazard and risk assessment considering climate change impact (Silva, et al., 2016; Shrestha & Lohpaisankrit, 2016; Tu & Tingsanchali, 2010). A number of studies have also been done for the major rivers and floodplains of Bangladesh (Tingsanchali & Karim, 2005; Nishat, 2017; Ali, et al., 2018). However, flood inundation of Arial Khan River has not been studied yet, let alone its hazard and risk assessment due to climate change scenarios. Hence, this study is designed for the flood hazard and risk assessment of Arial Khan River and its floodplain for predicted climate change scenarios using an open source numerical model.

Numerical modeling approach apparently plays a vital role in flood hazard and risk assessment being the only way which can provide the information of future changes in flood variables and consequent vulnerability under changing climate impact (Anh, et al., 2016). There are many commercial models and open source mathematical models for hydrodynamic assessments. However, open source software HEC-RAS (Hydrologic Engineering Center River's Analysis System) has been chosen to carry out this study due to its accuracy in analysis of river system and special feature of 1D-2D river-floodplain coupling simulation (HEC-RAS, 2016). The flood depth estimated from the HEC-RAS 1D-2D coupled model of Arial Khan is considered as the hazard parameter for flood hazard analysis. Later, the risk is assessed as the function of hazard, vulnerability and exposure as recently introduced in the AR5 (Fifth Assessment Report) of the IPCC (Intergovernmental Panel on Climate Change) (IPCC, 2014). However, this study assumes that indicators of exposure and vulnerability (e.g., population, land use and poverty rate) remain the same in the future. Although four climate scenarios are available, only two RCPs - RCP 2.6 and RCP 8.5 are selected being the optimistic (low emission mitigation scenario) and pessimistic (high emission scenario) scenario to construct the future climate scenarios to address the uncertainty in climate change projections.

1.2 Objectives of the Study

The specific objectives of this study are:

- I. To set up a calibrated and validated HEC-RAS 1D model of Ganges, Brahmaputra and Padma River to estimate future flow at the offtake of Arial Khan River
- II. To set up a calibrated and validated HEC-RAS 1D-2D coupled model of Arial Khan River and its floodplain
- III. To generate flood hazard and risk maps of Arial Khan River floodplain for present and future flood flow scenarios

1.3 Organization of the Thesis

Chapter 1 is an introduction to the thesis. Here, the background of the study and objectives of the thesis have been discussed.

Chapter 2 is the literature review. This chapter contains a review of the hydro-morphological status of the Arial Khan River. It discusses flood, causes of the flood, flood history and the flood mitigation strategies which are adopted in Bangladesh. Besides, the impact of future climate change on the flood scenario of Bangladesh has been discussed.

This chapter additionally, introduces the conceptual basis of recent vulnerability and risk concepts. Furthermore, it covers the previous studies on the flood hazard and risk assessment around the world as well as in Bangladesh and applicability of HEC-RAS 1D-2D coupled model in flood inundation assessment.

Chapter 3 is the salient features of the models. This chapter covers the features of the models used in this study. Besides, the basic concepts and theoretical background of HEC-RAS are also discussed.

Chapter 4 is the methodology of the study. This chapter discusses data collection, selection of RCP scenarios, generation of future flood hydrographs and the development of statistical relation. The chapter also broadly describes different steps of the hydrodynamic model set up in HEC-RAS. This chapter covers the selection of the hazard, exposure and vulnerability indicators as well.

Chapter 5 is the results and discussions. It contains calibration and validation of the hydrodynamic models, analysis of historical flood events and simulation of future floods and flood hazard and risk assessment for the future climate change scenarios of RCP 2.6 and RCP 8.5.

Chapter 6 is conclusions and recommendations. This chapter gives a summary of the results obtained in this study and also includes recommendations for further study relevant to this topic.

CHAPTER 2

LITERATURE REVIEW

2.1 Rivers of Bangladesh

Bangladesh is a riverine country with hundreds of rivers overlaying its landscape. The country consists of the floodplains of the Ganges, Brahmaputra and Meghna rivers and their numerous tributaries and distributaries. Their total catchment area of Ganges-Brahmaputra-Meghna (GBM) river basins is approximately 1.72 million sq. Km distributed between India, China, Nepal, Bangladesh, and Bhutan of which only about 7.5% lies in Bangladesh and the rest, 92.5% lies outside the territory (FFWC, 2017). Ganges, Brahmaputra and Meghna river systems together, drain a large amount of discharge and sediment load from upstream countries passes through Bangladesh towards the Bay of Bengal as shown in Figure 2.1. It is assumed that an average flow of 1,009,000 million cubic meters passes through these river systems during the monsoon season. Most of the rivers of Bangladesh are characterized by having sandy bottoms, flat slopes, substantial meandering, banks susceptible to erosion and channel shifting. The river system of Bangladesh is one of the most extensive in the world, and the Ganges and the Brahmaputra are amongst the largest rivers on earth in terms of catchment size, river length and discharge.

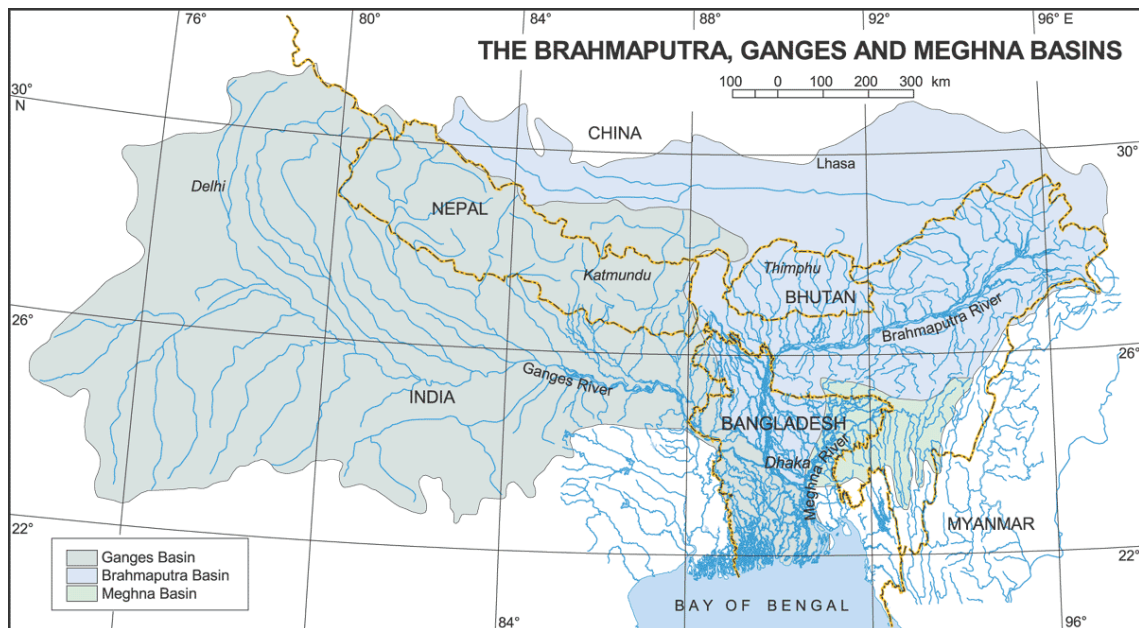


Figure 2.1: Ganges, Brahmaputra and Meghna Basins (*Source: Banglapedia*)

2.2 Arial Khan River

Arial Khan River one of the main south-eastward outlets of the river Padma. Bifurcating from the Padma at 51.5 km southeast of Goalundo in Rajbari district, the river flows through Faridpur and Madaripur districts before falling into the Tentulia at the north-eastern corner of Barisal. Madaripur and Shariatpur stand on the right and left bank of the Arial Khan. The river is navigable throughout the year and is under tidal influence. The river maintains a meandering channel through its course and is erosional.

The river has two parts, one of them is called as the Arial Khan Upper (AKU) and the other is called the Arial Khan Lower (AKL), both of them are distributaries of the Padma. The Arial Khan Upper originates at Chawdhury Char and Arial Khan Lower at Dubaldia. The length of Arial Khan Upper and the Arial Khan is about 70 km and 12.5 km respectively (Mamun, 2008). The Arial Khan Upper meets the Arial Khan Lower in Madaripur. Both the AKU and AKL are meander rivers with sharp curves and bends. After combining with the AKU, the AKL extends towards the downstream direction to meet various rivers such as Naya Banga, Babuganj, Kirtonkhola, etc. and finally meets Bishkhali river which discharges into the Bay of Bengal through the Sundarban forest. The upper reach of Arial Khan is vulnerable due to Monsoon Flood while the lower part is flooded due to coastal storm surge. The salient features of the Arial Khan River are given in Table 2.1.

Table 2.1: Salient features of Arial Khan River (*Source: BWDB, 2011*)

Offtake	Padma (Faridpur)
Outfall	Tetulia (Barisal)
District	Faridpur, Madaripur, Barisal
Tributary	Kumar (lower)
Distributary	Sandhya, Kumar, Kirtonkhola, Rongmatia
Length	155 km
Width	Max – 1940 m, Min – 86 m, Avg. – 300 m
Type	Meandering, slope – 3cm/km
Flow	Max – 5810 m ³ /s, Min - 0.83 m ³ /s

2.3 Hydro-Morphological Status of Arial Khan River

2.3.1 Hydrology

Discharge

The hydro-morphological condition of the river depends on the position of the off-take and the deviation of flow direction to the off-take from the parent river, the Padma. Analysis of annual maximum flow of Arial Khan at the off-take of the Arial Khan River at Chowdhury Char (SW 4A) station from 1965 to 2009 show that the flow trend is increasing in the Arial Khan River as shown in Figure 2.2 (Akter, et al., 2013). During the last few decades, the location and geometry of the off-take have been changed several times (CEGIS, 2010; Mamun, 2008).

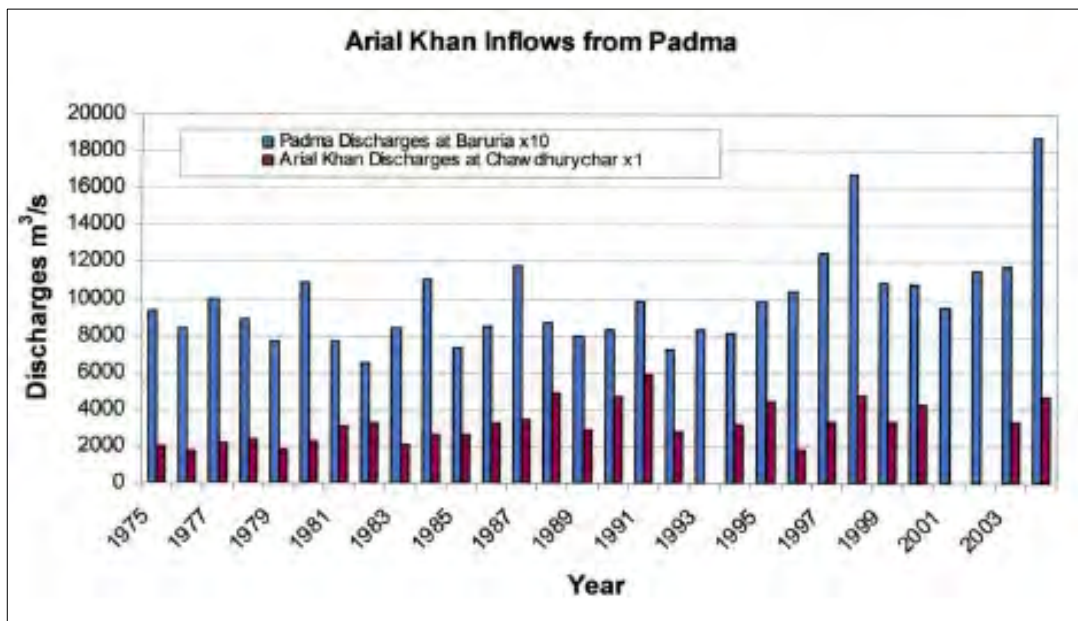


Figure 2.2: Yearly peak inflows in the Arial Khan River from the Padma River (*source*: Mamun, 2008)

Analysis of annual monthly flow of Arial Khan River from 1965 to 2007 indicates high season variation in the flow in the Arial Khan River (Figure 2.3). The average flow during February and March is less than 50 m³/s, whereas the average flow of August and September is more than 2000 m³/s, indicating a very high variability of mean monthly flow. A study conducted by (CEGIS, 2010) predicts that the flow into the Arial Khan River would increase in future both dry and wet seasons. Subsequently, the increase of monsoon discharge would increase river bank erosion as well.

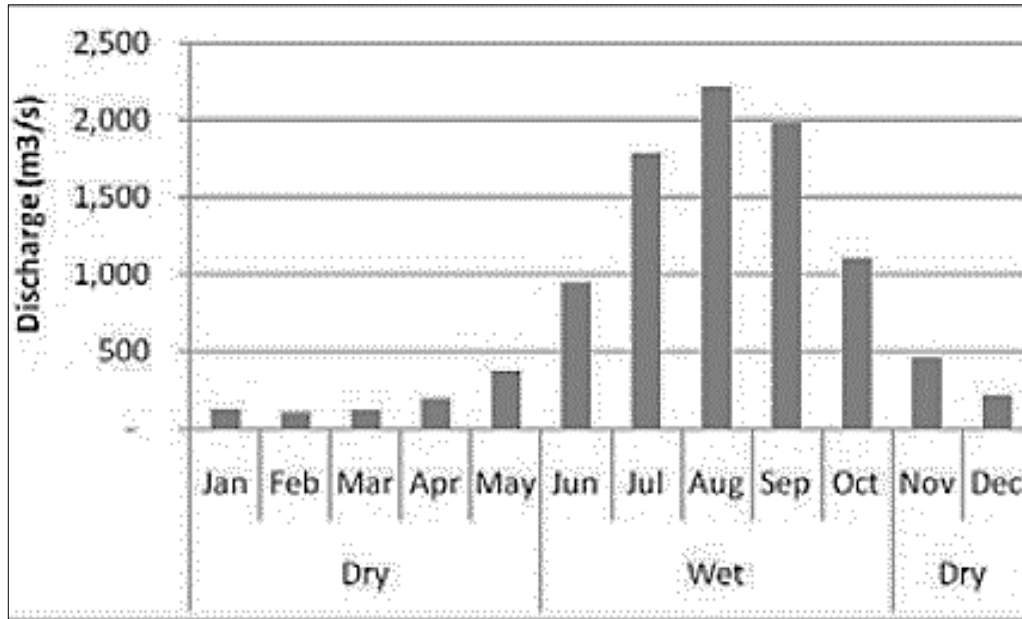


Figure 2.3: Annual stream flow of the Arial Khan River (1965-2007)
(source: Akter, et al., 2013)

Water level

Arial Khan River has two water level stations. One is at the offtake of the Arial Khan River (Chowdhury Char), another one is at Madaripur. The maximum water level of upstream Chowdhury Char station varies between 4.5 mPWD to 7.8 m PWD, whereas that of Madaripur varies between 3.8 mPWD to 6 mPWD. Maximum annual water levels of both the stations show no significant changes over time. However, annual minimum water levels of both the stations show a noticeable decreasing trend as shown in Figure 2.4 (Akter, et al., 2013).

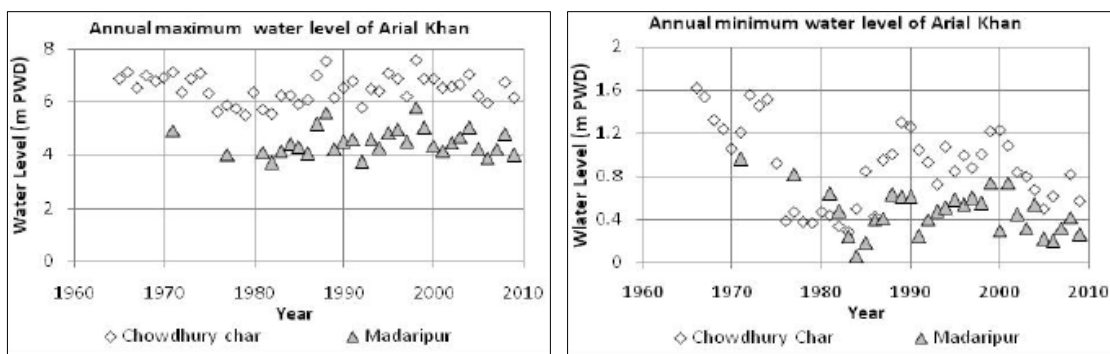


Figure 2.4: Annual maximum and minimum water levels (Source: Akter, et al., 2013)

2.3.2 Morphology

Bed materials in the Arial Khan River consist of fine sand. Most of the bed material transportation occurs in suspension mode. A few sediment datasets are found under the FAP 24 study during 1993-1996 as shown in Figure 2.5. Analysis of those datasets indicates that the sediment load in the Arial Khan River increased more substantially during the late 1980s, which was highly related to the discharge. The increase of bed material load was probably due to the favorable position of the off-take of the Arial Khan River. The decadal average bed material load in the Arial Khan River was about six million tonnes per year in the 1990s, when the average annual volume of discharge was about thirty billion cubic meter.

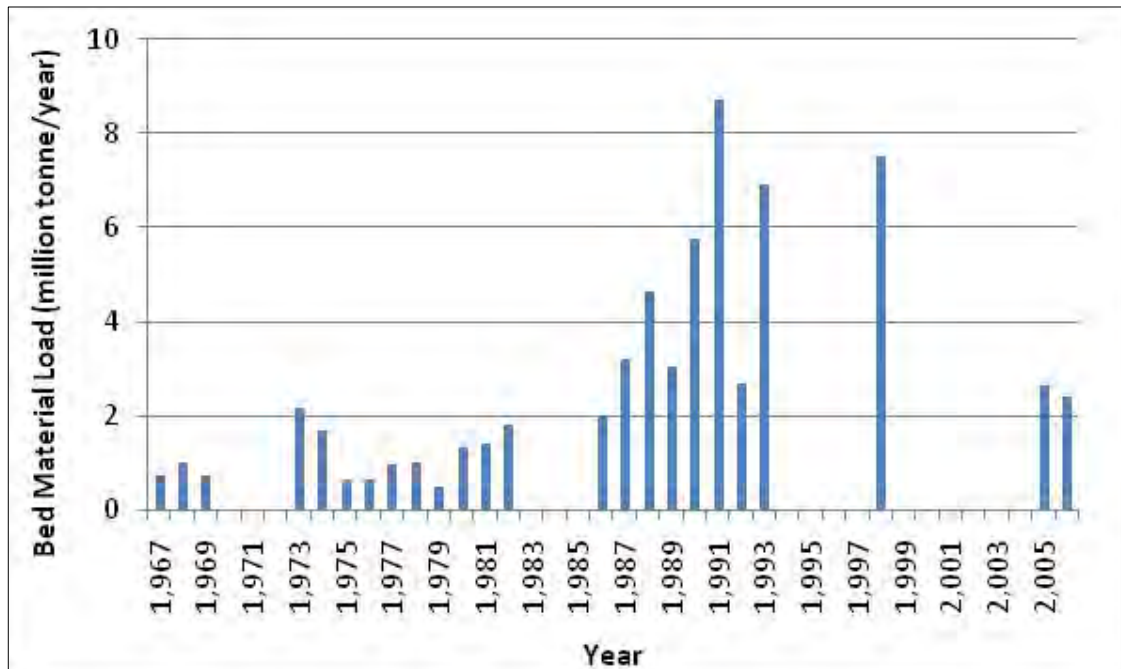


Figure 2.5: Yearly variation of bed material load (*source: Akter, et al., 2013*)

2.3.3 Instability/ Erosion

The river maintains a meandering channel through its course and is erosional in nature. The erosion rate varies between $0.2 \text{ km}^2\text{y}^{-1}$ to $1 \text{ km}^2\text{y}^{-1}$ while accretion rate varies between $0.18 \text{ km}^2\text{y}^{-1}$ to $0.6 \text{ km}^2\text{y}^{-1}$ (Akter, et al., 2013). Analysis of bank lines derived from time series satellite images of 1973 to 2010 reveals that erosion and accretion had occurred simultaneously.

2.4 Floods of Bangladesh

2.4.1 Floods and types of floods

Flood is an unusually high stage in the river - usually the level at which the river overflows its banks and inundates the adjoining area. Bangladesh is located at the confluence of the worlds' three largest basins – Ganges, Brahmaputra and Meghna, is forced to drain out huge cross-border monsoon runoff together with its runoff through a network of rivers to the Bay of Bengal. Most of the time, the volume of generated runoff exceeds the capacity of the drainage channels and this makes it one of the most flood vulnerable countries in the world. In Bangladesh, there are four types of floods that are typically encountered (WARPO, 2004).

Flash Flood from Hilly Areas

Intense local and short-lived rainfall often associated with mesoscale convective clusters is the primary cause of flash floods. These are characterized by a sharp rise followed by a relatively rapid recession. Often with high velocities of on-rush flood damages crops, properties and fish stocks of the wetland. Flash flood can occur within a few hours. Flash floods are frequent in the districts of Northeast and Southeast regions of the country. Flash flood naturally occurs in April and May and damage the Boro Crop of northeast Haor area.

Monsoon Floods or Normal flood or Fluvial flood from major rivers

River flood is a common phenomenon in this country caused by bank overflow. Of the total flow, around 80% occurs in the five months of monsoon from June to October (WARPO, 2004). A similar pattern is observed in the case of rainfall also. As a consequence of these skewed temporal distributions of river flow and rainfall, Bangladesh suffers from an abundance of water in monsoon, frequently resulting in floods. Climatologically, the discharge into Bangladesh, from upper catchments, occurs at the different time of the monsoon. In the Brahmaputra, maximum discharge occurs in an early monsoon in June and July whereas in the Ganga maximum discharge occurs in August and September. Synchronization of the peaks of these rivers results in devastating floods in the monsoon season in Bangladesh (WARPO, 2004). In this study, this type of flood is mainly focused as the area selected for this study is mainly vulnerable to fluvial or riverine flood.

Rain-fed Flood/ Urban Flood

This kind of flood generally occurs in many parts of the country but is mainly prevalent in the south-western part of the country. This kind of flood also occurs in the Floodplains where natural drainage systems have been disturbed either due to human interferences, e.g., construction of unplanned rural roads and encroachment of river courses, etc. or due to the gradual decay of the natural drainage system. When intense rainfall takes place in those areas, the natural drainage system cannot carry the run-off generated by the storm and causes temporary inundation in many localities. This kind of rain-fed flood is increasing in urban areas.

Floods Due to Storm Surges

This kind of flood mostly occurs along the coastal areas of Bangladesh over a coastline of about 800 km along the southern part. Continental shelves in this part of the Bay of Bengal are shallow and extend to about 20-50 km. Moreover, the coastline in the eastern portion is conical and funnel-like in shape. Because of these two factors, storm surges generated due to any cyclonic storm is comparatively high compared to the same kind of storm in several other parts of the world. In the case of super-cyclones, maximum heights of the surges were found to be 10-15 m, which causes flooding in the entire coastal belt. The worst kind of such flooding was on 12 Nov 1970 and 29 April 1991, which caused loss of 300,000 and 138,000 human lives respectively (FFWC, 2005). Coastal areas are also subjected to tidal flooding during the months from June to September when the sea is in spate due to the southwest monsoon wind.

2.4.2 Causes of Floods in Bangladesh

Floods in Bangladesh occur for many reasons. The main causes are given below:

Excessive Rainfall

Bangladesh is located at the foot of the highest mountain range in the world, the Himalayas, which is also the highest precipitation zone in the world. The influence of the south-west monsoon causes this rainfall. Cherapunji, highest rainfall in the world, is located a few kilometers northeast of the Bangladesh border (FFWC, 2017).

Geographical location

Bangladesh is located at the confluence of the world's three large river basins – Brahmaputra, Ganges, and Meghna. The runoff from their vast catchment (about 1.72

million km²) passes through a small area, only 7.5% of these catchments lie within Bangladesh. During the monsoon season, the amount of water entering Bangladesh from upstream is greater than the capacity of the rivers to discharge into the sea.

Flat Topography

The flat topography and flat slope are other significant reasons for the floods of Bangladesh. Due to its flat topography, when a massive amount of discharge occurs in monsoon, it gets stagnant within its topography and delays to discharge into the Bay of Bengal.

Synchronization of Monsoon Flow

The synchronization of flood peaks of the three major rivers - Padma, Meghna, and Jamuna is another main reason behind the floods in Bangladesh. A combination of heavy rainfall within and outside the country and synchronization of peak flows of the major rivers were the main reasons behind the floods of 1988 and 1998. It delays flood water to discharge into the BoB and increases flood height and causes prolong floods.

The influence of tides and cyclones

The frequent development of low-pressure areas and storm surges in the Bay of Bengal can impede drainage. The severity of flooding is highest when the peak floods of the major rivers coincide with these effects.

Riverbed Aggradation

The river gradient decreases rapidly if sedimentation continues on the riverbeds. Riverbed aggradations reduce the water carrying capacity of rivers, causing them to overflow their banks. The rise of riverbed levels is a major reason behind the increased flooding tendency in Bangladesh.

Drainage Congestion

The construction of embankments in the upstream catchments reduces the capacity of the floodplains to store water. The unplanned and unregulated construction of roads and highways in the flood plain without adequate opening creates obstructions to flow and drainage congestion.

Construction of Dams and Barrages in the River

Damming of a river reduces the velocity of water flow downstream. As a result, the sediments carried by the river start to settle down faster on the riverbed, causing riverbed aggradations. This also reduces the water carrying capacity of the river. So far, India's Farakka Barrage has tremendously damaged the agriculture, navigation, environment, and hydrodynamic equilibrium in Bangladesh.

Deforestation

A rapid increase in the population of South Asia has resulted in an acceleration of deforestation in the hills of Nepal and India to meet the increasing demand for food and fuelwood. Deforestation in hilly catchments causes more rapid and higher runoff, and hence more intense flooding.

Climate change

Climate changes could influence the frequency and magnitude of flooding. The increase of temperature will cause snow melting from glaciers and mountain peaks in the Himalaya. Besides the areas near the equator are likely to experience an increase in annual mean precipitation. Hence, the upstream flow from Ganges, Brahmaputra and Meghna basins will increase in the future. Additionally, a higher sea level will inhibit the drainage from the rivers to the sea and increase the impact of tidal surges. Hence, future climate change is going to be a significant driver of floods of Bangladesh.

2.4.3 Conventional Flood Mitigation Strategies

Structural Measures

For flood management, various options have been long practiced in Bangladesh. Among these, structural measures such as embankment, dredging, river training, polders are the principal strategies for the mitigation of flood loss and damage. Among these, embankments are the most commonly used structural measure in Bangladesh. Government always put more emphasis on protecting Medium High and Medium Low Lands from floods through the construction of embankments. Flooded, non-flooded and flood protected area of Bangladesh is shown in figure 2.6.

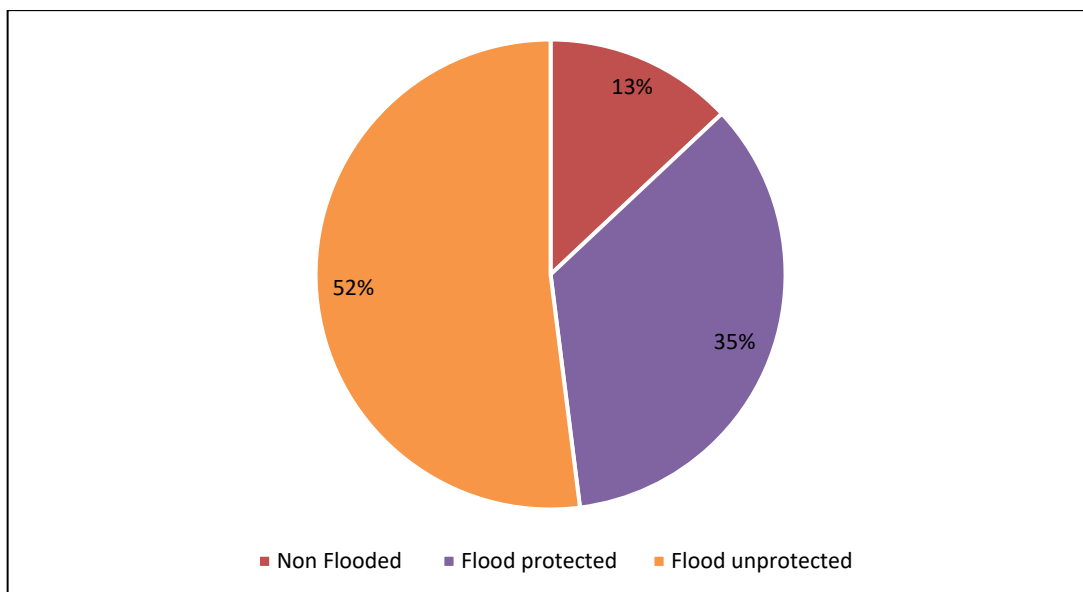


Figure 2.6: Percentage of Flooded, Non Flooded, Flood Protected Areas in 2003
(source: WMO, 2003)

Since the 1960s, Bangladesh has implemented about 628 nos. of large, medium and small-scale FCDI projects. Total investment was nearly US\$ 4.0 billion, and it provided flood protection to 5.37 million ha of land, which is about 35% of the area (WMO, 2003). A summary of structural measures is given in table 2.2.

Table 2.2: Structural measures taken in Bangladesh for Flood Mitigation

Item	Quantity
Embankment	10,000 km
Drainage Channel Improvement	3500 km
Drainage Structure	5000 nos.
Dam	1 no.
Barrage	4 nos.
Pump House	100 nos.
River Closure	1250 nos.

Non-Structural Measures

Despite all the structural activities, it is found that the people living in the Medium High and Medium Low Lands are not immune to flooding during moderate to extreme flood

events. Additionally, with the experience over the last few decades, it is observed that the structural measures do not usually bring only blessings. They also have adverse effects such as a rise in bed levels and obstruction to drainage (Islam, et al., 2010). Hence, the government realized that minimizing flood loss through non-structural means like flood forecasting and warning system and flood hazard and risk maps are also very important. With this end in view, Flood Forecasting and Warning System (FFWS) was established in 1972 with 10 Flood Monitoring Stations on the major river systems. After the disastrous floods of 1987 and 1988, the Government realized the importance of FFWS and took steps to modernize the system. New FF model was developed based on the Mike-II hydrodynamic model and flood-monitoring stations were increased to 30 in 1996. In 1998 flood, FFWS was found to be very useful providing the early warning and information on the flood. With the experience of the 1998 flood, the Government decided to improve it further to cover all the flood-prone areas of the country under real-time flood monitoring.

However, the success story was not within a satisfactory mark. It is also perceived that flood forecasting and warning alone cannot solve the problem of flood damage. Because most of the residents in the floodplain are not sufficiently aware of the consequences flood. Thus, land with a high risk of flooding is carelessly developed for housing and infrastructure purposes with few measures against flood damages. Hence, the main facilities damaged by the floods of 1987, 1988 and 1998 are housing and infrastructure (Tingsanchali & Karim, 2005). Hence, after the big flood event in 1998, experts from different fields recommended the use of flood hazard and flood risk maps for developing an effective flood management plan (Nishat, 1998) which provides information to residents in flood-prone areas about flooding consequences. If residents and persons in charge of flood loss prevention understand the susceptibility to flood correctly, flood loss mitigating measures in the floodplain could be developed smoothly. These measures could further minimize damages by establishing proper flood protection, warning and evacuation system. From then, the studies on flood hazard and risk are initiated in Bangladesh as a non-structural flood management measures and now it is a well-accepted form of flood mitigation all over the world as well as in Bangladesh.

2.4.4 Flood Statistics in Bangladesh

Flood is a natural phenomenon in Bangladesh and occurs on an annual basis. Percent of the total area of Bangladesh affected by the flood are available since 1954 is presented in Table 2.3. The table shows that the flood of 1955, 1974, 1987, 1988, 1998, 2004, 2007 and 2017 inundated more than 50000 sq. Km of the area and caused enormous damages to properties and considerable loss of life. Recent notable and catastrophic floods have occurred in 1987, 1988, 1998, 2004 and 2007.

The catastrophic floods of 1987 occurred throughout July and August and affected 57,300 km² of land, (about 40% of the total area of the country) and were estimated as a once in 30-70 year event (Flood Archive, 2003). The severely affected regions were on the western side of the Brahmaputra, the area below the confluence of the Ganges and the Brahmaputra and considerable areas north of Khulna.

The flood of 1988, which was also of catastrophic consequence, occurred throughout August and September. The waters inundated about 82,000 km² of land, (about 60% of the area) and its return period was estimated at 50–100 years. Rainfall together with synchronization of unusually high flows of all the three major rivers of the country in only three days aggravated the flood. Dhaka, the capital of Bangladesh, was severely affected. The flood lasted 15 to 20 days.

In 1998, over 75% of the total area of the country was flooded, including half of the capital city Dhaka (Reliefweb, 1998). It was similar to the catastrophic flood of 1988 in terms of the extent of the flooding. A combination of heavy rainfall within and outside the country and synchronization of peak flows of the major rivers contributed to the river. Thirty million people were made homeless and the death toll reached over a thousand (Reliefweb, 1998). The flooding caused contamination of crops and animals and unclean water resulted in cholera and typhoid outbreaks. Few hospitals were functional because of damage from the flooding and those that were had too many patients, resulting in common injuries becoming fatal due to lack of treatment. 700,000 hectares of crops were destroyed, 400 factories were forced to close, and there was a 20% decrease in economic production (BBC News, 1998). Communication within the country also became difficult.

Table 2.3: Year-wise Flood affected area in Bangladesh (*source: FFWC, 2017*)

Year	Flood affected area		Year	Flood affected area		Year	Flood affected area	
	sq. km	%		sq. km	%		sq. km	%
1954	36800	25	1977	12500	8	2000	35700	24
1955	50500	34	1978	10800	7	2001	4000	2.8
1956	35400	24	1980	33000	22	2002	15000	10
1960	28400	19	1982	3140	2	2003	21500	14
1961	28800	20	1983	11100	7.5	2004	55000	38
1962	37200	25	1984	28200	19	2005	17850	12
1963	43100	29	1985	11400	8	2006	16175	11
1964	31000	21	1986	6600	4	2007	62300	42
1965	28400	19	1987	57300	39	2008	33655	23
1966	33400	23	1988	89970	61	2009	28593	19
1967	25700	17	1989	6100	4	2010	26530	18
1968	37200	25	1990	3500	2.4	2011	29800	20
1969	41400	28	1991	28600	19	2012	17700	12
1970	42400	29	1992	2000	1.4	2013	15650	10.6
1971	36300	25	1993	28742	20	2014	36895	25
1972	20800	14	1994	419	0.2	2015	47200	32
1973	29800	20	1995	32000	22	2016	48675	33
1974	52600	36	1996	35800	24	2017	61979	42
1975	16600	11	1998	100250	68			
1976	28300	19	1999	32000	22			

The 2004 floods lasted from July to September and covered 50% of the country at their peak. At the time of the July 2004 floods 40% of the capital, Dhaka was under water. In this flood, 600 deaths were reported, and 30 million people were homeless. 100,000 people alone in Dhaka suffered from diarrhea from the flood waters. Bridges were destroyed, the death toll rose to 750, and the airport and major roads were flooded — this hampered relief efforts. The damage to schools and hospitals was estimated at \$7 billion. Rural areas also suffered, the rice crop was devastated as were important cash crops such as jute and sugar.

In 2007, more than half of Bangladesh was severely affected by monsoon flooding. Caused by excessive rainfall in catchment areas of Nepal, Bhutan and Northern Indian, floods in July and September affected 13.3 million people – 6 million of them children – in 46 districts. The flood peak and duration of the flood of 2004 and 2007 in the major three rivers- Ganges, Brahmaputra and Meghna are given in Table 2.4.

Table 2.4: Hydrological characteristics of Floods of 2004 and 2007

(Source: Islam, et al. (2010))

Parameters	Rivers	Stations	2004	2007
Peak Flood level (m) above DL	Brahmaputra	Bahadurabad	0.68	0.88
	Ganges	Hardinge Bridge	-	-
	Meghna	Bhairab Bazar	1.53	0.69
Duration of Flood (days) above DL	Brahmaputra	Bahadurabad	15	21
	Ganges	Hardinge Bridge	0	0
	Meghna	Bhairab Bazar	38	37

Flood of 2017 was also a severe one. The rise of water levels in the various rivers in the northern part of the country due to heavy rainfalls as well as water flow from the upstream hills in India have led to the inundation of the river basin areas in the northern parts of Bangladesh. Almost 42% of the country got flood affected which corresponded to 35 districts namely: Kurigram, Rangpur, Lalmonirhat, Nilphamari, Gaibandha, Bogra, Sirajganj, Tangail, Jamalpur, Natore, Pabna, Manikganj, Narayanganj, Rajbari, Faridpur, Manikganj, Munshiganj, Shariatpur, Panchagarh, Thakurgaon, Dinajpur, Naogaon,

Chapai Nawabganj, Jessore, Sylhet, Sunamganj, Netrokona, Brahmanbaria, Habiganj, Moulvibazar, Sherpur, Chittagong, Bandarban, Cox’s Bazar and Feni (FFWC, 2017).

2.4.5 Flood History in the Study Area

Arial Khan River is a major river of the south-west region. It is the major distributary of the Padma River. The danger level at Madaripur station (SW 5) of Arial Khan River is 4.20 m. It has been recorded that during the historical flood event in Bangladesh, the water level in Arial Khan River was above the danger level and caused the floodplain nearby flooded severely. The maximum recorded water level in Arial Khan River was 5.80 mPWD in the Madaripur station during the flood of 1998 (FFWC, 2019). During the devastating floods of 1987 and 1988 in Bangladesh, the water level in Arial Khan was 5.17 m and 5.60 m respectively. Figure 2.5 shows the water level at Madaripur station of Arial Khan River for the year 1987, 1988, 1998, 2004, 2007, 2010, 2015 and 2017.

It is observed from Figure 2.7 that the water level of 1987, 1988, 1998, 2004, 2007 and 2010 was above the danger level. Hence, it can be observed that Arial Khan river usually is flooded during the high impact flood events.

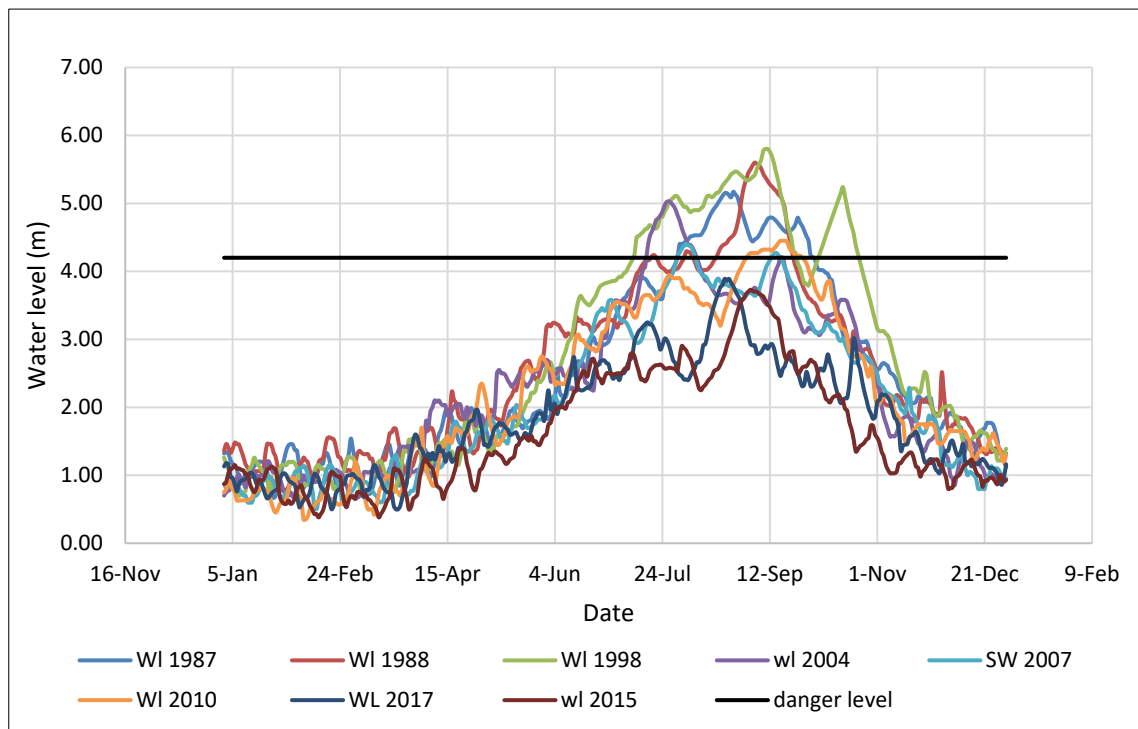


Figure 2.7: Comparison of flood hydrographs at Madaripur station of Arial Khan River

The water level condition of Arial Khan River during the peak monsoon season is documented in different Annual Flood Reports of FFWC. In 2011, the WL of Arial Khan at Madaripur flowed above the DL from 5th August to 4th September for 30 days. The WL attained its highest peak of 4.37 m on the 15th of August, which was 20cm above the DL at Madaripur (FFWC, 2011). In 2012, the WL of Arial Khan at Madaripur did not flow above the DL. The WL attained its highest peak of 3.71 m on the 30th of September, which was 46cm below the DL at Madaripur (FFWC, 2012). In 2013, the WL of Arial Khan at Madaripur flowed below the DL. The WL attained its highest peak of 3.61 m on the 12th of September, which was 56cm below the DL at Madaripur (FFWC, 2013).

In 2014, The WL of Arial Khan at Madaripur flowed below the DL. The WL attained its highest peak of 3.76 m on the 1st of September, which was 41cm below the DL at Madaripur (FFWC, 2014). In 2015 the WL attained its highest peak of 3.73 m on the 3rd of September, which was 34cm below the DL at Madaripur (FFWC, 2015). In 2016, WL of Arial Khan at Madaripur flowed below the DL. The WL attained its highest peak of 3.87 m on the 5th of August, which was 24cm below the DL at Madaripur (FFWC, 2016). The WL of Arial Khan at Madaripur flowed below the DL throughout the monsoon in 2017. The WL attained its highest peak of 3.89 m on 22nd August, which was 28 cm below the DL at Madaripur (FFWC, 2017).

2.5 Impact of Climate Change on Flood Situation of Bangladesh

Climate change and its impact is a significant concern of the twenty-first century. Global warming induced changes in temperature, rainfall and sea level are already evident in many parts of the world, as well as in Bangladesh (Ahmed & Alam, 1999; Stocker, et al., 2013). Climate change is enhancing hazards such as floods, droughts, cyclones and other hydro-climatic disasters (Kay, et al., 2015; Mohammed, et al., 2018).

According to the fifth assessment report (AR5) of IPCC (International Panel on Climate Change), the global mean surface temperature may increase between 0.3°C to 4.8°C for low (RCP 2.6) to high (RCP 8.5) emission scenarios from its baseline (1985-2005) by the end of 21st century (IPCC, 2014). At the same time, the high altitude and equilateral pacific are likely to experience an increase in annual mean precipitation under the RCP 8.5 scenario (IPCC, 2014) (Figure 2.8). Increase in global temperature and precipitation will significantly increase the monsoon flows of the GBM rivers.

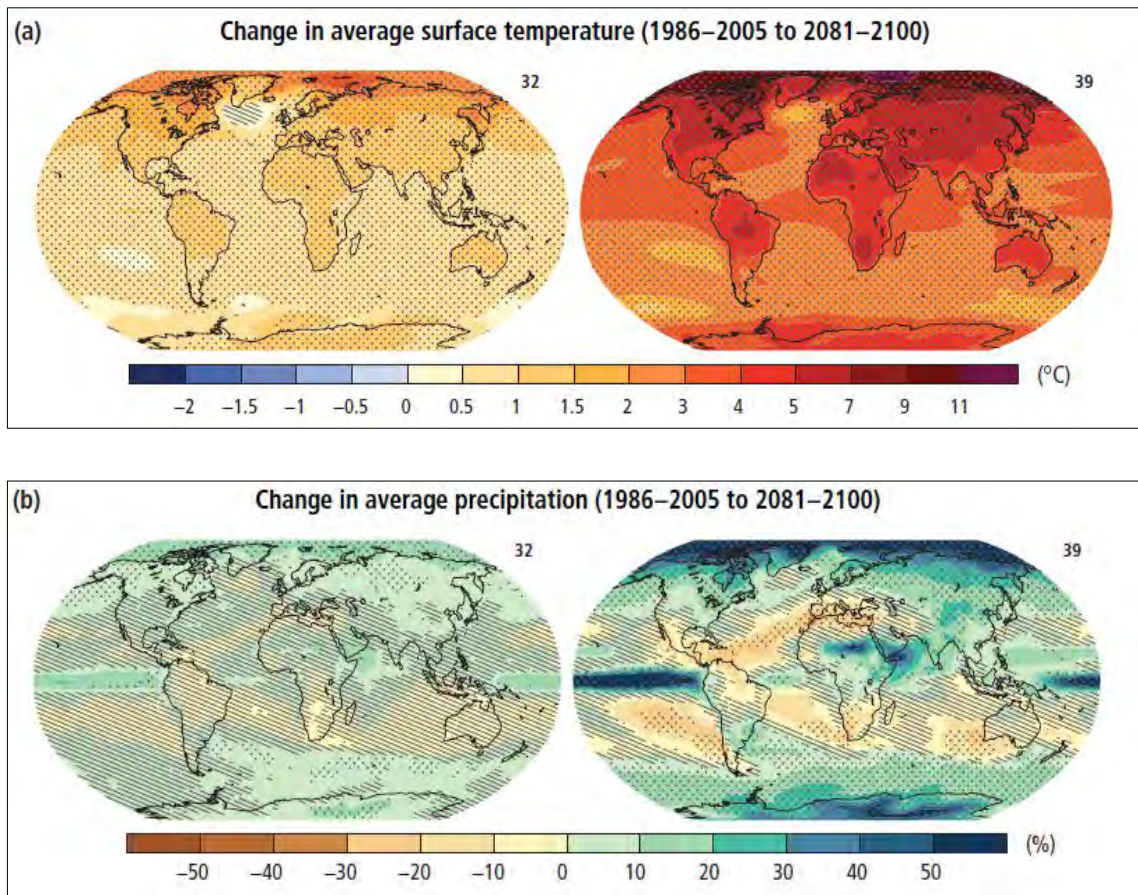


Figure 2.8: Changes in temperature and precipitation from the baseline by the end of the 21st Century for RCP 2.6 and RCP 8.5 (*source*: Stocker, et al., 2013)

The study of Masood, et al. (2015) estimated that by the end of 21st century, the entire GBM basin is projected to be warmed by ~ 4.3 °C and the changes of mean precipitation (runoff) are projected to be +16.3% (+16.2%), +19.8% (+33.1%), and +29.6% (+39.7%) in the Brahmaputra, Ganges, and Meghna, respectively.

Table 2.5: Mean GBM Flows m^3/s under 3 SSPs and 3 Climate Realisations (Whitehead, et al., 2015)

	Q0			Q8			Q16		
	BaU	MS	LS	BaU	MS	LS	BaU	MS	LS
1990s	31742.1	31742.1	31742.1	32327.0	32327.0	32327.0	29101.6	29101.6	29101.6
2050s	32695.4	32705.5	32187.1	31282.5	31290.1	30777.5	30771.0	30780.8	30263.9
2090s	32921.2	32926.6	32098.4	35317.5	35325.8	34491.7	33916.0	33922.0	33093.9

Whitehead, et al. (2015) projected the GBM flow using the SRES (Special Report on Emission Scenarios) scenarios of IPCC (Table 2.5). This study also shows an increase in the flow of GBM basins by the end of the 21st century.

The changes in extreme flows of the Ganges-Brahmaputra-Meghna river system under the RCP 8.5 scenario is recently modeled by Mohammed, et al. (2019) in SWAT (Soil and Water Assessment Tool). This study also finds that mean monthly flows and flood flows will significantly increase in the 2080s of the RCP 8.5 scenario. The Percentage of changes in mean flood flow in GBM basins at different time slices compared to the baseline period are shown in Table 2.6.

Table 2.6: Percentage changes in ensemble-mean of flood flows at different time slices compared to the baseline period (*Source*: Mohammed, et al., 2019)

Return Period (years)	Ganges			Brahmaputra			Meghna		
	2020s	2050s	2080s	2020s	2050s	2080s	2020s	2050s	2080s
2	12	19	33	11	12	22	10	23	33
5	13	22	37	13	13	25	14	28	40
10	13	24	39	14	15	28	16	32	45
20	14	25	41	15	16	32	17	36	49
50	14	27	44	16	20	36	19	41	54
100	14	28	46	16	24	40	21	45	58

All the studies mentioned above show that monsoon flows of the GBM rivers will increase manifolds by the end of the 21st century and all the flow will ultimately discharge into the Bay of Bengal through Bangladesh. So it's certain that Bangladesh will face more intense and frequent floods in the near future (Hasan & Islam, 2018; Fahad, et al., 2018). To cope with future flood situation and minimize potential flood losses & damages, it is necessary to plan a long-term sustainable flood mitigation strategy for the flood-prone rivers of Bangladesh considering future climate change impact.

2.6 Concepts of Hazard, Exposure, Vulnerability & Risk

2.6.1 General Concept of Vulnerability and Risk

The study of vulnerability and risk involves experts from a wide range of fields including climate science, development studies, disaster management, health, social science, policy development, economics, engineering etc. Researchers from respective fields bring their conceptual models to the study of vulnerability and risk addressing similar problems and processes using different languages. There are several terms associated with vulnerability and risk assessment, e.g., hazard, exposure, sensitivity, adaptive capacity, resilience, adaptation, adaptation baseline, coping range, vulnerability, risk etc. The same term appears to have different meanings when used in different contexts and by different authors from different fields of study (Adger, et al., 2002). Despite some divergence over the meaning of vulnerability, understanding vulnerability requires more than analyzing the direct impacts of a hazard, as agreed by most experts. Vulnerability also concerns the wider environmental and social conditions that limit people and communities to cope with the impact of a hazard (Birkmann, 2006). Therefore, it is very important to understand the concepts associated with vulnerability and risks to climate variability and the interaction of climatic factors with socio-economic factors and environmental system.

2.6.2 IPCC conceptualization of Vulnerability and Risk

The Intergovernmental Panel on Climate Change (IPCC) is an intergovernmental panel of the United Nations dedicated to providing scientific, technical and socio-economic information relevant to understanding the scientific basis of risk of human-induced climate change, its potential impacts and options for adaptation and mitigation. At present, it is considered as the most important guidelines or basis for any climate change studies. Many studies have been conducted based on the conceptual framework of vulnerability and risk given by the Intergovernmental Panel on Climate Change (IPCC) in its Third Assessment Report (TAR) and Fourth Assessment Reports (AR4) (Schneider, 2007). It defines vulnerability as a function of the character, magnitude, and rate of climate variation to which a system is exposed, its sensitivity, and its adaptive capacity (IPCC, 2001). According to the 4th assessment report of IPCC, Vulnerability (V) is defined as a consequences of Hazard (H), Exposure (E) and Adaptive Capacity (AC) as in Eqn. (2.1).

$$V = f(H, E, AC) \quad (2.1)$$

Recently, IPCC has introduced the new concept of risk in its Special Report Managing the Risks of Extreme Events and Disasters to Advance Climate Change Adaptation and in the Fifth Assessment Report (AR5) which includes hazard, exposure and vulnerability as shown in Figure 2.8 (Oppenheimer, et al., 2014; Cardona, et al., 2012).

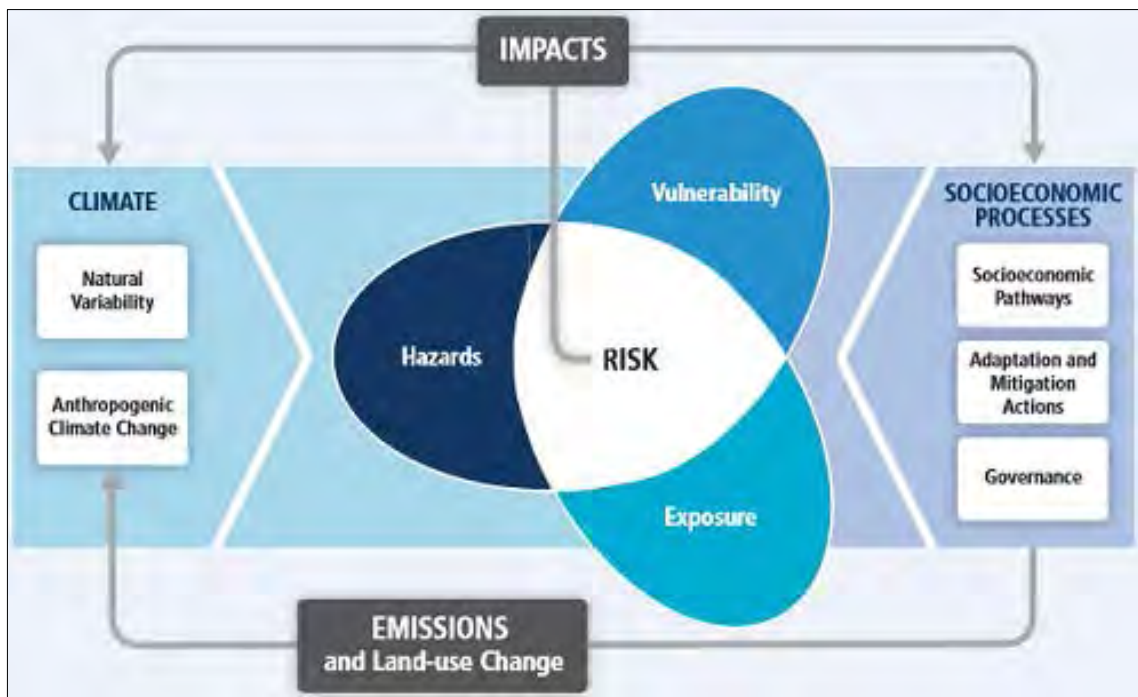


Figure 2.9: IPCC AR5 concept of risk (*source: IPCC, 2014*)

IPCC AR5 defines Risk as “the potential for consequences where something of value is at stake and where the outcome is uncertain, recognizing the diversity of values.” The risk is often represented as the probability of occurrence of hazardous events or trends multiplied by the impacts of these events or trends occur. Risk results from the interaction of vulnerability, exposure, and hazard” (Agard & Schipper, 2015).

It defines Hazard as the potential occurrence of a natural or human-induced physical event that may cause loss of life, injury, or other health impacts, as well as damage and loss to property, infrastructure, livelihoods, service provision, and environmental resources. It defines vulnerability as “the propensity or predisposition to be adversely affected.” Vulnerability encompasses a variety of concepts including sensitivity or susceptibility to harm and lack of capacity to cope and adapt” (Agard & Schipper, 2015).

On the other hand, exposure is defined as “the presence of people, livelihoods, species or ecosystems, environmental services and resources, infrastructure, or economic, social, or cultural assets in places that could be adversely affected” (Agard & Schipper, 2015). By this definition, exposure is often assessed using population and infrastructural objects’ location in a zone potentially affected by a natural hazard.

A key distinction made by IPCC in their Fifth Assessment Report of the IPCC (2014) from the earlier vulnerability assessment frameworks (e.g. as used in the IPCC Fourth Assessment Report), is that exposure is considered independently from vulnerability, recognizing that a community may be exposed to a climate-related hazard, but not vulnerable (for example, if there are sufficient resources to protect a community living on a floodplain). Hence, in the 5th assessment report of IPCC, climate risk (R) has been assessed as the consequence of the physical hazard (H), intersecting with vulnerable (V) and exposed people (E) as shown in Eqn. (2-2).

$$R = H * E * V \quad (2-2)$$

By IPCC AR5 definition, risks are considered “key” when societies and systems exposed are impacted by high hazard or characterized by high vulnerability, or both. In this study, the risk concept is framed by the integrative concept of climate risk, introduced by the IPCC (Intergovernmental Panel on Climate Change) in the Fifth Assessment Report of the IPCC (2014).

2.7 Previous Studies

2.7.1 Studies on Flood Hazard and Risk Assessment around the World

Worldwide many studies have been conducted so far on potential flood hazard and risk assessment. Some of them considered future climate change impact while others did not. Tu & Tingsanchali (2010) studied the flood hazard and risk assessment of the Hoang Long River basin of Vietnam. In this study, the design flow hydrograph for different return period is found from the rainfall-runoff model MIKE-NAM. Later these hydrographs are fed to hydrodynamic model MIKE 11 to simulate flood flow in Hoang Long Basin. The flood hazard map has been prepared considering two parameters – flood depth and duration. Finally, the risk map is prepared multiplying the hazard with population density as a vulnerability unit.

Later, the Event-Based Flood Inundation Mapping for Lower Kelani River Basin of Sri Lanka under A2 (high emission) and B2 (low emission) climate change scenarios of IPCC Special Report on Emissions Scenarios (SRES) has been assessed by Silva, et al. (2016). Hydrological model HEC-HMS has been used to generate future flood discharge under the mentioned climate change scenarios. Later, flood discharge and inundation along the Kelani River has been analyzed by the application of the two-dimensional flood simulation model (FLO-2D).

Recently, Shrestha & Lohpaisankrit (2016) studied the flood hazard assessment of Yang River Basin of Thailand for climate change scenarios of RCP 4.5 and RCP 8.5. They used a physically-based distributed hydrological model, Block-wise use of TOPMODEL and a hydraulic model, HEC-RAS to simulate the floods under future climate scenarios. The study result showed that both the minimum and maximum temperature of the basin would increase in the future. Similarly, average annual rainfall would also project to increase in the future, higher in the near future and lower in the far future. Not only that, the intensity of The intensity of annual floods is expected an increase for both RCP 4.5 and 8.5 scenarios. It is also found from this study that compared to the baseline period, an additional 60 km² area of the basin is projected to be flooded with the return period of 100 years.

2.7.2 Studies on Flood Hazard and Risk Assessment of Bangladesh

Though the world's research on hazard and risk assessment under different climate change scenarios are quite in an advanced stage, hazard assessment is still in an early stage in Bangladesh. Additionally, very few useful studies on comprehensive hazard mapping and flood risk assessment are found. A few relevant literatures about the hazard and risk assessment carried out in Bangladesh have been reviewed here.

Chowdhury & Karim (1997) developed risk-based zoning maps for Ganges tidal flood-prone area considering only cyclonic storm surge floods. In this study, the hazard factors were based on the simulated spatial distribution of 100-year flood depths while the vulnerability factors were based on the distribution of population densities. Finally, the land units are grouped into low risk, moderate risk, high risk, and severe risk zones.

Islam & Sado (2000) prepared hazard maps based on the 1988 flood. In this study, flood depth and flood-affected frequency were considered for the evaluation of flood hazard

assessment. The hazard parameters were estimated using NOAA satellite dataset while flood hazard rank assessment was undertaken on the basis of land cover classification, physiographic divisions, geological divisions, elevations intervals and administrative districts.

Masood & Takeuchi (2012) studied flood hazard and risk assessment in the mid-eastern part of Dhaka. DEM data were collected from Shuttle Radar Topography Mission (SRTM) and the observed flood data for 32 years (1972-2004) were used. The inundation simulation has been conducted using the HEC-RAS program for the 100-year flood. Risk index has been calculated by multiplying vulnerability and hazard index. The average depth of inundation has been assigned as a hazard index. Moreover, for calculating vulnerability index, the percentage of area covered with house/living place and agricultural land have been considered. The study result showed that though the western built-up area is densely populated, there is no inundation in this area, so it is entirely risk-free. On the other hand, a southern area where inundation depth is maximum falls in the medium risk category due to its low population with high agricultural land.

Hossain (2013) studied the flood damage and risk assessment model in the haor basin of Bangladesh. The primary objective of this study was to assess flood damage and risk of agricultural Boro crop due to pre-monsoon flash flood. The inundation information has been extracted from a 2D hydrodynamic flood model (MIKE 21) for 2year, 10year, 20year and 100year recurrence intervals. Then, the flood hazard map has been developed considering two combinations of hazard parameter. In the first combination, flood depth and flooding duration were considered whereas, in the second combination, flood depth and flood velocity were considered. The assessment of the agricultural Boro crop loss is estimated by developing a crop damage assessment model for the Haor basin. Finally, for risk assessment, risks of 2Year, 10Year, 20Year and 100Year return period flood events are calculated by developing a risk model.

2.7.3 Studies on Arial Khan River

Though a few studies on hazard and risk analysis have done, no studies on the flood hazard and risk mapping of Arial Khan River. Tingsanchali & Karim (2005) studied the flood hazard and risk analysis in the southwest region of Bangladesh, where the floodplains of the Arial Khan River were also included. However, the main focus was the

flood inundation of the whole southwest river system. Moreover, the primary objective of this study was to develop flood hazard and risk maps for a flood with a return period of 100 years. No specific climate change scenario was considered.

Additionally, the flooding depth was estimated from a commercial hydrodynamic model MIKE 11. Later, flood vulnerability is assessed on the basis of only one vulnerability indicator – population density. Other important vulnerability indicators such as poverty rate, agriculture land, crop productivity are not considered. Finally, the risk is calculated multiplying hazard with vulnerability. Except for this study, no hazard or risk assessment studies is found for Arial Khan River flood plain.

Few studies are done on the morphological process and instability problems of Arial Khan River (Akter, et al., 2013; Winkley, et al., 1994; Mamun, 2008). However, flood inundation of Arial Khan River has not been studied yet, let alone its hazard and risk assessment due to climate change scenarios. Hence, the flood hazard and risk assessment of Arial Khan river considering new concepts of climate change scenarios along with different exposure and vulnerability indices are very required. That's why, this study is designed for the fluvial flood hazard and risk assessment of Arial Khan River and its floodplain for predicted climate change scenarios using an open source numerical model.

2.7.4 Application of HEC-RAS in Floodplain Inundation Modelling

There many numerical models both commercial and open source available for flood inundation assessment. Among the commercial models, MIKE 11 is a reliable one. Delft3D, HEC-RAS, River2D are the name of some open source software. However, HEC-RAS is very notable in flood inundation mapping due to its accuracy in river analysis and recently launched a feature of 1D-2D coupling capacity (HEC-RAS, 2016).

Previously, HEC-RAS 1D and HEC-GeoRAS were being used widely to develop flood inundation map in many studies (Knebl, et al., 2005; Hicks & Peacock, 2005; Yang, et al., 2006; Abera, 2011; Rouf, 2015). The accuracy of the flood inundation map depends on the water surface elevation. In GIS tools providing water surface elevation is difficult and we have to consider additional construction in the 1D model to separate the river from the floodplain. So, both the GIS and HEC-RAS 1D model may not be adequate to represent the actual conditions.

Besides, 1D modeling approaches could be useful in some contexts, mainly for artificial channels or simple reaches but it presents several limitations for overflow analysis (Srinivas, et al., 2009). When water begins to overflow, it becomes a 2D phenomenon. Hence, the automatic floodplain mapping and analysis using HEC-RAS 2D provides more efficient, effective and standard results and saves time and resources. At the same time, this requires very high-resolution bathymetry data for the river as well (Nishat, 2017). However, fine resolution bathymetry data is not available for most of the rivers of Bangladesh. Hence, the 1D-2D coupling is more appropriate for the flooding for the rivers of Bangladesh.

The main advantage of 1D-2D coupled models is the similarity between model behavior and physical behavior (Moore, 2011). For Koiliaris River, China, the combined 1D-2D HEC- RAS model performed better than the 1D HEC- RAS model for a specific study reach by using topographic data at a high spatial resolution (Patel, et al., 2017).

Some studies are done the flood inundation mapping using the 1D-2D coupling model in Bangladesh as well. Anik & Khan (2016) studied the flood inundation of the Jamuna River using HEC-RAS 1D-2D coupling. Das, et al. (2018) studied the flood inundation mapping on Surma-Kusiyara floodplain using the HEC-RAS 1D-2D coupled model. Very recently, Tazin (2018) studied flood hazard mapping of Dharala floodplain using the HEC-RAS 1D-2D coupled model incorporating agricultural land use pattern.

2.8 Summary

From the above literature reviews, it can be summarized that though the world's research on hazard and risk assessment under different climate change scenarios are quite in an advanced stage, hazard assessment is still in an early stage in Bangladesh. A few studies on hazard and risk analysis have done, but flood inundation of Arial Khan River has not been studied yet, let alone its hazard and risk assessment due to climate change scenarios. Hence, the flood hazard and risk assessment of Arial Khan river considering new concepts of climate change scenarios along with different exposure and vulnerability indices are very necessary. That's why, this study is designed for the fluvial flood hazard and risk assessment of Arial Khan River and its floodplain under climate change impact. In this study, the RCP scenarios of IPCC –AR5 will be used both for low (RCP 2.6) to high (RCP 8.5) emission scenarios along with its new risk framework. Besides, some

important indicators, for example, population, households, cropped land, disable population, dependent population ratio, communication infrastructure, crop productivity, poverty rate, literacy rate, flood center, etc. will be incorporated too.

Among many numerical hydrodynamic models, open source HEC-RAS has been chosen to carry out this study. Because the performance of HEC-RAS 1D is quite acceptable for one-dimensional simulation of artificial channels or simple reaches. On the other hand, the HEC-RAS 1D-2D coupled model is highly recommended for flood inundation modeling which includes floodplains as 2D part and river as 1D part. Hence, in this study, for generation of future flood hydrograph incorporating the discharge outputs of the hydrological model, a 1D model of Ganges-Brahmaputra-Padma River has been prepared. On the other hand, for flood hazard assessment of Arial Khan River Floodplain, HEC-RAS 1D-2D coupled model is used.

CHAPTER 3

SALIENT FEATURES OF THE MODELS

3.1 General

Several numbers of commercial and non-commercial software tools available for numerical modeling and analysis. The major tools used in this study are one and two-dimensional numerical model HEC-RAS 5.0.3 beta version and Arc GIS for spatial data processing and HEC-GeoRAS for interfacing between HEC-RAS and Arc GIS. HEC-RAS and HEC-GeoRAS, an open source model which have excellent Graphical User Interfaces (GUI), were developed by the US Army Corps of Engineers. Arc GIS was developed Environmental Systems Research Institute (ESRI) which enables to view, edit, create and analyze geospatial data. Descriptions of these software tools are presented below.

3.2 HEC-RAS

HEC-RAS is a computer program that models the hydraulics of water flow through natural rivers and other channels. The program was developed by the US Department of Defense, Army Corps of Engineers in order to manage the rivers, harbors and other public works under their jurisdiction. It has found wide acceptance by many others since its public release in 1995. Before the recent update to Version 5.0, the program was one-dimensional, meaning that there is no direct modeling of the hydraulic effect of cross-section shape changes, bends, and other two- and three-dimensional aspects of flow. The release of version 5.0 introduced two-dimensional modeling of flow as well as sediment transfer modeling capabilities. Besides, it is also capable of performing one and two-dimensional hydraulic calculations for a full network of natural and constructed channels.

3.2.1 Theoretical Basis for Hydrodynamic Calculation in HEC-RAS

Theoretical Basis for One Dimensional Hydrodynamic Calculation

1D Steady Flow Water Surface Elevation

HEC-RAS is currently capable of performing 1D water Surface profile calculations for steady gradually varied flow in natural or constructed channels, subcritical, supercritical and mixed flow regime water surface profiles can be calculated. Topics discussed in this

section include equations for basic profile calculations and applications of the momentum equation.

Equations for Basic Profile Calculations

Water surface profiles are computed from one cross-section to the next by solving the Energy equation with an iterative procedure called the standard step method. From Figure 3.1, the Energy the equation is written as follows (HEC-RAS, 2016):

$$Z_2 + Y_2 + \frac{\alpha_2 V_2^2}{2g} = Z_1 + Y_1 + \frac{\alpha_1 V_1^2}{2g} + h_e \quad (3-1)$$

Where,

Z_1, Z_2 = elevation of the main channel inverts

Y_1, Y_2 = depth of water at cross sections

V_1, V_2 = average velocities (total discharge/ total flow area)

α_1, α_2 = velocity weighting coefficients

g = gravitational acceleration

h_e = energy head loss

A diagram showing the terms of the energy equation is shown in Figure 3-1.

The energy head loss (h_e) is expressed as

$$h_e = L\bar{S}_f + C \left| \frac{\alpha_2 V_2^2}{2g} - \frac{\alpha_1 V_1^2}{2g} \right| \quad (3-2)$$

Where,

L = discharge-weighted reach length

\bar{S}_f = representative friction slope between two sections

C = expansion or contraction loss coefficient

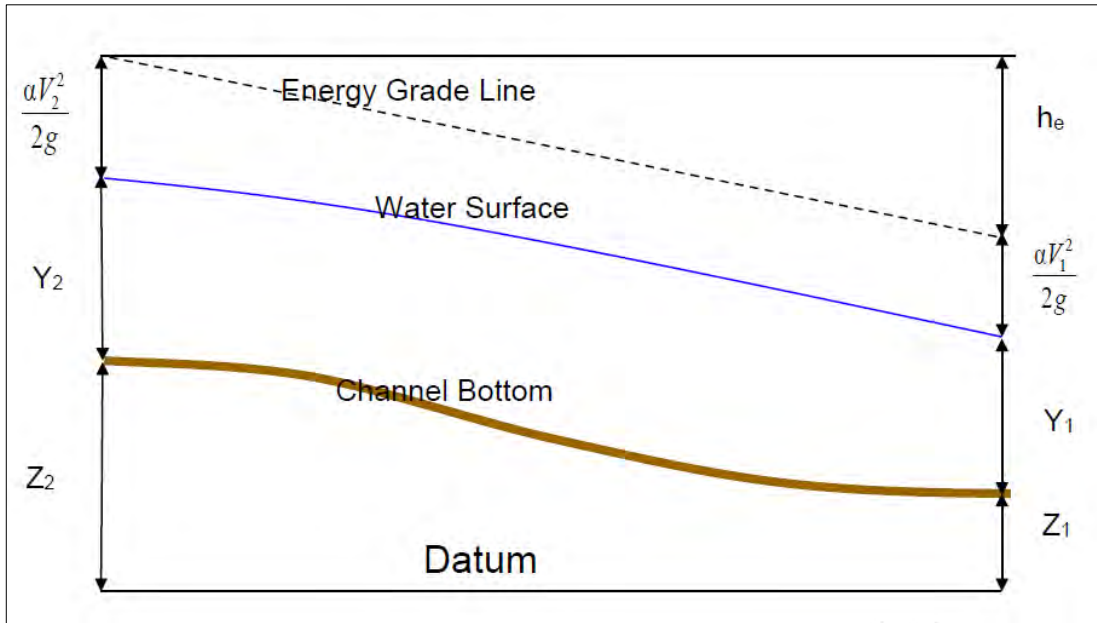


Figure 3.1 Representation of terms in the energy equation

The distance weighted reach length, L , is calculated as:

$$L = \frac{L_{lob}Q_{lob} + L_{ch}Q_{ch} + L_{rob}Q_{rob}}{Q_{lob} + Q_{ch} + Q_{rob}} \quad (3-3)$$

Where,

$L_{lob}L_{ch}L_{rob}$ = x-section reach length specified for flow in the left overbank, main channel and right overbank respectively

$Q_{lob} + Q_{ch} + Q_{rob}$ = arithmetic average of the flows between sections for the left overbank, main channel and right overbank respectively

Application of Momentum Equation

Whenever the water surface passes through critical depth, the energy equation is not considered to be applicable. The energy equation is only applicable to gradually varied flow situations and the transition from subcritical to supercritical or supercritical to subcritical is a rapidly varying flow situation. There are several instances when the transition from subcritical to supercritical and supercritical to subcritical flow can occur. These include significant changes in channel slope, bridge constrictions, drop structures and weirs and stream junctions. In some of these instances, empirical equations can be used (such as at drop structures and weirs), while at others it is necessary to apply the

momentum equation in order to obtain an answer. The momentum equation is derived from Newton's second law of motion:

$$\sum F_x = ma \quad (3-4)$$

Force = Mass x Acceleration (change in momentum)

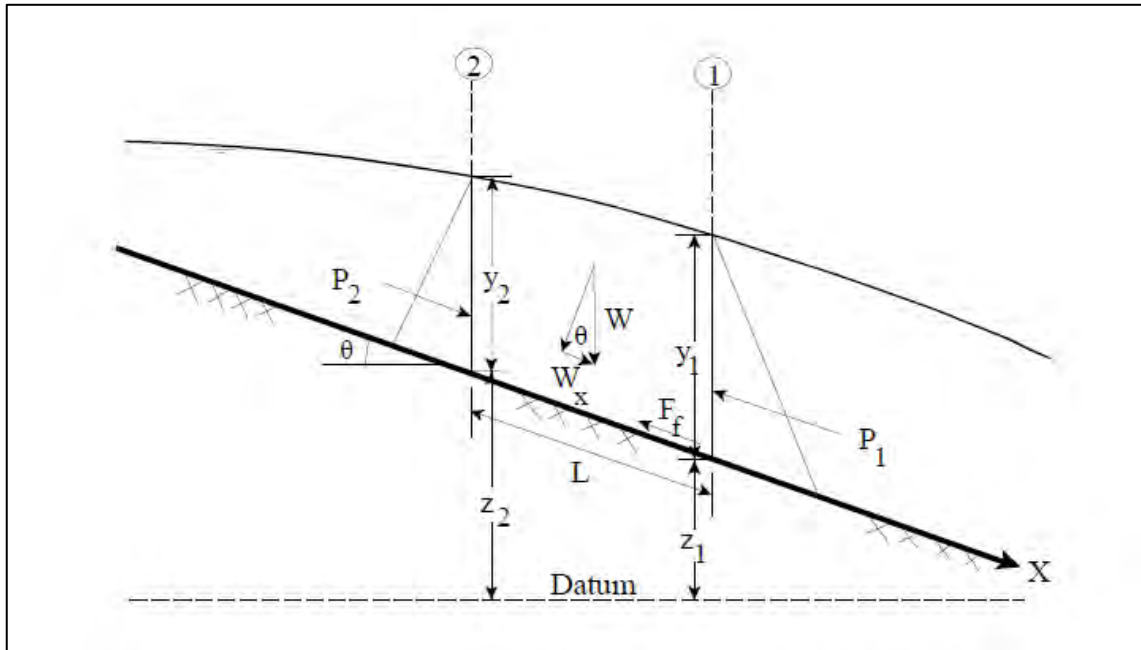


Figure 3.2 Application of the momentum principle

Applying Newton's second law of motion to a body of water enclosed by two cross sections at location 1 and 2 (Figure 3.2), the following expression for the change in momentum over a unit time can be written:

$$P_2 - P_1 + W_x - F_f = Q\rho\Delta V_x \quad (3-5)$$

Where,

P = Hydrostatic pressure force at location 1 and 2

W_x = Force due to the weight of water in the X direction

F_f = Force due to external friction losses from 2 and 1

Q = discharge

ρ = Density of Water

ΔV_x = Change on velocity from 2 to 1, in the X direction.

Hydrostatic Pressure Force:

The force in the X direction due to hydrostatic pressure is:

$$P = \gamma A \bar{Y} \cos \theta \quad (3-6)$$

The assumption of hydrostatic pressure distribution is only valid for slopes less than 1:10. The $\cos \theta$ for a slope of 1:10 (approximately 6 degrees) is equal to 0.995. Because the slope of ordinary channels is far less than 1:10, the $\cos \theta$ correction for depth can be set equal to 1.0. Therefore, the equations for the hydrostatic pressure force at section 1 and 2 are as follows:

$$P_1 = \gamma A_1 \bar{Y}_1 \quad (3-7)$$

$$P_2 = \gamma A_2 \bar{Y}_2 \quad (3-8)$$

Where,

γ = unit weight of water

A_i = wetted area of the cross section at location 1 and 2

\bar{Y}_i = depth measured from water surface to the centroid of the cross sectional area at location 1 and 2.

The Weight of Water Force:

Weight of water = (unit weight of water) x (volume of water)

$$W = \gamma \left(\frac{A_1 + A_2}{2} \right) L \quad (3-9)$$

$$W_x = W \times \sin \theta \quad (3-10)$$

$$\sin \theta = \frac{z_2 - z_1}{L} = S_0 \quad (3-11)$$

$$W_x = \gamma \left(\frac{A_1 + A_2}{2} \right) L S_0 \quad (3-12)$$

Where,

L = Distance between sections 1 and 2 along the X axis

S_0 = Slope of the channel, based on mean bed elevations

z_i = Mean bed elevation at locations 1 and 2

Force to External Friction:

$$F_f = \tau \bar{P} L \quad (3-13)$$

Where,

τ = Shear Stress

\bar{P} = Average wetted perimeter between section 1 and 2

$$\tau = \gamma \bar{R} \bar{S}_f \quad (3-14)$$

Where,

\bar{R} = Average Hydraulic Radius ($R=A/P$)

\bar{S}_f = Slope of the energy grade line (friction slope)

$$F_f = \tau \frac{\bar{A}}{\bar{P}} S_f L \quad (3-15)$$

$$F_f = \gamma \left(\frac{A_1 + A_2}{2} \right) \bar{S}_f L \quad (3-16)$$

Mass time acceleration :

$$ma = Q \rho \Delta V_x \quad (3-17)$$

$$\rho = \frac{\gamma}{g} \text{ and } \Delta V_x = (\beta_1 V_1 - \beta_2 V_2)$$

$$ma = \frac{Q\gamma}{g} (\beta_1 V_1 - \beta_2 V_2) \quad (3-18)$$

Where, B = momentum coefficient that accounts for a varying velocity distribution in irregular channels

Substituting back into equation 3-4 and assuming Q can vary from 2 to 1

$$\gamma A_2 \bar{Y}_2 - \gamma A_1 \bar{Y}_1 + \gamma \left(\frac{A_1 + A_2}{2} \right) L S_0 - \gamma \left(\frac{A_1 + A_2}{2} \right) L \bar{S}_f = \frac{Q_1 \gamma}{g} \beta_1 V_1 - \frac{Q_2 \gamma}{g} \beta_2 V_2 \quad (3-19)$$

$$\frac{Q_2 \beta_2 V_2}{g} + A_2 Y_2 + \left(\frac{A_1 + A_2}{2} \right) L S_0 - \gamma \left(\frac{A_1 + A_2}{2} \right) L \bar{S}_f = \frac{Q_1 \beta_1 V_1}{g} + A_1 \bar{Y}_1 \quad (3-20)$$

$$\frac{Q_2^2 \beta_2}{g A_2} + A_2 \bar{Y}_2 + \left(\frac{A_1 + A_2}{2} \right) L S_0 - \gamma \left(\frac{A_1 + A_2}{2} \right) L \bar{S}_f = \frac{Q_1^2 \beta_1}{g A_1} + A_1 \bar{Y}_1 \quad (3-21)$$

This is the functional form of the momentum equation that is used in HEC-RAS. All applications of the momentum equation within HEC-RAS are derived from this equation.

Theoretical Basis for One - Two Dimensional Hydrodynamic Calculation

This study is focused on the development of 1D-2D coupled hydrodynamic modeling for the Arial Khan River floodplain through HEC-RAS 5.0.3 published by USACE. The equations for 1D-2D coupled modeling have been stated in (Patel, et al., 2017). The HEC-RAS 5.0.3 is fully solved using the 2D Saint-Venant equation (Brunner, 2016; Brunner, 2016b; HEC-RAS, 2016; Quiroga, et al., 2016):

$$\frac{\delta \zeta}{\delta t} + \frac{\delta \rho}{\delta t} + \frac{\delta q}{\delta t} = 0 \quad (3-22)$$

$$\frac{\delta \rho}{\delta t} + \frac{\delta}{\delta x} \left(\frac{p^2}{h} \right) + \frac{\delta}{\delta x} \left(\frac{pq}{h} \right) = - \frac{n^2 p g \sqrt{p^2 + q^2}}{h^2} - g h \frac{\delta \xi}{\delta x} + p f + \frac{\delta}{p \delta x} (h \tau_{xx}) + \frac{\delta}{p \delta y} (h \tau_{xy}) \quad (3-23)$$

$$\frac{\delta q}{\delta t} + \frac{\delta}{\delta y} \left(\frac{q^2}{h} \right) + \frac{\delta}{\delta y} \left(\frac{pq}{h} \right) = - \frac{n^2 q g \sqrt{p^2 + q^2}}{h^2} - g h \frac{\delta \xi}{\delta y} + q f + \frac{\delta}{p \delta y} (h \tau_{yy}) + \frac{\delta}{p \delta x} (h \tau_{xy}) \quad (3-24)$$

Where, h is the water depth (m), p and q are the specific flow in the x and y-direction ($m^2 s^{-1}$), ξ is the surface elevation (m), g is the acceleration due to gravity (ms^{-2}), n is the

Manning resistance, ρ is the water density ($kg m^{-3}$), τ_{xx} , τ_{yy} and τ_{xy} are the components of the effective shear stress and f is the Coriolis (s^{-1}) (Quiroga, et al., 2016).

3.2.2 Capabilities of HEC-RAS

The following is a description of the major capabilities of HEC-RAS.

- User Interface
- Hydraulic Analysis Components
- Data Storage and Management
- Graphics and Reporting

- RAS Mapper

User Interface

The user interacts with HEC-RAS through a graphical user interface (GUI). The main focus in the design of the interface was to make it easy to use the software, while still maintaining a high level of efficiency for the user. The interface provides for the following functions:

- File Management
- Data Entry and Editing
- Hydraulic Analyses
- Tabulation and Graphical Displays of Input and Output Data
- Inundation mapping and animations of water propagation
- Reporting Facilities
- Context Sensitive Help

Hydraulic Analysis Components

The HEC-RAS system contains several river analysis components for (i) Steady flow water surface profile computations; (ii) one – and two- dimensional unsteady flow simulation; (iii) movable boundary sediment transport computations; and (iv) water quality analysis. A key element is that all four components use a common geometry data representation and common hydraulic computation routines. In addition to these river analysis components, the system contains several hydraulic design features that can be addressed once the basis water surface profiles are computed.

Steady Flow Water Surface Profile

This component of the modeling system is intended for calculating water surface profiles for steady gradually varied flow. The system can handle a full network of channels, a dendritic system or a single river reach. The steady flow component is capable of modeling subcritical, supercritical, and mixed flow regimes water surface profiles. The basic computational procedure is based on the solution of the one-dimensional energy equation. Energy losses are evaluated by friction (Manning's equation) and contraction/expansion (coefficient multiplied by the change in velocity head). The momentum equation may be used in situations where the water surface profile is rapidly

varied. These situations include mixed flow regime calculations (i.e., hydraulic jumps), hydraulics of bridges and evaluating profiles at river confluences (stream junctions).

One and Two Dimensional Unsteady Flow Simulation

This component of the HEC-RAS modeling system is capable of simulating one – dimensional; two-dimensional and combined unsteady flow through a full network of open channels, floodplains and alluvial fans. The unsteady flow component can be used to performed subcritical, supercritical, and mixed flow regime (subcritical, supercritical, hydraulic jumps and drawdowns) calculations in the unsteady flow computations module.

The hydraulic calculations for cross-sections, bridges, culverts and other hydraulic structures that were developed for the steady flow component were incorporated into the unsteady flow module.

Special features of the unsteady flow component include: extensive hydraulic structure capabilities Dam break analysis; levee breaching and overtopping; Pumping stations; navigation dam operations; pressurized pipe systems; automated calibration features; User-defined rules; and combined one and two-dimensional unsteady flow modeling.

Sediment Transport/ Movable Boundary Computations

This component of the modeling system is intended for the simulation of one-dimensional sediment transport/movable boundary calculations resulting from scouring and deposition over moderate periods (typically years, although applications to single flood events are possible).

The sediment transport potential is computed by grain size fraction, thereby allowing the simulation of hydraulic sorting and armouring. Major features include the ability to model a full network of streams, channel dredging, various levee and encroachment alternatives, and the use of several different equations for the computation of sediment transport. The model is designed to simulate long-term trends of scour and deposition in a stream channel that might result from modifying the frequency and duration of the water discharge and stage, or modifying the channel geometry. This system can be used to evaluate deposition in reservoirs, design channel contractions required to maintain navigation depths, predict the influence of dredging on the rate of deposition, estimate maximum possible scour during large flood events and evaluate sedimentation in fixed channels.

Water Quality Analysis

This component of the modeling system is intended to allow the user to perform riverine water quality analyses. An advection-dispersion module is included with this version of HEC-RAS, adding the capability to model water temperature. This new module uses the QUICKEST-ULTIMATE explicit numerical scheme to solve the one-dimensional advection-dispersion equation using a control volume approach with a fully implemented heat energy budget. Transport and Fate of a limited set of water quality constituents are now also available in HEC-RAS. The currently available water quality constituents are Dissolved Nitrogen (NO₃-N, NO₂-N, NH₄-N, and Org-N); Dissolved Phosphorus (PO₄-P and Org-P); Algae; Dissolved Oxygen (DO) and Carbonaceous Biological Oxygen Demand (CBOD).

Data Storage and Management

Data storage is accomplished through the use of "flat" files (ASCII and binary), the HEC-DSS (Data Storage System), and HDF5 (Hierarchical Data Format, Version 5). User input data are stored in flat files under separate categories of project, plan, geometry, steady flow, unsteady flow, quasi-steady flow, sediment data, and water quality information. Output data is predominantly stored in separate binary files (HEC and HDF5). Data can be transferred between HEC-RAS and other programs by utilizing the HEC-DSS.

Data management is accomplished through the user interface. The user is requested to enter a single filename for the project being developed. Once the project filename is entered, all other files are automatically created and named by the interface as needed. The interface provides for renaming, moving and deletion of files on a project-by-project basis.

Graphics and Reporting

Graphics include X-Y plots of the river system schematic, cross-sections, profiles, rating curves, hydrographs and inundation mapping. A three-dimensional plot of multiple cross-sections is also provided. Inundation mapping is accomplished in the HEC-RAS Mapper portion of the software. Inundation maps can also be animated, and contain multiple background layers (terrain, aerial photography, etc.). Tabular output is available. Users can select from pre-defined tables or develop their own customized tables. All graphical

and tabular output can be displayed on the screen, sent directly to a printer (or plotter), or passed through the Windows Clipboard to other software, such as a word-processor or spreadsheet. Reporting facilities allow for printed output of input data as well as output data. Reports can be customized as to the amount and type of information desired.

RAS-Mapper

HEC-RAS can perform inundation mapping of water surface profile results directly from HEC-RAS. Using the HEC-RAS geometry and computed water surface profiles, inundation depth and floodplain boundary datasets are created through the RAS Mapper. Additional geospatial data can be generated for analysis of velocity, shear stress, stream power, ice thickness and floodway encroachment data. In order to use the RAS Mapper for analysis, it is necessary to have a terrain model in the binary raster floating-point format (.flt). The resultant depth grid is stored in the .flt format while the boundary dataset is stored in ESRI's Shapefile format for use with geospatial software.

3.3 ArcGIS

GIS is defined as computer systems capable of assembling, storing, manipulating, and displaying geographically referenced information (USGS, 1998). Originally developed as a tool for cartographers, GIS has recently gained widespread use in engineering design and analysis, especially in the fields of water quality, hydrology, and hydraulics. GIS provides a setting in which to overlay data layers and perform spatial queries, and thus create new spatial data.

The results can be digitally mapped and tabulated, facilitating efficient analysis and decision-making. Structurally, GIS consists of a computer environment that joins graphical elements (points, lines, polygons) with associated tabular attribute descriptions.

This characteristic sets GIS apart from both computer-aided design software (geographic representation) and databases (tabular descriptive data). For example, in a GIS view of a river network, the graphical elements represent the location and shape of the rivers, whereas the attributes might describe the stream name, length, and flow rate. This one-to-one relationship between each feature and its associated attributes makes the GIS environment unique. In order to provide a conceptual framework, it is necessary first to define some basic GIS constructs.

3.3.1 Data Model

Geographic elements in a GIS are typically described by two data models: vector and raster. Each of these is described below:

Vector

Vector objects include three types of elements: points, lines, and polygons. A point is defined by a single set of Cartesian coordinates [easting (x), northing (y)]. A line is defined by a string of points in which the beginning and end points are called nodes, and intermediate points are called vertices (Smith, 1995). A straight line consists of two nodes and no vertices whereas a curved line consists of two nodes and a varying number of vertices. Three or more lines that connect to form an enclosed area define a polygon. Vector feature representation is typically used for linear feature modeling (roads, lakes, etc.), cartographic base maps and time-varying process modeling.

Triangular Irregular Network (TIN)

A TIN is a vector-based representation of the physical land surface or sea bottom, made up of irregularly distributed nodes and lines with three-dimensional coordinates (x, y, and z) that are arranged in a network of non-overlapping triangles.

A TIN is used to represent the terrain of the digital elevation model (DEM), which can be further used to produce digital surface models (DSM) or digital terrain models (DTM). An advantage of using a TIN over a rasterized digital elevation model (DEM) in mapping and analysis is that the points of a TIN are distributed variably based on an algorithm that determines which points are most necessary to create an accurate representation of the terrain. Data input is therefore flexible and fewer points need to be stored than in a raster DEM, with regularly distributed points. While a TIN may be considered less suited than a raster DEM for certain kinds of GIS applications, such as analysis of a surface's slope and aspect, it is often used in CAD to create contour lines.

Raster

The raster data structure consists of a rectangular mesh of points joined with lines, creating a grid of uniformly sized square cells. Each cell is assigned a numerical value that defines the condition of any desired spatially varied quantity (Smith, 1995). Grids are the basis of analysis in raster GIS and are typically used for steady-state spatial

modeling and two-dimensional surface representation. A land surface representation in the raster domain is called a digital elevation model (DEM).

3.4 HEC-GeoRAS

HEC-GeoRAS is an ArcGIS extension specifically designed to process geospatial data for use with the HEC-RAS. The extension allows users to create an HEC-RAS import sample containing geometric attribute data from an existing digital terrain model (DTM) and complementary data sets. Water surface profile results may also be processed to visualize inundation depths and boundaries. HEC-GeoRAS extension for ArcGIS used an interface method to provide a direct link to transfer information between the ArcGIS and the HEC-RAS. Several requirements and tools of HEC-GeoRAS are described below: (HEC-GeoRAS, 2009)

3.4.1 Software Requirements

HEC-GeoRAS 10.2 is an extension used for ArcGIS 10.3. Both the 3D Analyst extension and the Spatial Analyst extension are required. The full functionality of HEC-GeoRAS 10.3 requires HEC-RAS 5.0 beta, or later, to import and export all of the GIS data options. Older versions of HEC-RAS may be used, however, with limitations on importing roughness coefficients, ineffective flow data, blocked obstructions, levee data, hydraulic structures, and storage area data. Further, data exported from older versions of HEC-RAS should be converted to the latest XML file structure using the SDF to XML conversion tools provided.

3.4.2 Data Requirements

HEC-GeoRAS requires a DTM in the form of a TIN or a GRID. The DTM must be a continuous surface that includes the bottom of the river channel and the floodplain to be modeled. Because all cross-sectional data will be extracted from the DTM, only high-resolution DTMs that accurately represent the ground surface should be considered for hydraulic modeling.

3.4.3 HEC-GeoRAS Menus

The HEC-GeoRAS menu options are RAS Geometry, RAS Mapping, ApUtilities, and Help. These menus are discussed below.

RAS Geometry

The RAS Geometry menu is for pre-processing geometric data for import into HEC-RAS. Items are listed in the RAS Geometry dropdown menu in the recommended (and sometimes required) order of completion. Items available in the RAS Geometry menu items are Create RAS Layers, Layer Set up, Stream Centerline Attributes, XS cutlines Attributes, Manning's n values, Export RAS Data, Terrain Tiles, Utilities, etc. This menu is also capable of incorporating Manning's n values, Levees, Ineffective flow areas, blocked obstructions, bridges/culverts, inline structures, Lateral Structures, Storage areas, storage area connections.

RAS Mapping

The RAS Mapping menu is for post-processing exported HEC-RAS results. Items available from the RAS Mapping dropdown menu are layer setup, import RAS data, inundation mapping, velocity mapping, Ice mapping, shear stress mapping, stream power mapping, visualization, post-processing utilities.

ApUtilities

Features available from the ApUtilities menu are used behind the scenes to manage the data layers created through GeoRAS. Also available from the ApUtilities menu is functionality to assign a unique HydroID to features. Only experienced users should use the items on the ApUtilities menu.

Help

The Help menu will provide general online help information. This version is consistent with the ArcGIS product with which it is being used.

HEC-GeoRAS Tools

There are several tools such as assign river and reach code, station code, assign flow path XS cutlines, etc. are provided in the toolbar. A tool waits for user action after being activated and will either invoke a dialog or change the mouse pointer, indicating the need for further action.

CHAPTER 4

METHODOLOGY

4.1 General

The primary objective of this study is to prepare flood hazard and risk maps for Arial Khan River floodplain under future climate change impact. For this purpose, the future flow hydrographs are collected from SWAT simulation. Later, an HEC-RAS 1D model and a linear regression analysis are performed to generate future flow hydrographs at the Offtake of Arial Khan for RCP 2.6 and RCP 8.5. Finally, a 1D-2D coupled model of Arial Khan River is set up to generate the flood hazard maps of the study area. The risk maps are prepared multiplying the hazard index with vulnerability and exposure indices as the new integrated risk framework of IPCC. Figure 4.1 shows the flow chart of the steps of the methodology to achieve the objectives of the study.

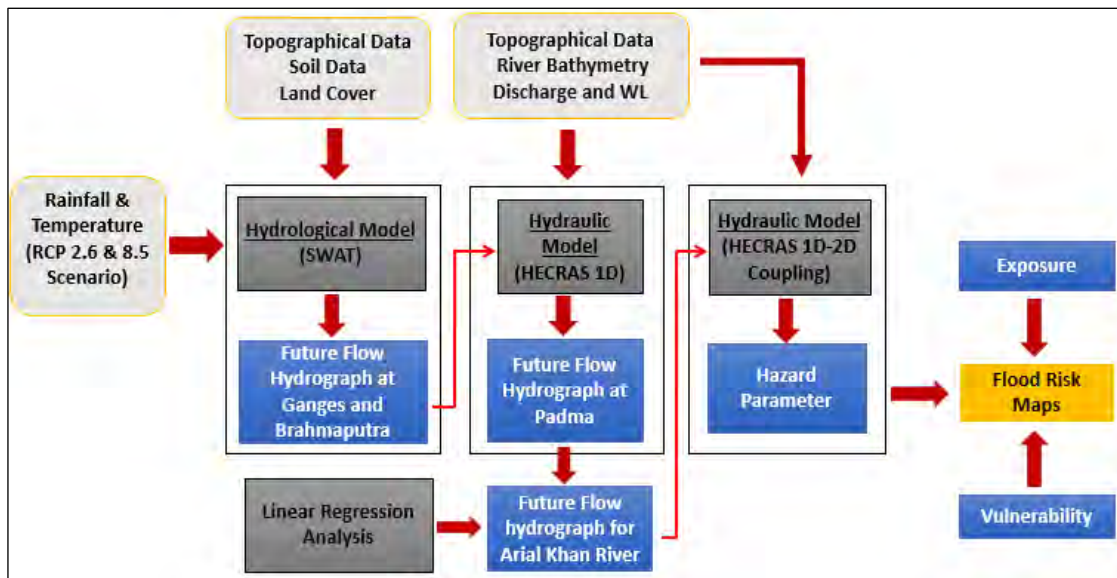


Figure 4.1: Summary of steps of methodology in the flow chart

4.2 Study Area

Arial Khan River is one of the major rivers of the south-west region of Bangladesh. Bifurcating from the Padma at 51.5-km southeast of Goalundo in Rajbari district, the river flows through Faridpur and Madaripur districts before falling into the Tentulia at the north-eastern corner of Barisal (BWDB, 2011). Madaripur and Shariatpur stand on the right and left bank of the Arial Khan. In this study, the upper reach of Arial Khan River and its adjacent floodplains have been proposed as the study area due to its existing

problems with monsoon flood inundation as shown in Figure 4.2 (Tingsanchali & Karim, 2005).

Arial Khan River is a meandering river and erosional in nature. The total length of this river is 160 km with an average bed slope of 0.00003 (BWDB, 2011). The selected reach length considered in this study is nearly 70 km. The floodplains of this portion of Arial Khan River is extended over eight upazilas – Bhanga, Sadarpur, Maksudpur, Madaripur, Shibchar, Rajoir, Janjira and Shariatpur of Faridpur, Gopalganj, Madaripur and Shariatpur districts. The total study area is nearly 1825 km². There is no polder in this study area.

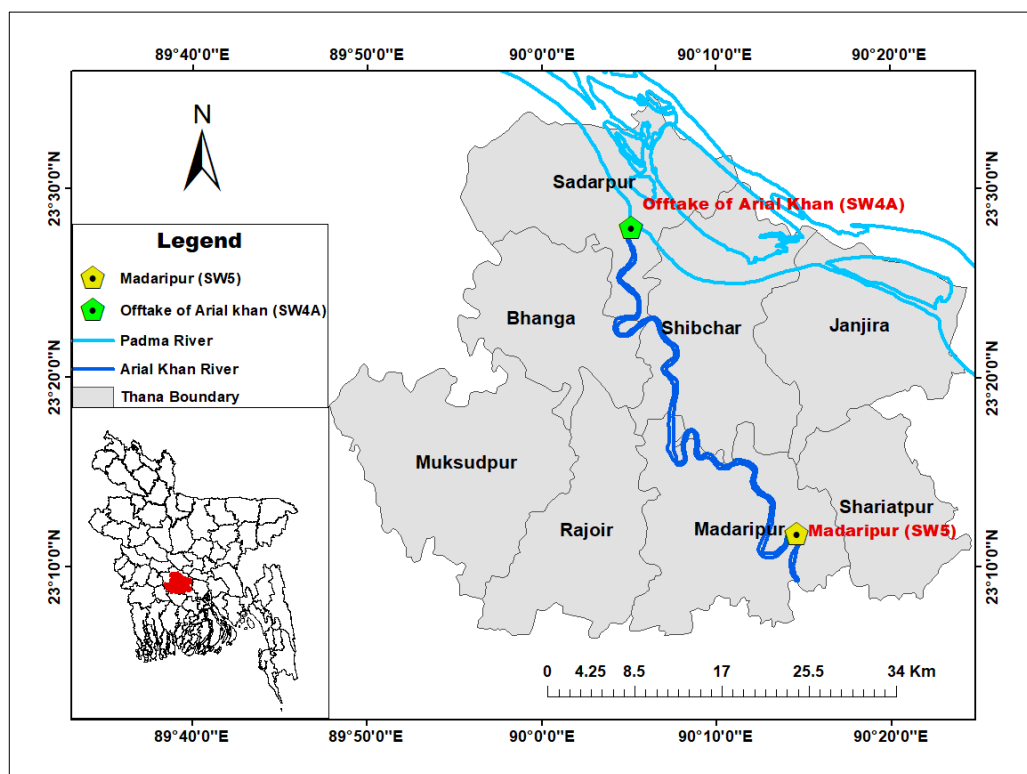


Figure 4.2: Arial Khan River and its floodplain

4.3 Data Collection

In order to develop a mathematical hydrodynamic model, various kinds of data of recent and previous years have been collected and compiled. These data also form the basis for further analysis and interpretation of model results leading to an accurate assessment of the hydrologic and hydrodynamic condition of the study area. According to the modeling requirements, the collected data includes geometric data (e.g., the bathymetry of the river), hydrologic data (e.g., discharge and water level), land topographic data (e.g., flood

inundation map and digital elevation model (DEM)). Basic data used in this study are tabulated in Table 4.1 including their source, location and time.

Table 4.1: Summary of the Data Types

Data Type	Data Source	Location	Period
SRTM DEM	USGS	Bangladesh	2015
Bathymetry	BWDB	Brahmaputra (Jamuna), Ganges, Padma & Arial Khan	2015-2016
Discharge	BWDB	Bahadurabad Transit (SW 46.9L), Hardinge Bridge (SW 90), Mawa (SW 93.5L) & Offtake of Arial Khan (SW 4A)	1965-2017
Water level	BWDB	Bahadurabad Transit (SW 46.9L), Hardinge Bridge (SW 90), Gualondu (SW 91.9R), Mawa (SW 93.5L), Sureswar (SW 95), Offtake of Arial Khan (SW 4A) & Madaripur (SW 5)	1985-2017
Satellite Image	MODIS	Bangladesh	2004-2010
Discharge for RCP scenarios	Previous Study SWAT Model Developed by (Mohammed, et al., 2018)	GBM Basins	Base year flow (1986-2005), 2020s (2006- 2035), 2050s (2036-2065), 2080s (2066-2095)
District Statistics	BBS	Faridpur, Gopalganj, Madaripur & Shariatpur	Population Census 2011& Agriculture Census 2008

4.3.1 Bathymetry

River cross-sections of Brahmaputra, Ganges, Padma & Arial Khan River are collected for the years of 2015-2016 from Bangladesh Water Development Board (BWDB). BWDB collects cross-section data at 39, 25, 15 and 12 different stations of Brahmaputra, Ganges, Padma, Arial Khan River designated by J1 – J17, G1 - G18, P0 - P7 and AKU-1 to AKU-12 respectively. These cross-sections depict the shape and bathymetry of the rivers.

4.3.2 Discharge Data

The discharged data of Bahadurabad Transit (SW 46.9L), Hardinge Bridge (SW 90), Mawa (SW 93.5L) & Offtake of Arial Khan (SW 4A) station were collected from the Bangladesh Water Development Board (BWDB) for the year 1965-2017. These discharge data are used as the upstream boundary of the hydrodynamic models.

The collected discharge comprises of data at an interval of one day from 1965-2006. For the years after 2006, the discharges were measured irregularly and so rating curves were used to generate a continuous daily time series of discharges from daily observed river stages. The general equation of the rating curves developed by (Kennedy, 1984) is used in this study is shown in Eqn. (4-1),

$$Q = C (h-a)^n \quad (4-1)$$

Where,

Q = discharge,

C and n = constants,

h = river stage and

a = river stage at which discharge is zero.

4.3.3 Water Level Data

The water level data of Bahadurabad Transit (SW 46.9L), Hardinge Bridge (SW 90), Gualondu (SW 91.9R), Mawa (SW 93.5L), Sureswar (SW 95), Offtake of Arial Khan (SW 4A) and Madaripur (SW 5) are collected from BWDB for the year 1985-2017. These water level data are used for defining the downstream boundary of the hydrodynamic models and calibrating and validating the models as well.

4.3.4 DEM

A digital elevation model (DEM) is a digital model or 3D representation of a terrain's surface, created from terrain elevation data. A DEM can be represented as a raster (a grid of squares, also known as a height map when representing elevation) or as a vector-based triangular irregular network (TIN). DEMs are commonly built using data collected from remote sensing techniques, but they may also be built from land surveying. This data is required to formulate the computational mesh of the 2D flow area. Each cell, and cell face, of the computational mesh of 2D flow area is pre-processed in order to develop detailed hydraulic property tables based on the underlying terrain used in the modeling process (Brunner, et al., 2015).

The Shuttle Radar Topography Mission (SRTM) data has emerged as a global elevation data in the past one decade because of its free availability, homogeneity and consistent accuracy compared to other global elevation datasets. In this study, the Digital Elevation Model (DEM) of Bangladesh in raster format has been collected from the FTP server of the Shuttle Radar Topographic Mission (SRTM) of National Aeronautics and Space Administration (NASA). The resolution of the collected DEM is 90m x 90m.

4.3.5 Satellite Image

MODIS (Moderate Resolution Imaging Spectroradiometer) is the key instrument aboard the Terra (EOS AM) and Aqua (EOS PM) satellites. Terra's orbit around the Earth is timed so that it passes from north to south across the equator in the morning, while Aqua passes south to north over the equator in the afternoon. Terra MODIS and Aqua MODIS are viewing the entire Earth's surface every 1 to 2 days, acquiring data in 36 spectral bands, or groups of wavelengths. The MODIS Flood Map, which has been used in this study, are collected from a previous study by Hussain (2012).

4.4 Generation of Future Flow Hydrograph

4.4.1 Selection of RCP Scenarios

A Representative Concentration Pathway (RCP) is a greenhouse gas concentration trajectory adopted by the IPCC for its fifth Assessment Report (AR5) in 2014. In this report, four pathways have been selected for climate modeling and research, which describe different climate futures, all of which are considered possible depending on how

much greenhouse gases are emitted in the years to come. The four RCPs are named: RCP2.6, RCP4.5, RCP6 and RCP8.5. They are labeled after a possible range of radiative forcing values in the year 2100 relative to pre-industrial values (+2.6, +4.5, +6.0, and +8.5 W/m², respectively). The RCPs are consistent with a wide range of possible changes in future anthropogenic greenhouse gas (GHG) emissions, and aim to represent their atmospheric concentrations (IPCC, 2014).

RCP 2.6 assumes that global annual GHG emissions (measured in CO₂-equivalents) peak between 2010–2020, with emissions declining substantially after that. Emissions in RCP 4.5 peak around 2040, then decline. In RCP 6, emissions peak around 2080, then decline. In RCP 8.5, emissions continue to rise throughout the 21st century (Meinshausen, et al., 2011) as shown in Figure 4.3.

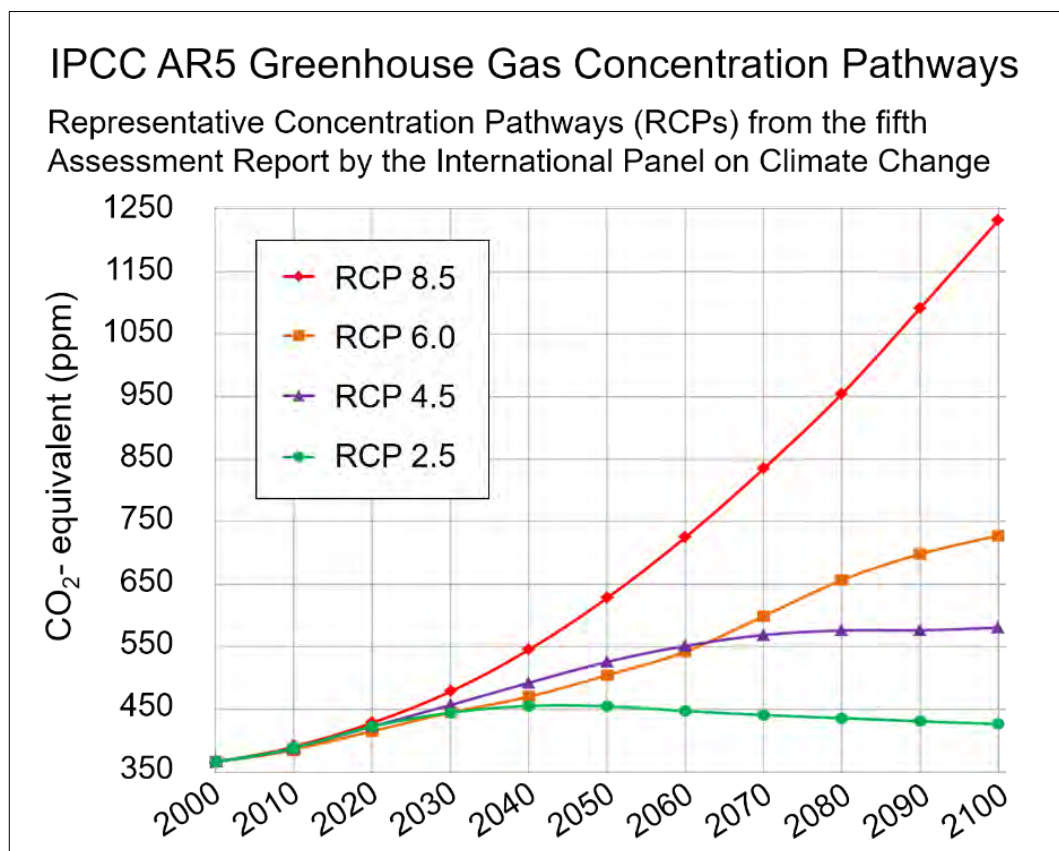


Figure 4.3: All forcing agents' atmospheric CO₂-equivalent concentrations (ppmv) according to four RCPs (*Source: IPCC, 2014*)

In this study, RCP 8.5 and RCP 2.6 are selected being the pessimistic (high emission) and optimistic (low emission) scenario among the 4 scenarios adopted by the 5th assessment

report of IPCC (IPCC, 2014) and to assess a comparison between them to explore a range of expected hazard and associated risk coming in the future.

4.4.2 Hydrological Model SWAT

In this study, a calibrated and validated hydrologic model of GBM basins, set up by (Mohammed, et al., 2018) in SWAT (Soil and Water Assessment Tool) has been used to estimate the future flow magnitudes at Bahadurabad Transit (Brahmaputra River) and Hardinge Bridge (Ganges River) (Mohammed, et al., 2018) as shown in Figure 4.4.

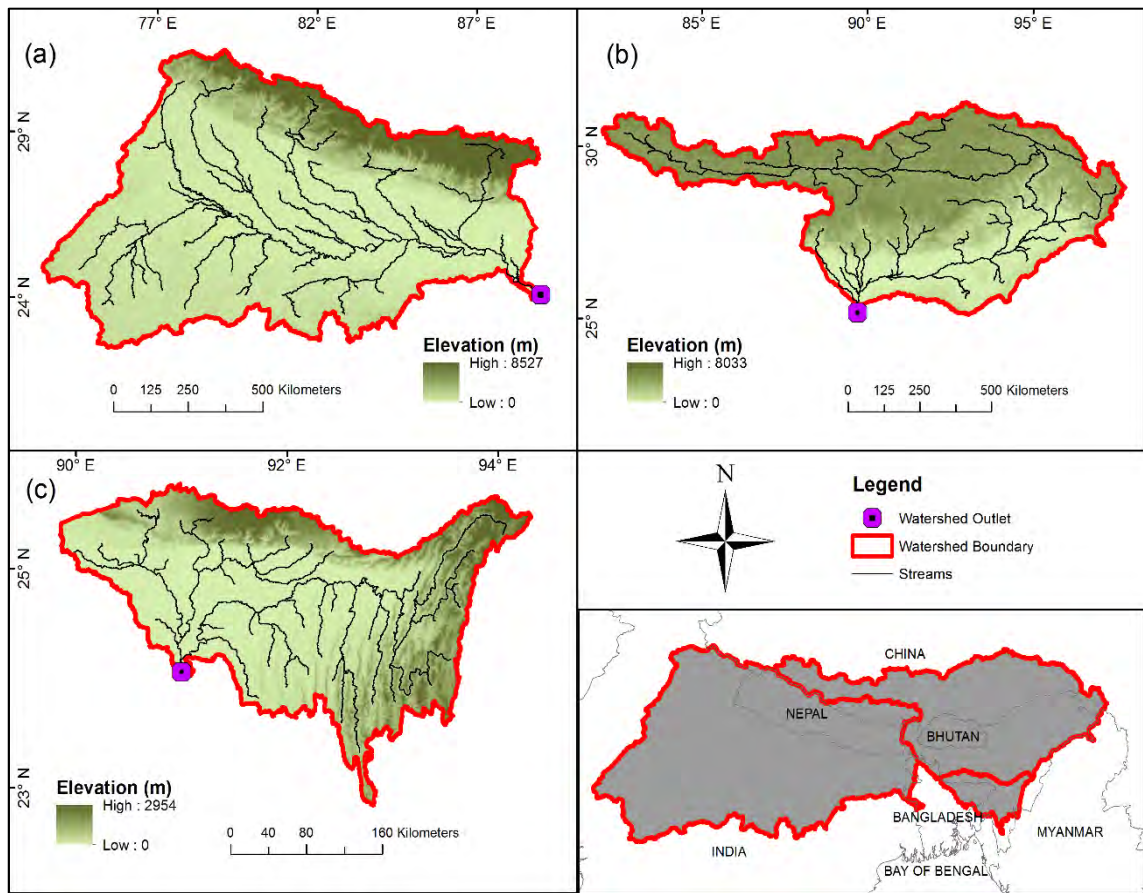


Figure 4.4: GBM basins (*Source: Mohammed, et al., 2018*)

This model has been set up using 90 m resolution DEM from HydroSHEDS (Hydrological data and maps based on SHuttle Elevation Derivatives at multiple Scales) to be used as topographic information of the GBM basins (Lehner, et al., 2008). The GlobCover land-use map prepared by the European Space Agency for the year 2009 with a 300 m resolution (Arino, et al., 2008) and the Digital Soil Map of the World prepared by the Food and Agricultural Organization of the United Nations has been used as land-

use and soil information of the model respectively (FAO, 1974). Daily precipitation and maximum/minimum temperature data from the global WFDEI (WATCH Forcing Data methodology applied to ERA-Interim data) dataset (Weedon, et al., 2014) and of the period 2000 to 2013 are used as meteorological inputs during the development of the SWAT models.

This model has been Calibrated for 2000-2006 and validated for 2007-2013 using the observed discharge data of BWDB. Before calibrating the models, global sensitivity analyses are performed on all hydrology-related parameters of SWAT using SWAT-CUP (Calibration and Uncertainty Program) (Abbaspour, et al., 2007).

4.4.3 Generation of Future Flow Hydrograph

The SWAT model of GBM basins developed by (Mohammed, et al., 2018) as mentioned in the section 4.4.3 has been used in this study to generate the future flow hydrographs at Bahadurabad Transit and Hardinge Bridge. For this study purpose, the model has been simulated using the projected daily precipitation and daily maximum/minimum temperature data of EC-EARTH3 dataset for RCP 2.6 and RCP 8.5 scenarios. These projections are generated by a combination of eight GCMs and three RCMs and these datasets are collected from Coordinated Regional Climate Downscaling Experiment (CORDEX) - South Asia domain database (Giorgi & Gutowski Jr, 2015).

The future flow hydrographs of Bahadurabad Transit (SW 46.9L) of Brahmaputra basin and Hardinge Bridge (SW 90) of Ganges from 1976-2100 for both RCP 2.6 and 8.5 scenarios simulated using the EC-EARTH3 data set are shown in Figure 4.5 and Figure 4.6. The hydrographs show that the future flow for RCP 2.6 and 8.5 are quite similar to 2040. After that, the future flow for the RCP 8.5 scenario is significantly higher than that of RCP 2.6 for both of the basins.

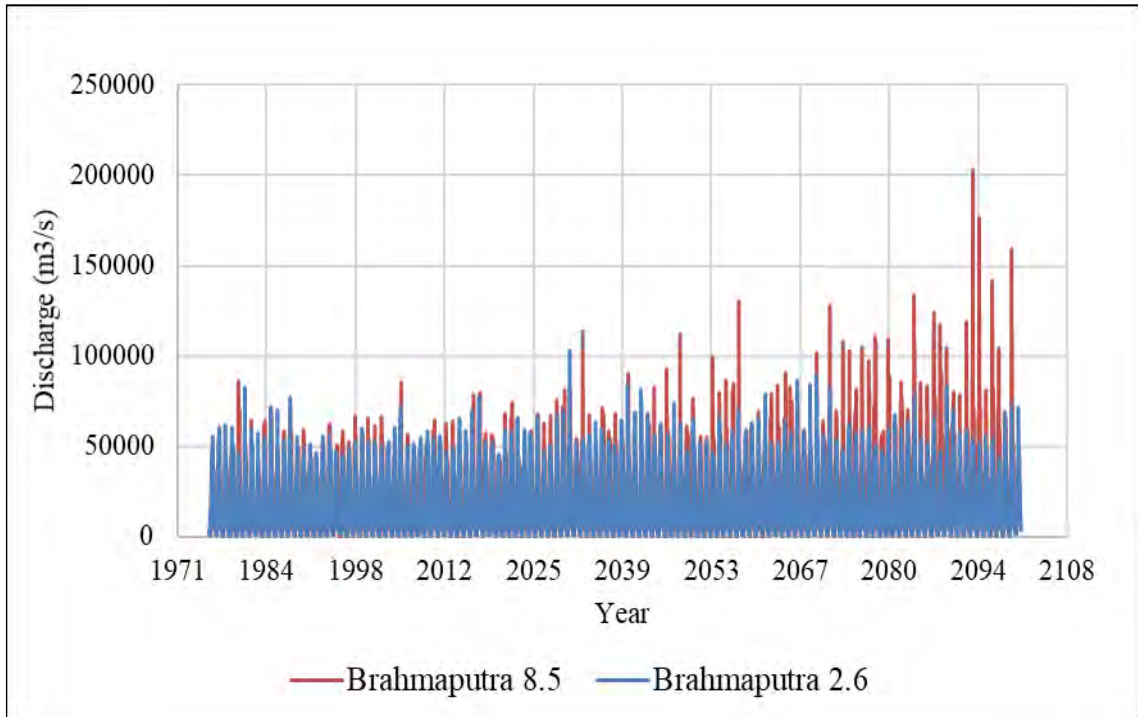


Figure 4.5: Flow hydrographs at Bahadurabad Transit (SW 46.9L) of Brahmaputra for RCP 2.6 & RCP 8.5 scenario

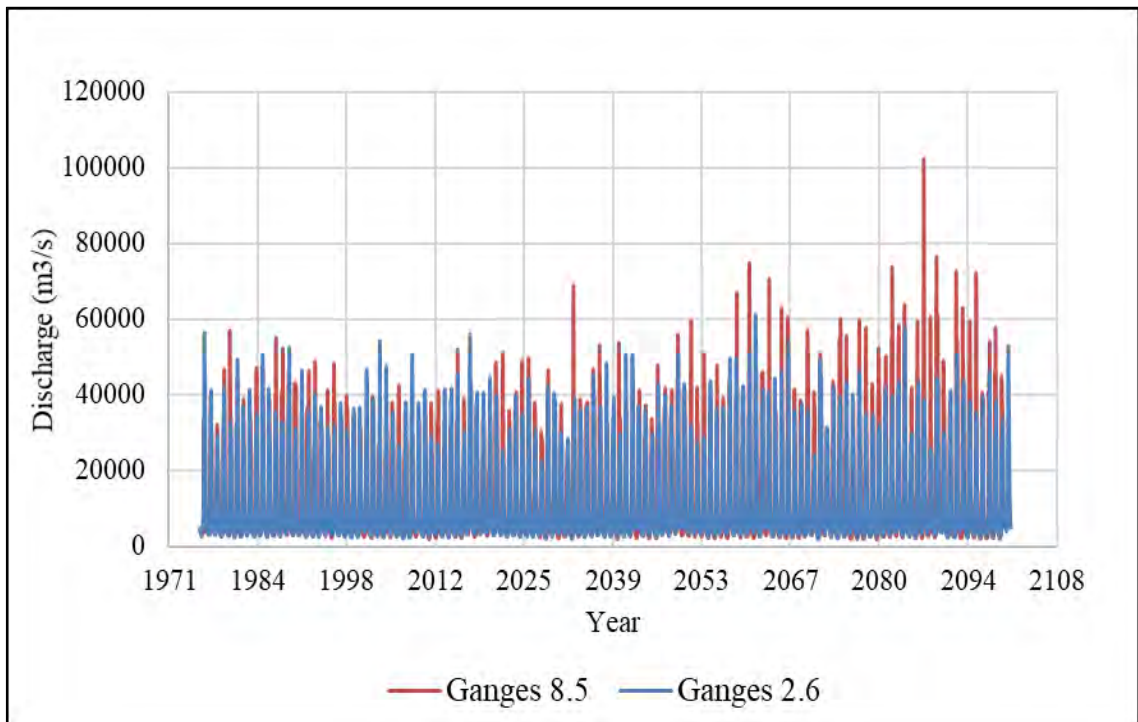


Figure 4.6: Flow hydrographs at Hardinge Bridge (SW 90) of Ganges for RCP 2.6 & RCP 8.5 scenario

Later, for the better understanding of the scenario analysis and ease of simulating the hydrodynamic models for future scenarios, 4 thirty-year long time slices are considered for each of the RCP scenarios, which are the baseline period (1976-2005), the 2020s (2006-2035), the 2050s (2036-2065) and the 2080s (2066-2095). After that, a hydrograph of each of these time slices has been prepared to be used in generating future scenarios.

As this study is mainly focused on the flood scenarios so maximum flood peaks would serve better than the mean values. However, the maximum of the dataset is usually avoided as climate data usually contains a lot of outliers. Hence, in the case of climate studies, it is usually suggested to take p^{th} percentile (where, $p = 90$ or 95 or 99) of the dataset rather than using the maximum of the dataset. The p^{th} percentile of a data sample means the value below which approximately $p\%$ of the data fall. Generally, extreme flood scenarios are defined by 90, 95 or 99th percentile (Bonsal, et al., 2001). This concept of using some percentile of climate data has been used in many climate studies for generating future climate change scenarios (Braun, et al., 2014; O'Connor & Costa, 2004; Beniston, et al., 2007; González, et al., 2010; Maurer & Hidalgo, 2008).

In this study, the 90th percentile flow of each of the day for above mentioned time slices have been extracted from the full data set using R software so that the upper limits of the flood parameters can be calculated. The 90th percentile daily flow hydrograph plots of Brahmaputra and Ganges for each of the time slices (baseline, the 2020s, 2050s, and 2080s) for both RCP 2.6 and 8.5 scenarios are shown in Figure 4.7 and Figure 4.8.

Figure 4.7 shows that for RCP 2.6 scenario the flows are not that much different for the Brahmaputra and Ganges Basin. On the hand, Figure 4.8 (a) shows that the future flow is remarkably higher for the 2080s for Brahmaputra Basin while Figure 4.8 (b) shows that the future flow is not that much higher for the Ganges Basin. These daily flow hydrographs are later used as the upstream flow boundary of the HEC-RAS 1D Brahmaputra, Ganges and Padma River model for generating future flow at the Mawa station (SW 93.5L) of Arial Khan River.

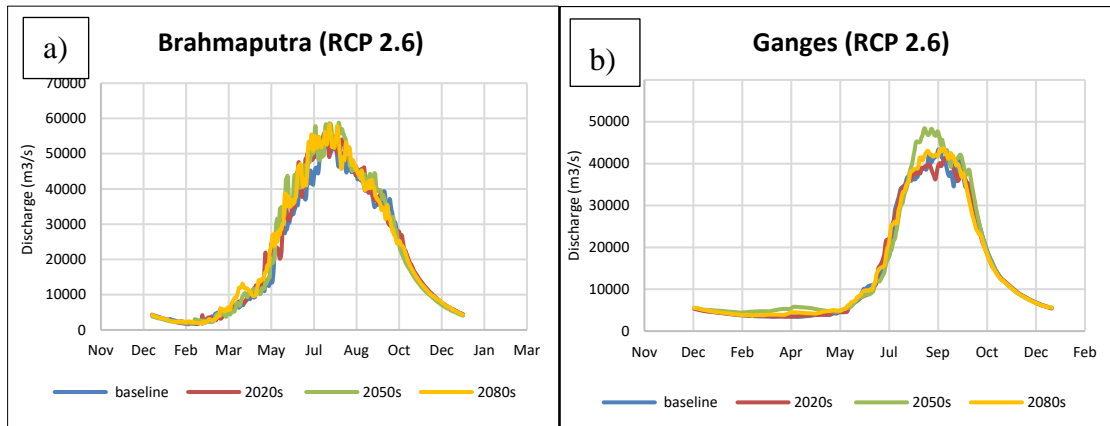


Figure 4.7: 90th Percentile daily flow hydrograph plots for the base period, 2020s, 2050s, 2080s of RCP 2.6 of a) the Brahmaputra and b) the Ganges

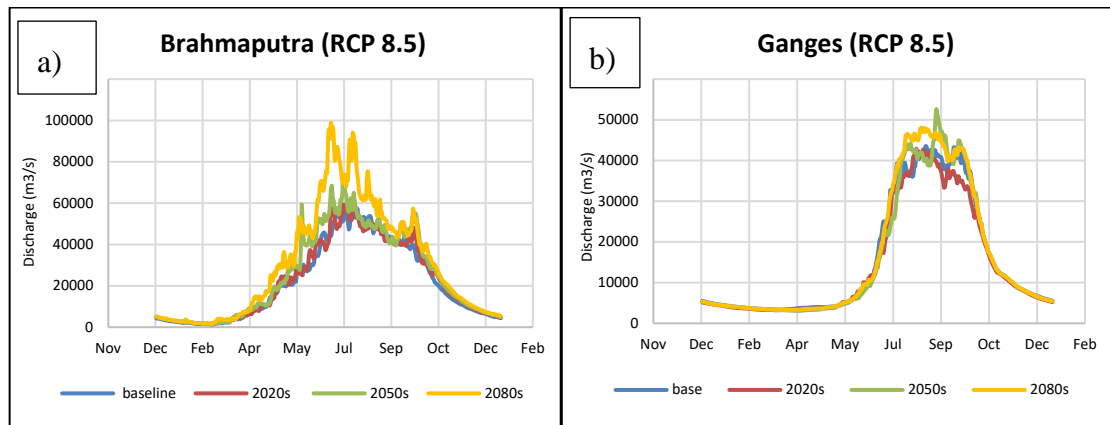


Figure 4.8: 90th Percentile daily flow hydrograph plots for the base period, 2020s, 2050s, 2080s of RCP 8.5 of a) the Brahmaputra and b) the Ganges

4.4.4 Statistical Relation between the Padma and Arial Khan River

The Padma is the parent river of Arial Khan River. Hence, the water level of the Arial Khan River shows a similar trend of rising and fall as the river Padma (FFWC, 2017). So, a statistical equation is developed to establish a relation between the discharge of the Padma River to Arial Khan River to generate future flow at the offtake of Arial Khan. Mawa (93.5L) is the nearest discharge station to the offtake of Arial Khan River. Additionally, there is no distributary between this part of Padma River except Arial Khan River. Previously, in many studies, the water level, discharge and sediment data of Mawa have been used for studies of Arial Khan River (Akter, et al., 2013; Winkley, et al., 1994). So, a linear regression equation has been developed between Mawa (SW 93.5L) station of Padma River and Chowdhury Para (SW 4A) station of Arial Khan River.

For this purpose, the time series discharge data of Mawa and Chowdhury Char is collected from 1965 to 2017 from Bangladesh Water Development Board. Then, a simple linear equation ($y=mx+c$) has been developed based on the monsoon flow as shown in Figure 4.9 by Eqn. (4.2).

$$Q_{\text{Arial Khan}} = 0.0358 * Q_{\text{Padma}} - 281.03 \quad (4-2)$$

Where, $Q_{\text{Arial Khan}}$ is the discharge of Chowdhury Char (SW 4A) and Q_{padma} is the discharge of Mawa (SW 93.5L). The performance of this equation has been assessed through R^2 and P value. The R^2 is found nearly 0.6 which is within the satisfactory range. The P value is found less than 0.001 which proves its statistical significance. After establishing that the equation performs reasonably well, it is used as the boundary condition of Arial Khan 1D-2D coupled model to estimate flood scenario for the base year, 2020s, 2050s and 2080s for both RCP 2.6 and 8.5.

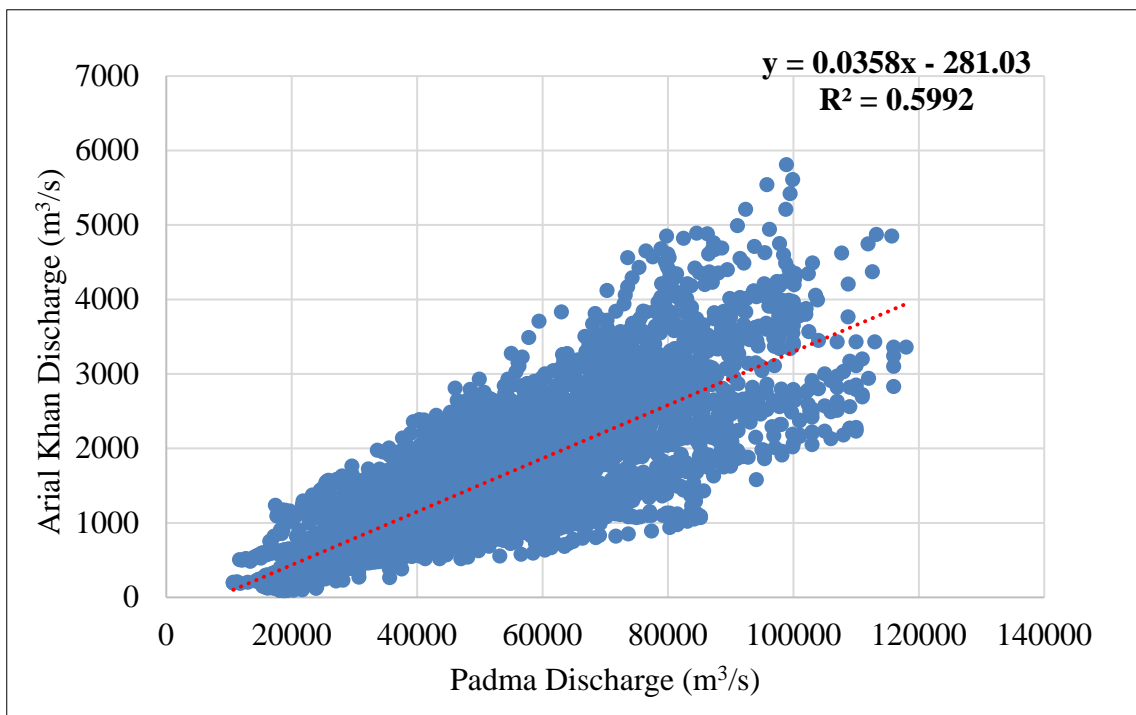


Figure 4.9: Statistical Relation between Arial Khan River and the Padma River

4.5 HEC-RAS 1D Model Set Up

4.5.1 Processing in HEC-RAS

A 1D HEC-RAS model has been set up for the Brahmaputra, Ganges and Padma River using the SWAT flow hydrographs at u/s boundaries. The model comprises 39, 25 and

15 cross-sections of Brahmaputra, Ganges, Padma River designated by RMJ1 to RMJ17, RMG1 to RMG18 and RMP0 to RMP7 as shown in Figure 4.10. The model has been set up using the bathymetry data for the year of 2015.

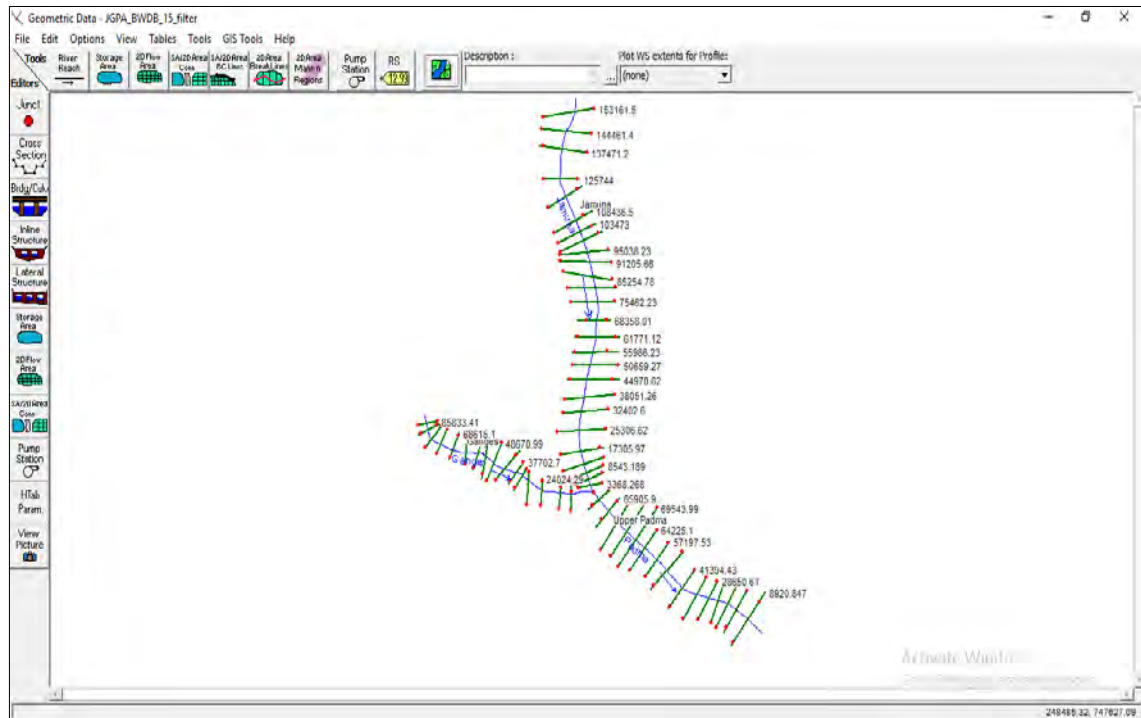


Figure 4.10: Cross-sections of Brahmaputra, Ganges and Padma River in HEC-RAS

4.5.2 Boundary Condition

The boundary condition is the conditions or phenomenon occurring at the boundaries of the model. There are several different types of boundary conditions available in HEC-RAS. They are Flow hydrograph, Stage hydrograph, Stage and flow hydrograph, Rating curve, Normal depth, Lateral inflow hydrograph, Groundwater inflow, Internal boundary stage and/or flow, etc.

For the 1D hydrodynamic model of Ganges-Brahmaputra-Padma, the discharge hydrographs at Bahadurabad Transit (SW 46.9L) and Hardinge Bridge (SW 90) are used as upstream boundary conditions and stage hydrograph of Sureswar (SW 95) is used as a downstream boundary condition.

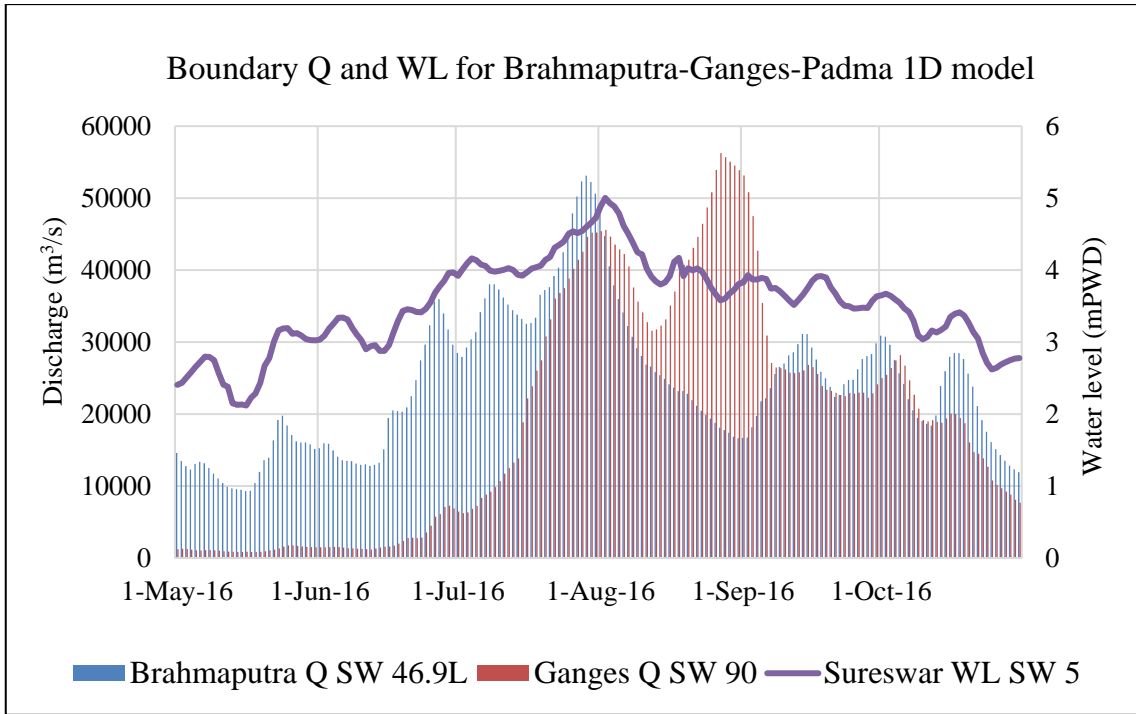


Figure 4.11: Boundary Q and WL for the Brahmaputra-Ganges-Padma Model for Calibration 2015

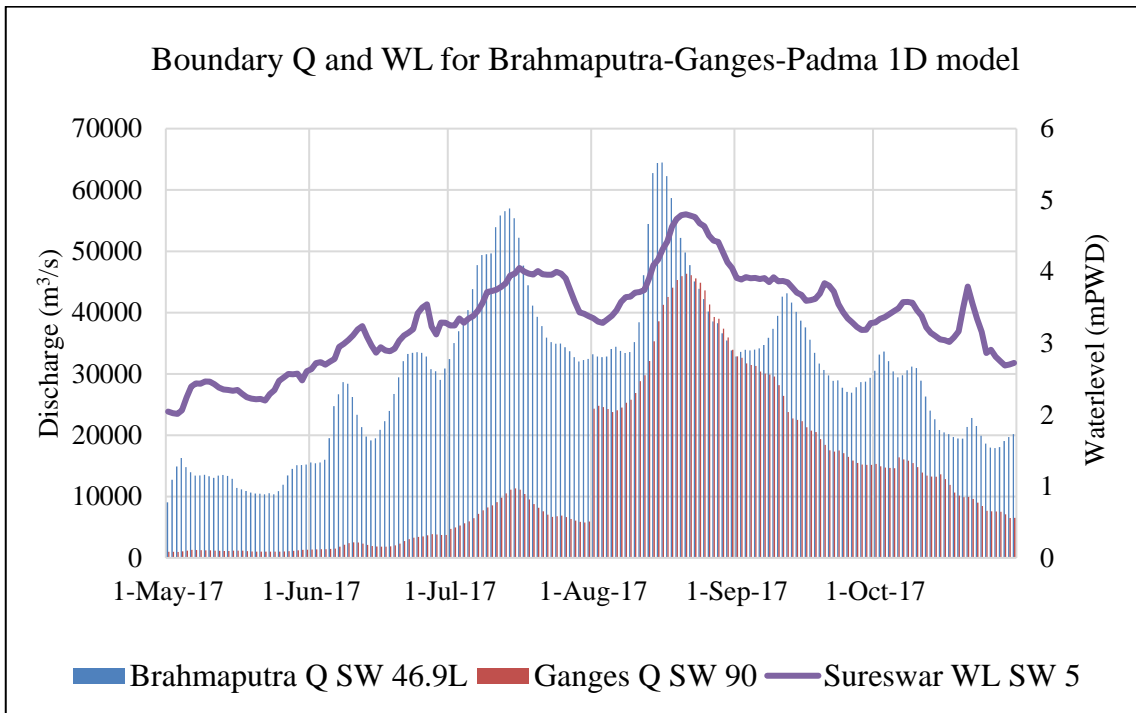


Figure 4.12: Boundary Q and WL for the Brahmaputra-Ganges-Padma Model for validation 2017

This model is calibrated for the year of 2015 and validated for the year 2016. The upstream discharge boundaries of Bahadurabad (SW 46.9L) and Hardinge Bridge (SW 90) and downstream water level boundary of Sureswar (SW 95) for calibration and validation are shown in Figure 4.11 and Figure 4.12 respectively.

4.6 HEC-RAS 1D-2D Coupled Model Set up

4.6.1 Datum Correction of Digital Elevation Model (DEM)

The Digital Elevation Model (DEM) of Bangladesh was collected from the FTP server of the Shuttle Radar Topographic Mission (SRTM) of National Aeronautics and Space Administration (NASA). The DEM was in the geographical coordinate system (GCS_WGS_1984). Geographic coordinate systems indicate location using longitude and latitude based on a sphere (or spheroid) while projected coordinate systems use X and Y based on a plane. All the data in the DEM have been projected on to the Bangladesh Transverse Mercator (BTM). The data comprises of a resolution of 90m x 90m.

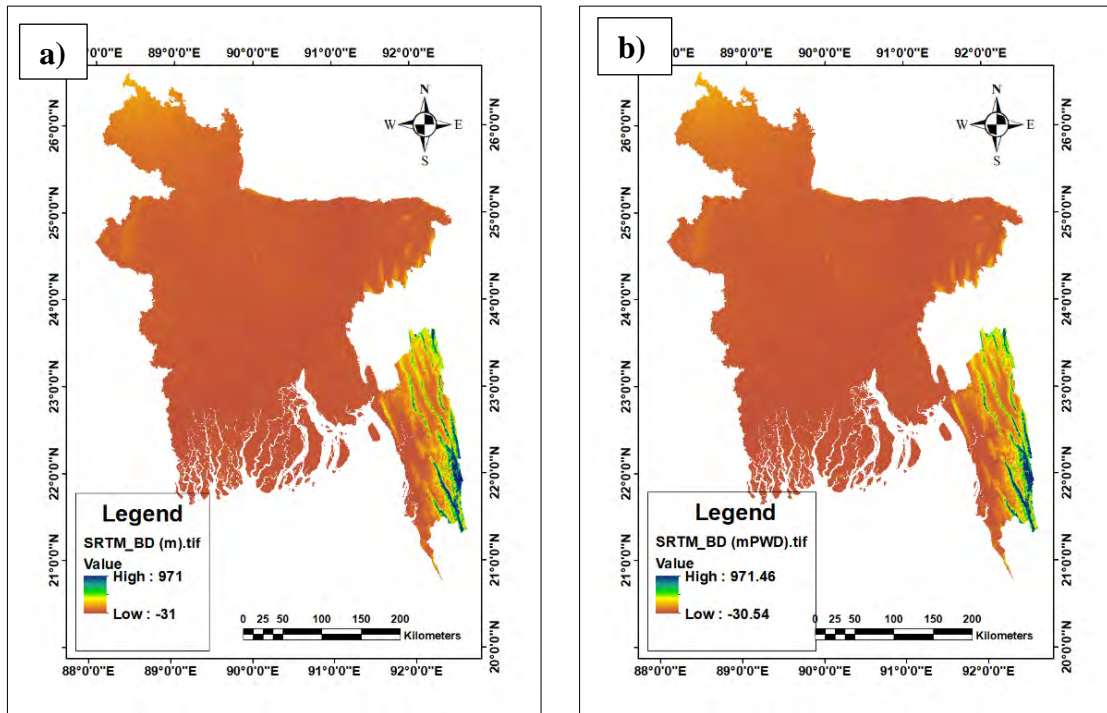


Figure 4.13 Digital Elevation Model (DEM) modification a) before modification b) after modification

The elevation of the DEM has been measured with respect to the mean sea level. In this study all the elevations including topography of river cross sections, water surface elevation has been considered are measured from Public Work Datum (PWD). PWD is a horizontal datum believed originally to have zero at Mean Sea Level (MSL) at Calcutta. PWD is located approximately 1.5 ft. below the MSL established in India under the British Rule and brought to Bangladesh during the Great Trigonometric. Survey. To adjust this difference in elevation, an elevation of 1.5ft (0.46m) is added to the collected DEM. The DEMs both before modification and after modification are shown in Figure 4.13.

4.6.2 Clipping of the Study Area from DEM

The Shapefile of the Upazilas which are adjacent to Arial Khan River is clipped from the Upazila shapefile of Bangladesh and superimposed on the modified DEM file mentioned above. Later, the DEM of these selected Upazillas has been clipped from the modified DEM using the Clipping Tool in Arc Toolbox. The clipped DEM of the study area is shown in Figure 4.14.

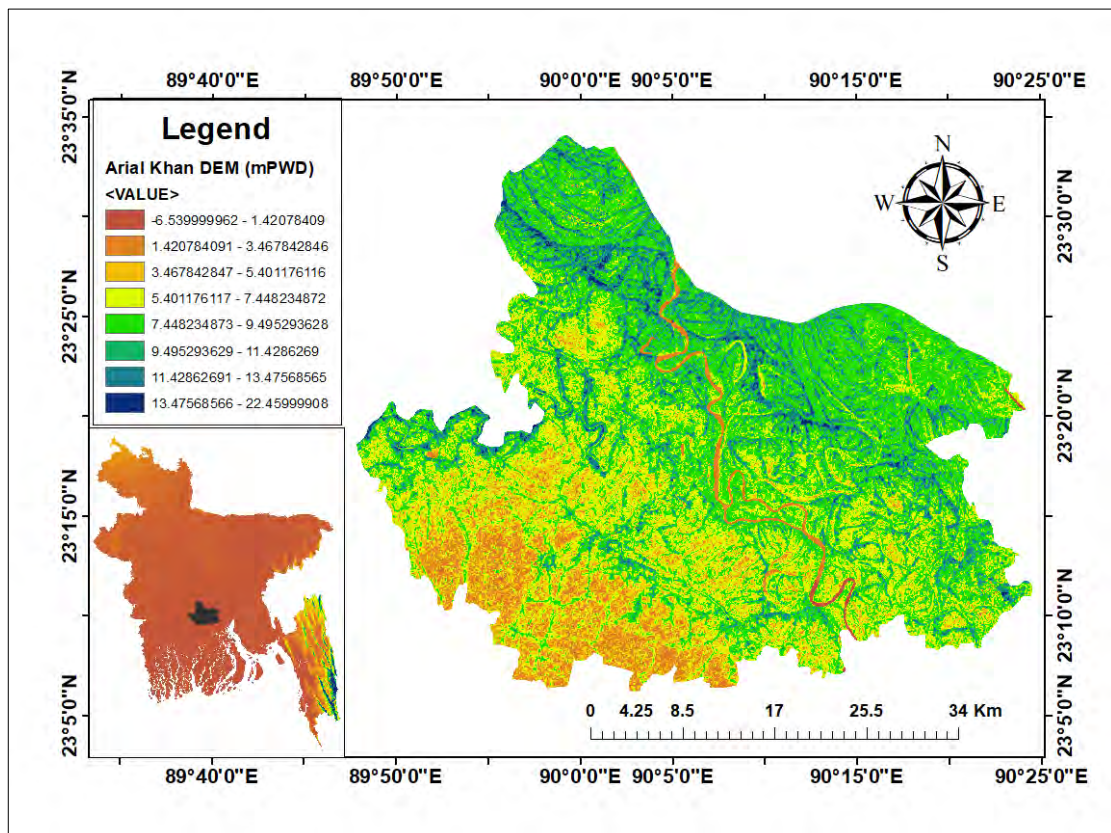


Figure 4.14: Clipped DEM of the study area

4.6.3 Generation of Triangulated Irregular Network (TIN)

A TIN is used to represent the terrain of the digital elevation model (DEM), which can be further used to produce digital surface models (DSM) or digital terrain models (DTM). TIN is a vector-based triangular representation whereas DEM is represented as a raster of a square grid. The purpose of the Raster to TIN tool is to create a Triangulated Irregular Network (TIN) whose surface does not deviate from the input raster by more than a specified Z tolerance. It is done by using the Raster to TIN tool in the ArcToolbox. TIN of the study area has been shown in Figure 4.15.

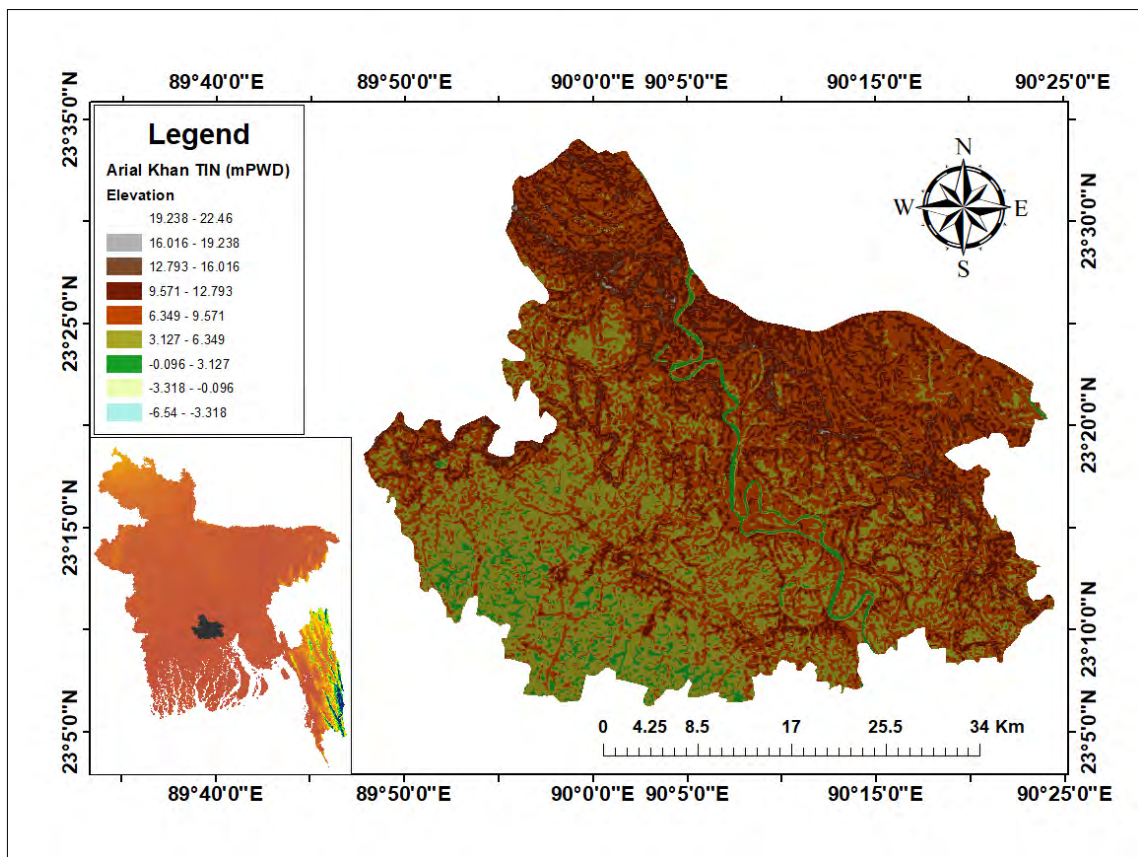


Figure 4.15: TIN of the study area

4.6.4 Pre-processing in HEC-GeoRAS

HEC-GeoRAS is an ArcGIS extension specifically designed to process geospatial data to incorporate for use with HEC-RAS. It is organized as a pre-processing (preRAS) and post-processing (postRAS) tool of HEC-RAS. This extension allows users to create an HEC-RAS import file containing geometric attribute data from an existing Digital Terrain Model (DTM) and complementary datasets. Water surface profile results may also be

processed to visualize inundation depths and boundaries. However, HEC-RAS 5.0 is capable of processing the results of the 2D and 1D-2D coupling in the newly added RASMapper tool of HEC-RAS. As this study is focused on 1D-2D coupling, HEC-GeoRAS is used to process the input 1D bathymetry only. The river centerline, bank lines, flow paths, and cross-section cutlines are drawn, and they are export from HEC-GeoRAS to be imported in HEC-RAS. The detail steps are given below:

River Centerline Creation

At first, the Arial Khan River has been drawn by the stream centerline layer. The river has been created by starting from the upstream end and working downstream following the middle part of the channel. The river name has been assigned as Arial Khan, and the reach name has been assigned as Upper Arial Khan. Figure 4.16 (a) shows river centerline created for this study.

Riverbanks Creation

The riverbanks separate the main channel from the overbank areas when flooding occurs. It differentiates the resistance of the main channel and the over banks. There are precisely two bank lines per cross-section, and it is important to define them as the left and right bank. Figure 4.16 (b) shows river centerline created for this study.

Flow Path Creation

The Flow Path Centerlines theme is used to identify the hydraulic flow path in the left overbank, the main channel and right overbank. Creating the flow path centerline layer assists in setting the cross-sectional cut lines correctly. As the stream centerline already exists in this study, river centerline has been copied for the flow path in the main channel. All flow paths (left overbank main channel and right overbank) are drawn from upstream to downstream. All three flow paths should be extended to each of the cross-sections. The flow paths are used to derive downstream reach lengths in HEC-RAS. Once the digitization of the flow paths was completed, each flow path must now be identified as a left, right or channel flow path. The channel is the flow path along the center of the river channel. Determining the left and right flow path is accomplished by an upstream to downstream perspective. Flow paths created for this study are shown in Figure 4.16 (c).

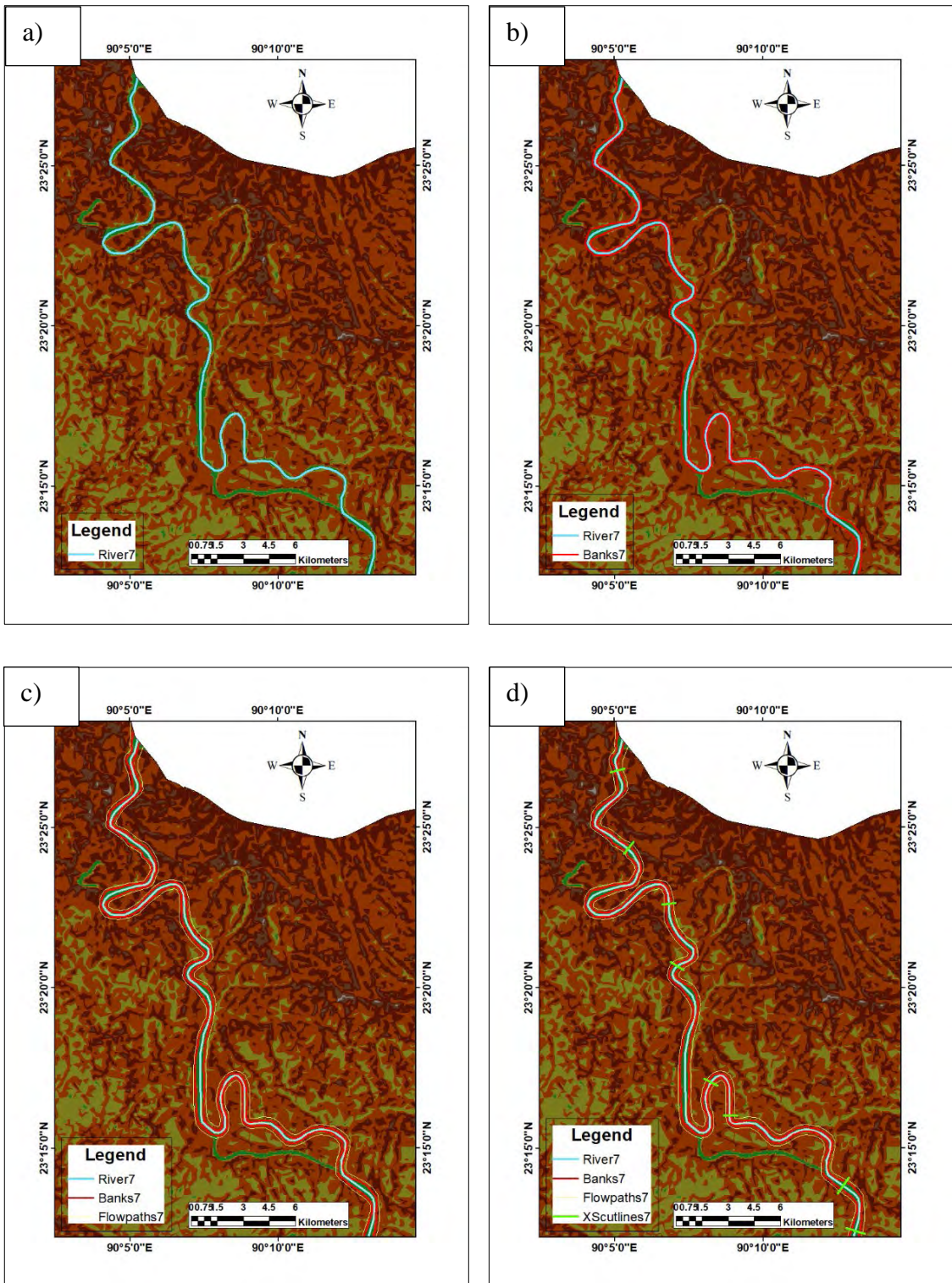


Figure 4.16: Processing in HEC-GeoRAS a) River Centerline b) Bank line c) Flow paths d) Cross-sections Cutlines of Arial Khan River

Cut Line theme. This theme will identify the planar location of the cross sections and the station elevation data being extracted from the DTM along each cut line for use in HEC-RAS. During drawing, cross-sectional cut lines must be pointed from the left overbank to the right overbank. Thus, each cut line from left to right was drawn, as it could look downstream. Cross-sectional cut lines must cross each of the three flow paths and the two banks exactly once. Cross-sectional cut lines should be perpendicular to the direction of flow, and they should not intersect each other. Ten cross-section locations RMAU 3 to RMAU 12 are chosen for the total study reach and drawn according to the morphological station position of BWDB as shown in Figure 4.16 (d).

Stream Centerline Attributes

After digitizing centreline, bankline, and flowpath, all the data such as topology, length/stations, and elevations need to be extracted. For this reason, all the above-mentioned features are extracted from the “Stream Centerline Attributes” menu of RAS Geometry toolbar. Then the attribute table was then checked to ensure the data are appropriately extracted or not.

XS Cutlines Attributes

It is also vital to ensure that all the cross-section data are correctly extracted. To complete this, all features such as River/Reach, Stationing, Bank stations, Downstream Reach Length, Elevations are extracted from the “XS Cut Line Attributes” of RAS Geometry toolbar. In this phase, the 2D feature class of XS Cut Lines is intersected with the TIN to create a feature class with 3D cross section. After that, the attribute table of 3D cross sections is examined in order to check their correctness.

Export RAS Data

The generation of the HEC-RAS import file is the last step of the HEC-GeoRAS pre-processing. In this phase, an HEC-RAS input file is created in RAS Import format which includes the terrain elevation extracted from the TIN, the 3-D stream centerline and the 3-D cross-sections themes as z values (z value is the elevation above public work datum and, for our case, is in units of the meter). The “Extract GIS DATA” is clicked under the menu “RAS Geometry” from the HEC-GeoRAS toolbar. The default name GIS2RAS is accepted and saved in the selected folder.

4.6.5 Processing on HEC-RAS

1D Hydrodynamic Model

The GIS format of the Arial Khan River bathymetry which has been processed in HEC-GeoRAS in the previous section has been incorporated in the Geometry Data window of HEC-RAS. The unit system is selected as SI units. The model comprises 10 number of cross-sections of the Arial Khan River named RMAK3 to RMAK12 which were imported for the development of the 1D hydrodynamic model. Initially, the geometry data include the elevation of the TIN from which it has been processed in HEC-GeoRAS.

Later, the bathymetry data of 2015 collected from BWDB has been incorporated in the cross-section data. The cross-sections of the Arial Khan River are shown in Figure 4.17. Then, the roughness of the river is incorporated manually, and the river is interpolated with a distance of 200 m between the cross sections as shown in Figure 4.18.

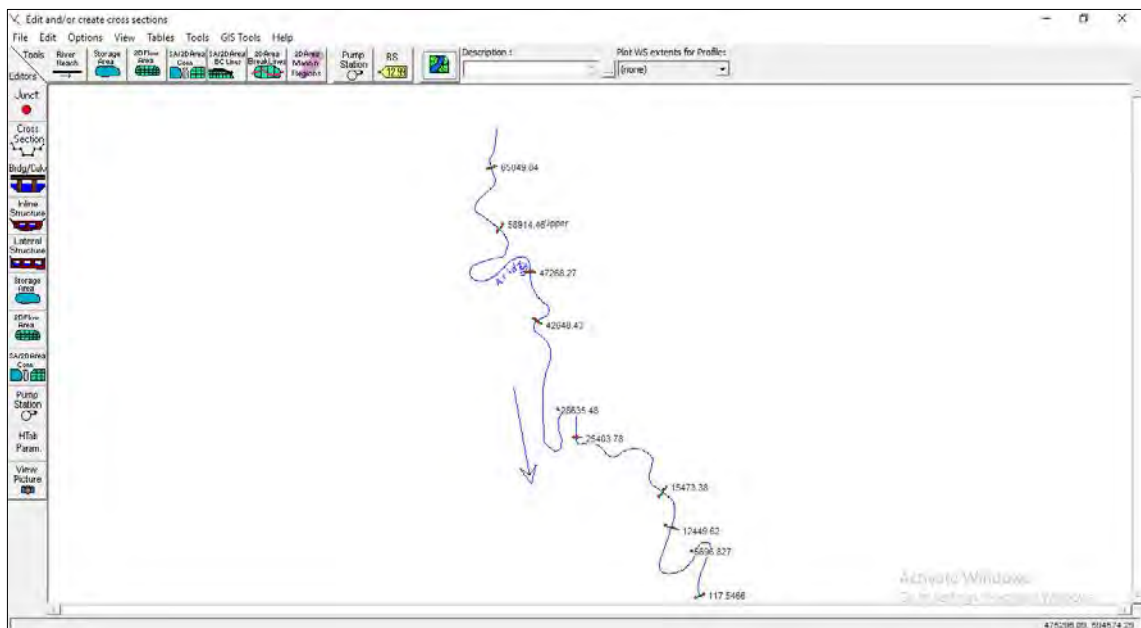


Figure 4.17: Arial Khan cross-section in HEC-RAS

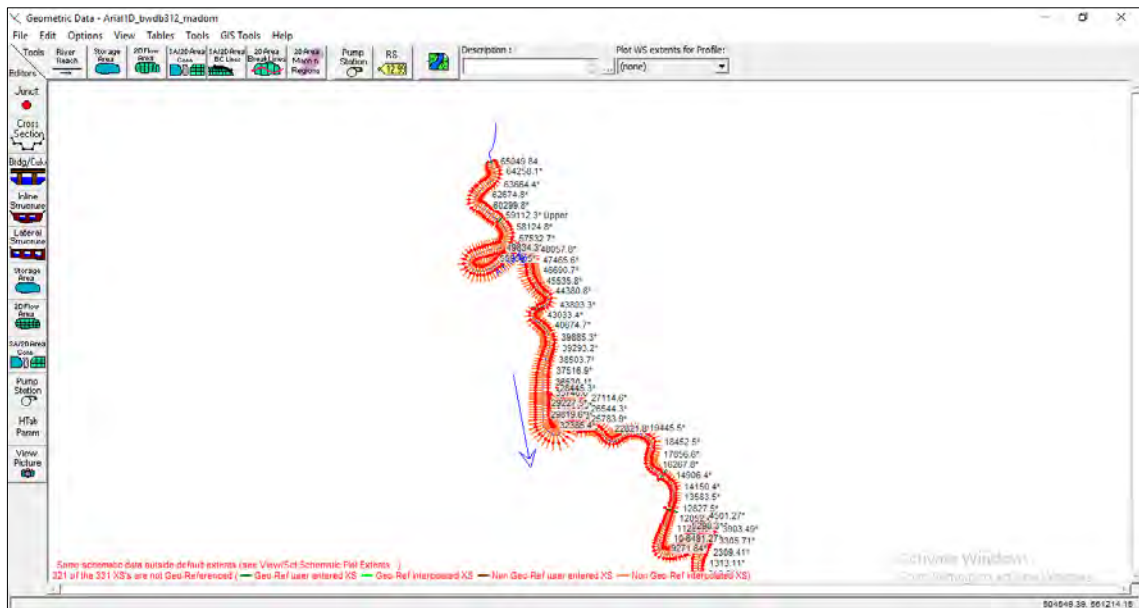


Figure 4.18: Interpolated Cross-sections of Arial Khan River

Developing a Terrain Model

A terrain layer is of primary importance for computing hydraulic properties (elevation-volume, elevation-wetted perimeter, elevation profiles, etc.), inundation depths and floodplain boundaries. HEC-RAS supports the terrain model in Geo Tiff format. So, after preparing the 1D river bathymetry, the raster file of the study area is added using the new terrain layer tool of RAS-Mapper as shown in Figure 4.19.

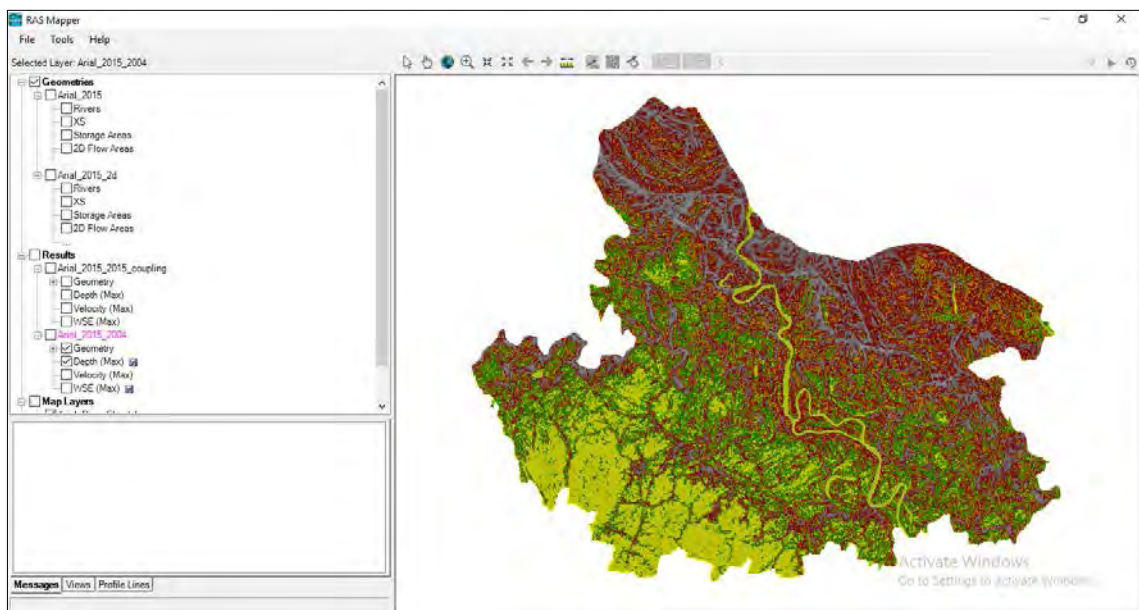


Figure 4.19: Incorporation of the Terrain of the study area in RAS-Mapper

RAS Mapper converts this raster file into the GeoTIFF (*.tif) file format. Later, this terrain is used for pre-processing geometric data for 2D flow areas, computing flood depths and inundation boundaries from simulation results. However, prior to creating a terrain layer, the projection has been specified by selecting Bangladesh Transverse Mercator as an ESRI projection file (*.prj). Once a projection has been included, all the data will be projected into the selected coordinate system. Then, this terrain file is opened in Geometry Editor window of HEC-RAS for generating 2D flow area.

2D Flow Area Computational Mesh

2D flow area is a region of a model in which the flow through that region is generated with the HEC-RAS 2D flow computational algorithm. 2D Flow area is defined by laying out a polygon that represents the outer boundary of the 2D flow area.

In this study, two 2D flow areas have been drawn in the right side and left the side of Arial Khan River following the Terrain file. The HEC-RAS 2D modeling uses a Finite-Volume solution scheme. This algorithm is developed to allow for the use of a structured or unstructured computational mesh. A mesh of 150m*150m grid resolution has been defined for each of the 2D flow areas as shown in Figure 4.20. Initially, the mesh is generated for Manning's roughness, $n=0.06$. Later, this roughness of the mesh/ floodplain can be changed according to the user's choice.

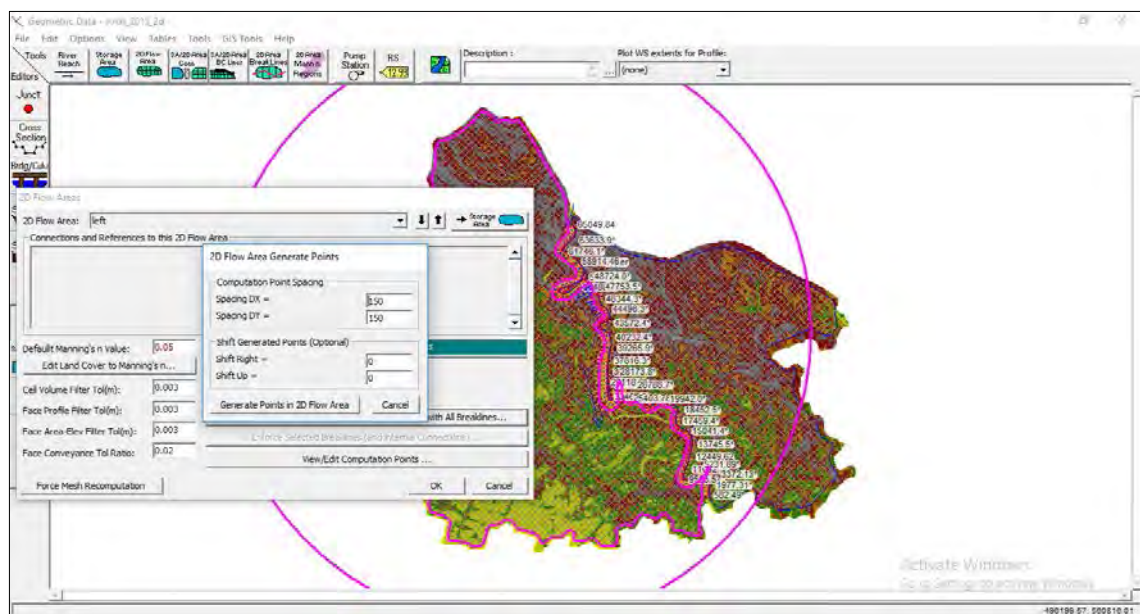


Figure 4.20: 2D flow area computational mesh

1D-2D Coupling through Lateral Structure

A lateral structure can be connected to a 1D river reach or 2D flow area or 2D storage area. Here, the lateral structure is used to create a connection between the 1D river and 2D flow area, which will generate a movement of water between the 1D river and the 2D flow area. A series of (4 on each of the banks) lateral structures have been created from the upstream to downstream of the river as shown in Figure 4.21. Red line of the figure represents where HEC-RAS has a link the lateral structure to the 2D flow area. Figure 4.22 shows a vertical cross-section of one of the eight lateral structures. The elevation of the connected lateral structure needs to be above the TW (Tail Water) cell min elevation.

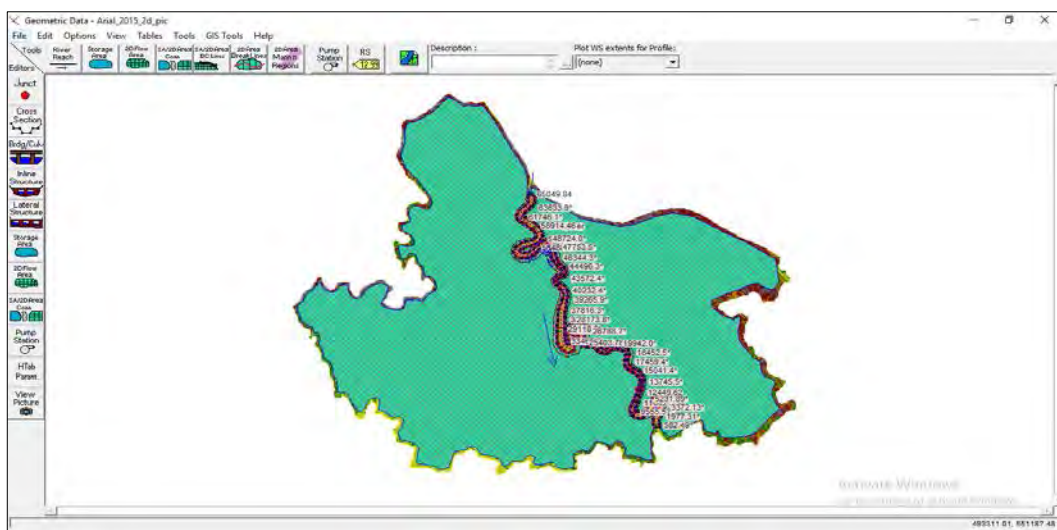


Figure 4.21: Incorporation of Lateral Structures

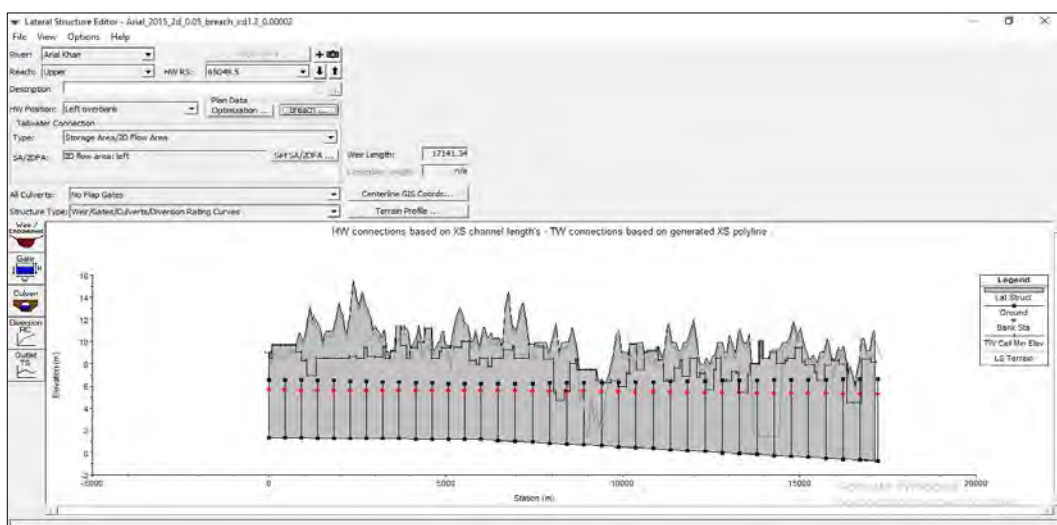


Figure 4.22: Elevation of 1 of the 8 lateral structures

Boundary Conditions

In this study, the one-dimensional hydrodynamic model has one upstream boundary and one downstream boundary. Here, the discharge hydrograph of Chowdhury Char (SW 4A) and water level hydrograph of Madaripur (SW 5) is used as upstream and downstream boundary respectively.

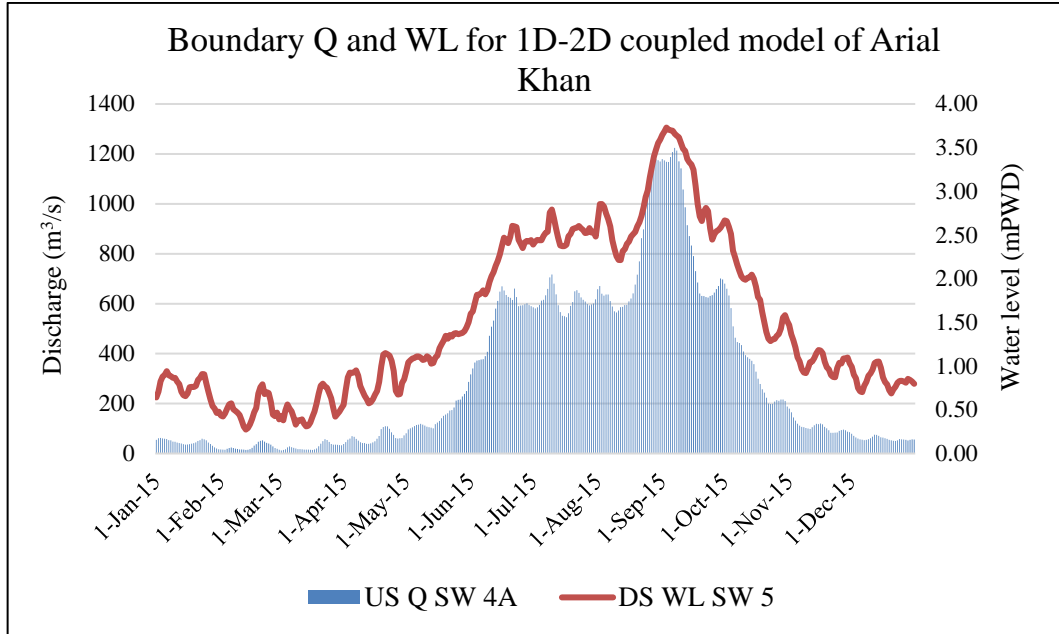


Figure 4.23: Boundary Q and WL for Arial Khan River for Calibration 2015

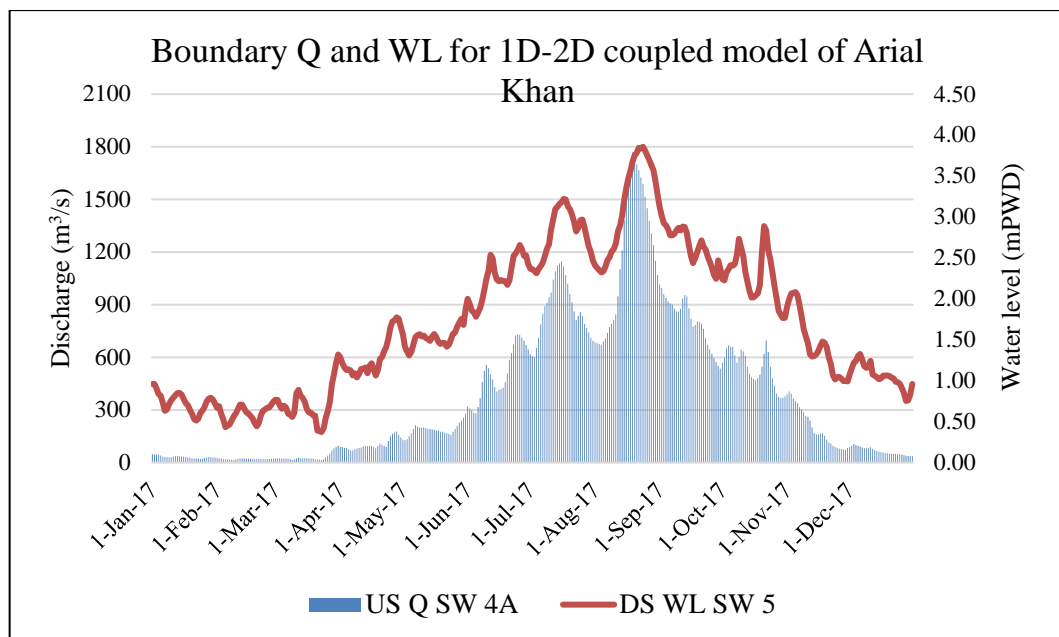


Figure 4.24: Boundary Q and WL for Arial Khan River for Validation 2015

The upstream discharge boundary and downstream water level boundary condition for calibration and validation are shown in Figure 4.23 and Figure 4.24. Later, boundary conditions have been applied to the 2D flow area too. There are six peripheral boundaries incorporated in the model of the study area out of which 2 are inflow boundaries, and the other 4 are outflow boundaries as shown in Figure 4.25.

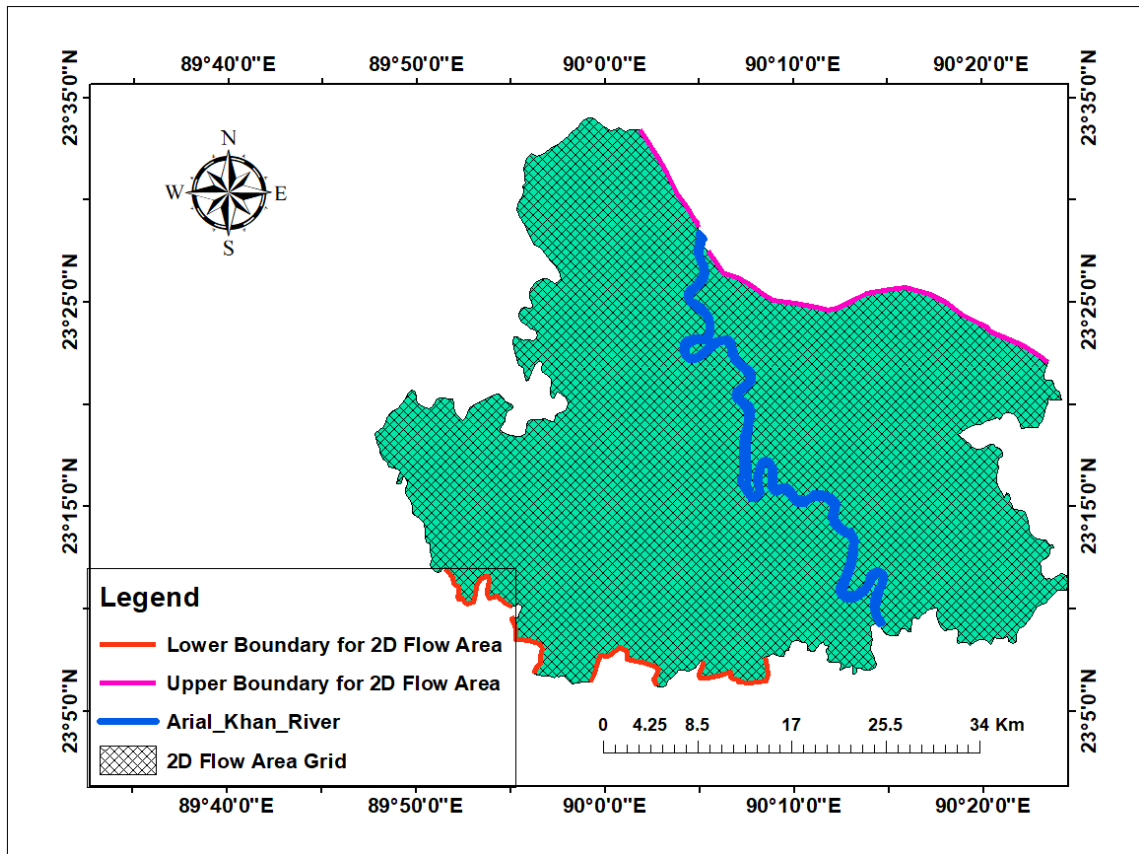


Figure 4.25: Incorporation of upper and lower boundary condition for 2D flow area

Two inflow boundaries are used on the upper left periphery to consider the effect of the Padma River. Stage hydrographs of Goalundo Transit (SW 91.9R) are used as the boundary conditions of these boundaries. Another four boundaries are used in the lower periphery for the purpose of passing out the water from the floodplain. In these boundaries, normal depth condition has been used. The threshold value used for the normal depth is 0.1m.

4.6.6 Model Performance Evaluation

To simulate the model with base and different flow conditions, it is necessary to test the model's performance. This testing provides an idea about the degree of the accuracy of the model in reproducing the real river dynamics. This process is known as calibration. The calibration of hydrodynamic model generally, includes the choice of an appropriate value of roughness coefficient (Manning's 'n') such that simulated values from the model should be close to the observed values in the river (Timbadiya, et al., 2011). Model validation involves testing of the calibrated model with a definite Manning's n with a different set of data. This step is very important before the widespread application of model output.

For calibrating and validating the model, there are many model performance evaluators who assess the model performance quantitatively. In this study, two widely used quantitative statistical performance indicators named Coefficient of Determination (R^2) and Coefficient of Nash-Sutcliffe Efficiency (NSE) have been used for comparison of simulated flow hydro-graph with the observed flow hydrograph for various Manning's "n" (Tazin, 2018).

Coefficient of Determination (R^2)

The coefficient of determination is the proportion of the variance in the dependent variable that is predictable from the independent variable(s). It provides a measure of how well-observed outcomes are replicated by the model, based on the proportion of total variation of outcomes explained by the model. It is denoted as R^2 or r^2 and pronounced "R squared". For simple linear regression, r^2 is used instead of R^2 where r^2 is simply the square of the sample correlation coefficient (i.e., r) between the observed outcomes and the observed predictor values as shown in Eqn. (4-3).

$$r = \frac{n(\sum(xy) - (\sum x)(\sum y))}{\sqrt{[n\sum x^2 - (\sum x)^2][n\sum y^2 - (\sum y)^2]}} \quad (4-3)$$

Where, x is the observed value for the constituent being evaluated, and y is the simulated value for the constituent being evaluated.

If additional regressors are included, R^2 is the square of the coefficient of multiple correlation. An R^2 of 0 means that the dependent variable cannot be predicted from the independent variable. An R^2 of 1 means the dependent variable can be predicted without

error from the independent variable. An R^2 between 0 and 1 indicates the extent to which the dependent variable is predictable. An R^2 of 0.10 means that 10 percent of the variance in y is predictable from x ; an R^2 of 0.20 means that 20 percent is predictable; and so on. Typically values greater than 0.5 are considered acceptable (Legates & McCabe, 1999).

Nash-Sutcliffe Efficiency coefficient (NSE)

The Nash-Sutcliffe efficiency (NSE) is a normalized statistic that determines the relative magnitude of the residual variance (noise) compared to the measured data variance (information) (Nash & Sutcliffe, 1970). NSE is computed as shown in Eqn. (4-4).

$$NSE = 1 - \left[\frac{\sum_{i=1}^n (y_i^{obs} - y_i^{sim})^2}{\sum_{i=1}^n (y_i^{obs} - y^{mean})^2} \right] \quad (4-4)$$

Where, y_i^{obs} is the i th observed value for the constituent being evaluated, y_i^{sim} is the i th simulated value for the constituent being evaluated, y^{mean} is the mean of the observed data being evaluated and n is the total number of the observations.

Nash–Sutcliffe efficiency coefficient ranges from $-\infty$ to 1. An efficiency of 1 ($NSE = 1$) corresponds to a perfect match of modeled discharge to the observed data. The closer the model efficiency is to 1, the more accurate the model is. Values between 0.0 and 1.0 are generally viewed as acceptable levels of performance, whereas values <0.0 indicates unacceptable performance. Generally, threshold values have been suggested between $0.5 < NSE < 0.65$ to indicate a model of sufficient quality (Moriasi, et al., 2007). Previously, it is used by Parhi (2012) and Tazin (2018) for comparing simulated flow with the observed flow for different n value (Parhi, et al., 2012; Tazin, 2018).

4.7 Preparation of Flood Inundation, Hazard and Risk Maps

4.7.1 Flood Inundation Classification

The depth files are exported directly from RAS-Mapper. Later they are processed in ArcGIS. In this study Inundated are classified into five classes: F0 (0-0.3 m), F1 (0.3 m-0.9 m), F2 (0.9 m-1.8 m), F3 (1.8 m-3.6 m) and F4 (>3.6 m). This inundation classification is developed by the National Water Management Plan (NWMP). Later, this classification is used in many flood studies of Bangladesh (Tazin, 2018; Rouf, 2015; IWM, 2014; DDM, 2016).

4.7.2 Selection of Indicators

Hazard Indicator

Generally, flood hazard assessment is the calculation of adverse effects of flooding for a particular area. One or more parameters, such as flood depth, flood duration, flood wave velocity and rate of rise of water level can be used to estimate flood hazard. The selection of the hazard parameters mainly depends on the characteristics of the study area and flood (UN, 1991). In this study, flood hazard has been prepared on the basis of flood depth.

Indicator of Exposure & Vulnerability

Indicator of Exposure

The indicators of Exposure are selected following the exposure definition of IPCC AR5 (IPCC, 2014) which defines exposure as the presence of people, livelihoods, environmental services, infrastructure and other resources that could be adversely affected by a potential hazard. The indicators selected for this study are – population density, number of households and proportion of cropped land as shown in Table 4.2.

Indicator of Vulnerability

Similar to exposure, the indicators of vulnerability are also chosen according to the vulnerability concept of AR5. There are ongoing scientific debates on how best to quantify vulnerability and which indicators should be included (Birkmann, 2014). However, the social vulnerability index has emerged as a most widely accepted and implemented approach (Cutter, et al., 2003; Cutter & Finch, 2008; Chen, et al., 2013). Related indexes typically draw on Census data, which provides a regular, transparent, homogeneous sampling of socio-economic conditions at the national scale. Here, the approach of the social vulnerability index is broadly followed, and Population Census 2011 and Agriculture Census 2008 are used to quantify 11 indicators representing the socio-economic components of vulnerability for flood across all Upazilas of the study area as given in Table 4.2.

The selection of these indicators are made on the basis of the type of the hazard encountering (in this study, flood hazard) and knowledge and perception on the local communities and their livelihoods and their relation with flood risk assessment. The list has also been improved looking into various literatures, expert opinion, and data

availability. These selected indicators are used in the risk assessment of many recent studies (Allen, et al., 2016; Jahan, 2018; Kabir, et al., 2017).

Table 4.2: List of Indicators used in this study

Hazard	Exposure	Vulnerability	
		Sensitivity (-) ¹	Adaptive Capacity (+) ¹
Flood Depth	Population Density	Disable Population	Paka and Semi Paka House
	No. of Household	Dependent Population Ratio	Communication Infrastructure
	Cropped Land	Female to Male Ratio	Crop Productivity
		Poverty Rate	Literacy Rate
			Health Centre
			Flood Shelter
			Growth Centre

Among these 11 indicators, 4 are the indicators of Sensitivity, and the rest are the indicators of Adaptive capacity. The sensitivity indicators are giving positive dependency on estimating vulnerability while Adaptive capacity is providing the negative dependency. Broadly, positive (+) dependency defines that an increase in the variable indicates an increase in vulnerability whereas negative (-) dependency defines that an increase in the measured variable indicates a decrease in vulnerability. This approach of quantifying vulnerability in terms of positive and negative dependency is introduced by (Cutter, et al., 2003) and used by (Allen, et al., 2016) and (Jahan, 2018) for vulnerability assessment.

¹ A positive (+) dependency means that an increase in the variable indicates an increase in vulnerability whereas a negative (-) dependency means that an increase in the measured variable indicates a decrease in vulnerability.

4.7.3 Normalization of the Indicators

Normalization is essential to ensure that all indicators in the particular index are comparable among each other regardless of their units of measurement (Kabir, et al., 2017). In this study, for each of the indicators of hazard, exposure, and vulnerability, a normalized index is established with dimensionless values ranging from 1 (indicating low value) to 100 (indicating high value), ensuring all components contribute an equal weighting to the final risk index. For each indicator (I), Upazila values (I_t) are normalized (I_{nor}) to values in a common range of 1 to 100 using Eqn. (4-5) and Eqn. (4-6) as used by (Jahan, 2018).

$$I_{nor} = 1 + \frac{(I_t - I_{min})(100-1)}{(I_{max} - I_{min})} \quad (4-5)$$

In the case of high values indicating higher vulnerability (positive dependency) or:

$$I_{nor} = 1 + \frac{(I_{max} - I_t)(100-1)}{(I_{max} - I_{min})} \quad (4-6)$$

In the case of high values indicating reduced vulnerability (negative dependency).

After normalization, a weighted score is given to each of the indicators. Weighting is very important in the development of a composite index to ensure the most influential indicators that are treated differently from the other indicators and vice versa (Kabir, et al., 2017). In this study, equal weighting is given to all indicators, such that the final vulnerability index (VI) and exposure index (EI) for each Upazila is calculated as the average across all normalized scores as shown in Eqn. (4-7).

$$VI \text{ or } EI = \frac{\sum I_{nor}}{N} \quad (4-7)$$

4.7.4 Risk Assessment

In this study, flood risk has been assessed following the IPCC concept of climate risk according to the 5th assessment report of IPCC where flood risk (R) is calculated as the consequence of the physical hazard (H), intersecting with vulnerable (V) and exposed people (E) as shown in Eqn. (4-8). This approach of integrated flood risk assessment is a new concept which has been recently adopted by some recent studies like Koks, et al. (2015) and Allen, et al. (2016).

$$R = H * E * V \quad (4-8)$$

Finally, hazard, exposure, vulnerability, and risk have been classified into five categories, maintaining an equal interval for each case, 0-20, 20.01-40, 40.01-60, 60.01-80 and 80.01-100 for Very Low, Low, Medium, High and Very High respectively. By this categorization, Upazila-wise hazard, exposure, vulnerability and risk maps have been prepared in ArcGIS.

CHAPTER 5

RESULTS AND DISCUSSIONS

5.1 Calibration and Validation of the Ganges-Brahmaputra-Padma 1D model

In this study, the one-dimensional model of the Ganges-Brahmaputra-Padma River system has been calibrated and validated for the year of 2016 and 2017 respectively. Flow hydrograph and stage hydrograph are used as the upstream and downstream boundary condition respectively. Then, the mean daily discharge data at the observed station is compared with the model simulated daily discharge. Generally, the water level time series is compared instead of the flow series. However, this study flow is used for calibration and validation because the flow will be further used for projecting future flow at the Offtake of Arial Khan River. The model is calibrated and validated at Mawa (SW 93.5L) gauge station of Padma River. This station is selected for calibration and validation because the statistical equation of Arial Khan Offtake (Chowdhury Char SW 4A) has been developed with respect to this station of Padma River.

5.1.1 Calibration

In this study, simulation is made for the one dimensional model of the Ganges-Brahmaputra-Padma River using the daily hydrograph for six months from May to October. Manning's n is the main calibration parameter of the HEC-RAS model.

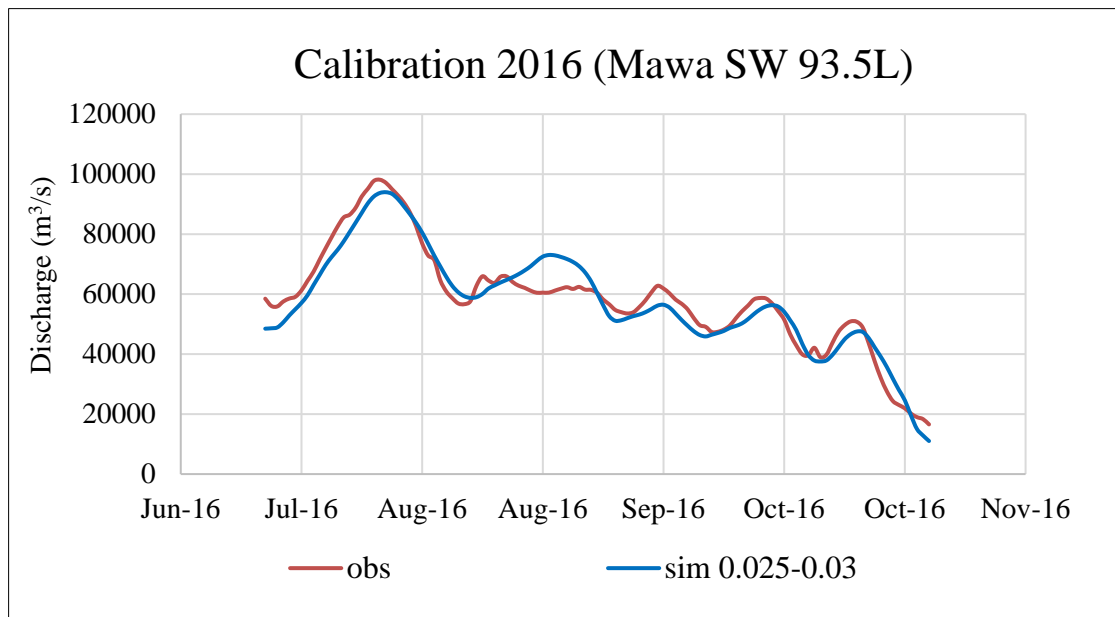


Figure 5.1: Calibration of the Ganges-Brahmaputra-Padma 1D model

Various sets of Manning's roughness coefficients, $n = 0.015 - 0.02$, $0.02 - 0.025$, $0.025 - 0.03$, $0.03 - 0.035$ are adopted for various simulations. All simulations are run in unsteady state condition. Finally, the roughness of $n = 0.025$ for the main channel and $n = 0.03$ for the floodplains has been fixed for all the rivers of the system. The comparison of observed and simulated flow hydrograph at Mawa (SW 93.5L) station for various Manning's n is shown in Figure 5.1.

Apart from the visual comparison, the model has been assessed statistically as well using two widely used statistical indicators - Coefficient of Determination (R^2) and Nash Sutcliffe Efficiency (NSE). The values of R^2 and NSE have been found 0.9168 and 0.9138 respectively which indicate that the simulated value is very close to the observed value and also within the satisfactory range.

5.1.2 Validation

Using the calibrated Manning's roughness coefficient (n) value, validation has been performed for the year 2017. The validation has also shown a satisfactory result. The comparison of observed and simulated discharge hydrograph at Mawa (SW 93.5L) is shown in Figure 5.2. Figure 5.2 shows the simulated stage hydrograph is in close agreement with observed hydrograph. In the case of validation, the coefficient of determination R^2 and Nash and Sutcliffe Efficiency (NSE) have been found 0.8212 and 0.7424 respectively which indicate that the validated value is closer to the observed value.

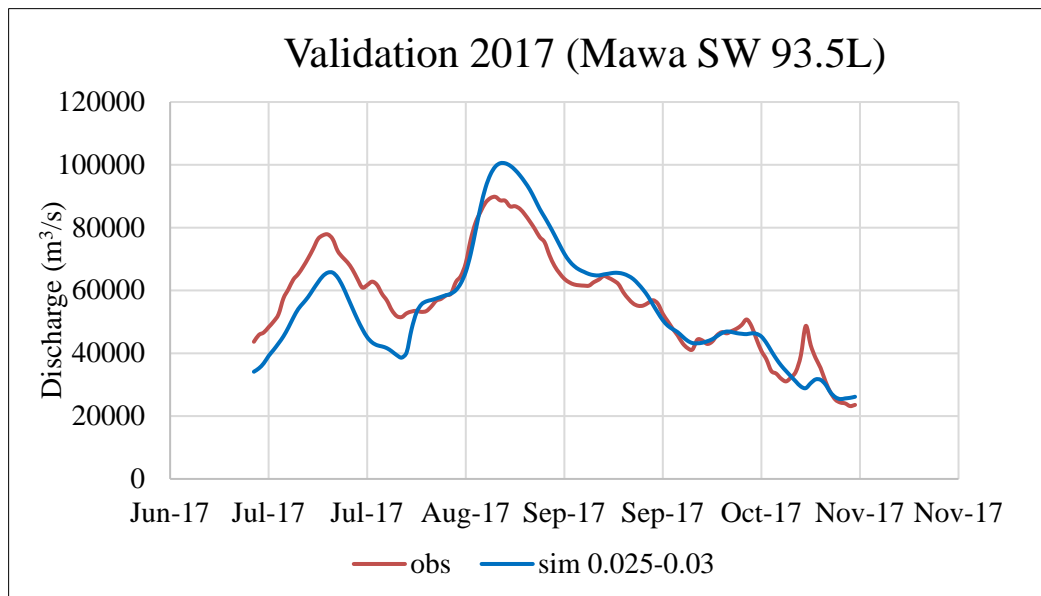


Figure 5.2: Validation of the the Ganges-Brahmaputra-Padma 1D model

5.2 Calibration and Validation of Arial Khan 1D-2D coupled Model

5.2.1 Calibration & Validation of the 1D Model

In this study, the calibration and validation of the one-dimensional model of Arial Khan River 1D-2D coupled model are done for the year 2015 and 2017 respectively. Flow hydrograph and stage hydrograph are used as the upstream and downstream boundary condition respectively. Then, the mean daily water level data at the observed station is compared with the model simulated daily water level. Since there is no intermediate hydrologic station in between upstream Chowdhury Char (SW 4A) and downstream Madaripur (SW 5) station, calibration has been done in upstream Chowdhury Char (SW 4A) station.

Calibration

One dimensional model of Arial Khan River has been simulated using the daily hydrograph for twelve months from January to December. Manning's n is the main calibration parameter of the HEC-RAS model. Hence, various Manning's roughness coefficients, $n = 0.010-0.15, 0.015-0.02, 0.02-0.025, 0.025-0.03, 0.03-0.035$ are adopted for various simulations. All simulations are run in the unsteady state. The result shows that the upstream water surface elevation is increased by increasing Manning's roughness coefficient value. These are consistent with the law of water flowing.

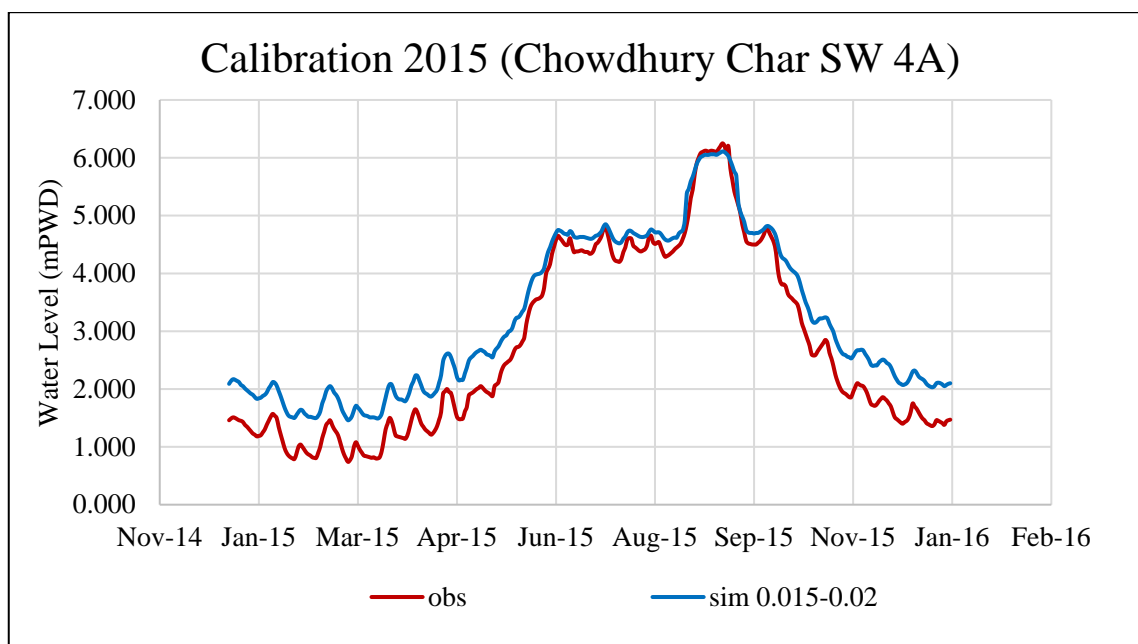


Figure 5.3: Calibration of the Arial Khan 1D model

The simulated hydrograph of $n = 0.015$ for the main channel and $n = 0.02$ for the floodplain matches more accurately with the observed hydrograph. The comparison of observed and simulated stage hydrographs at Chowdhury Char (SW 4A) station for Manning's 'n' are shown in Figure 5.3. Figure 5.3 shows that the trend and shape of the observed and hydrograph are almost similar. The simulated water level and observed water level almost matches in the monsoon period from June to September. There are little differences in the dry season from January to May and October to December. This may be occurred because of the low flow profile at the beginning of the year and the end of the year. However, as the main focus of this study is monsoon flood hazard assessment, so this is almost accepted for our study purpose. The R^2 and NSE values of $n = 0.015-0.02$ are found 0.9974 and 0.892, which are within satisfactory range too.

Validation

Using the calibrated Manning's roughness coefficient (n) value, validation for the model has been performed for the year 2017. The validation has also shown a satisfactory result. The comparison of observed and simulated stage hydrographs at Mawa (SW 93.5L) gauge station is shown in Figure 5.4.

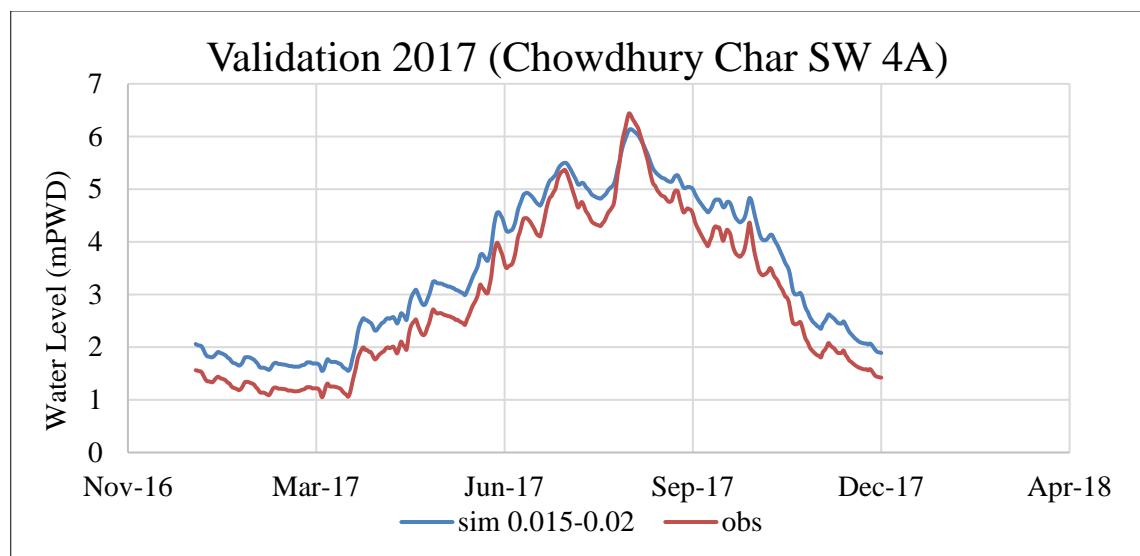


Figure 5.4: Validation of the Arial Khan 1D model

Figure 5.4 shows that the simulated stage hydrograph is in close agreement with observed hydrograph where there were slight differences in simulated water level and observed water level as like as calibration. In unsteady validation, the coefficient of determination R^2 and NSE have been found 0.989 and 0.882 respectively which indicate a good

correlation between the observed and simulated data and indicates the model's accuracy for further analysis.

5.2.2 Comparison of 2D Flood Inundation

After the calibration and validation of the 1D model, a 1D-2D coupled model is set up to simulate the flood inundation in the floodplain. However, it is necessary to validate the

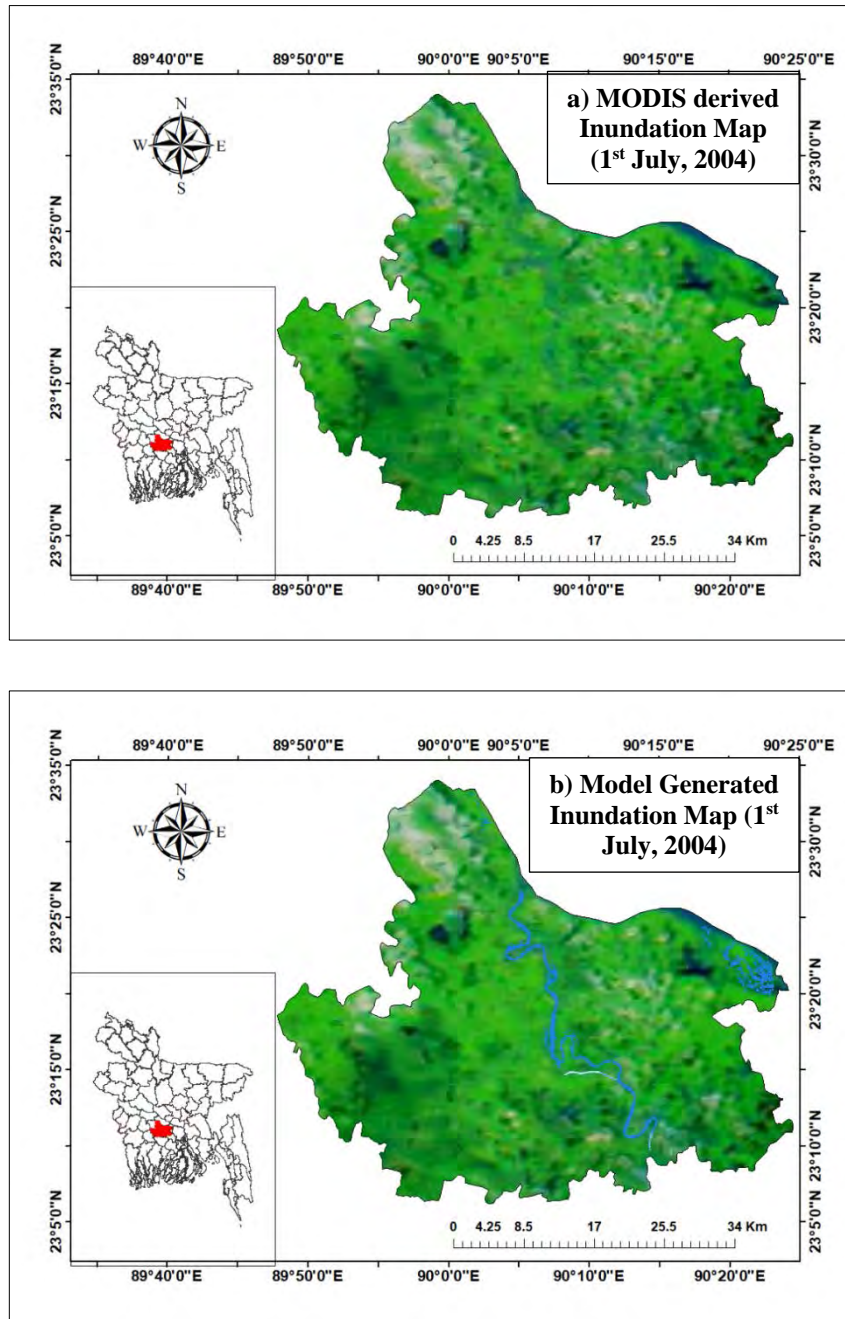


Figure 5.5: Qualitative comparison between a) MODIS derived inundation Map and b) model generated inundation map (before the flood)

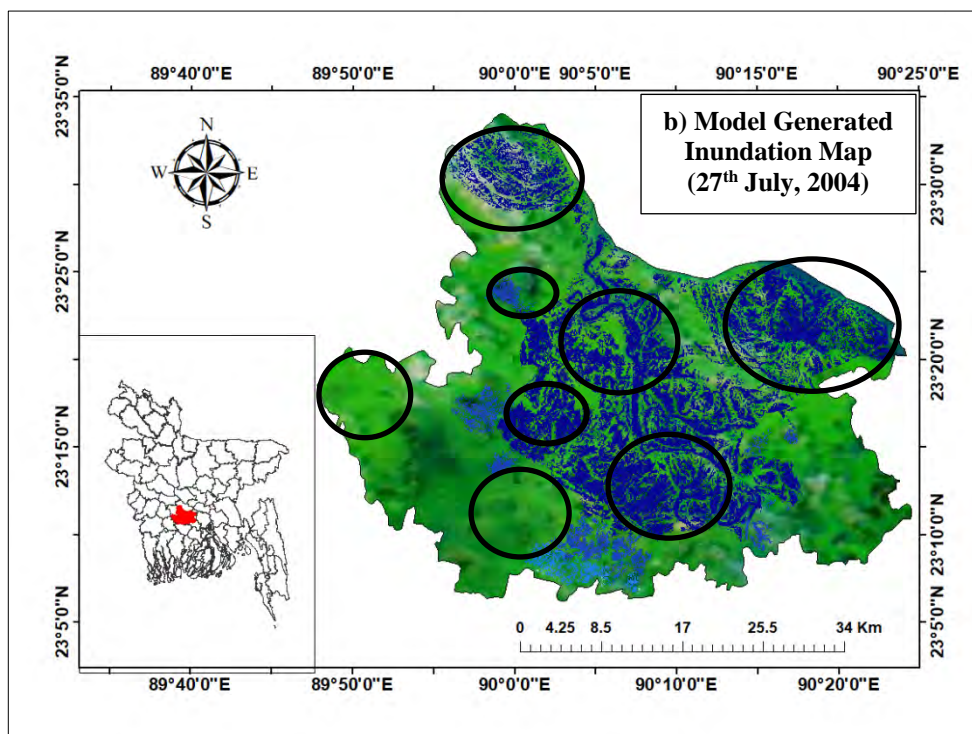
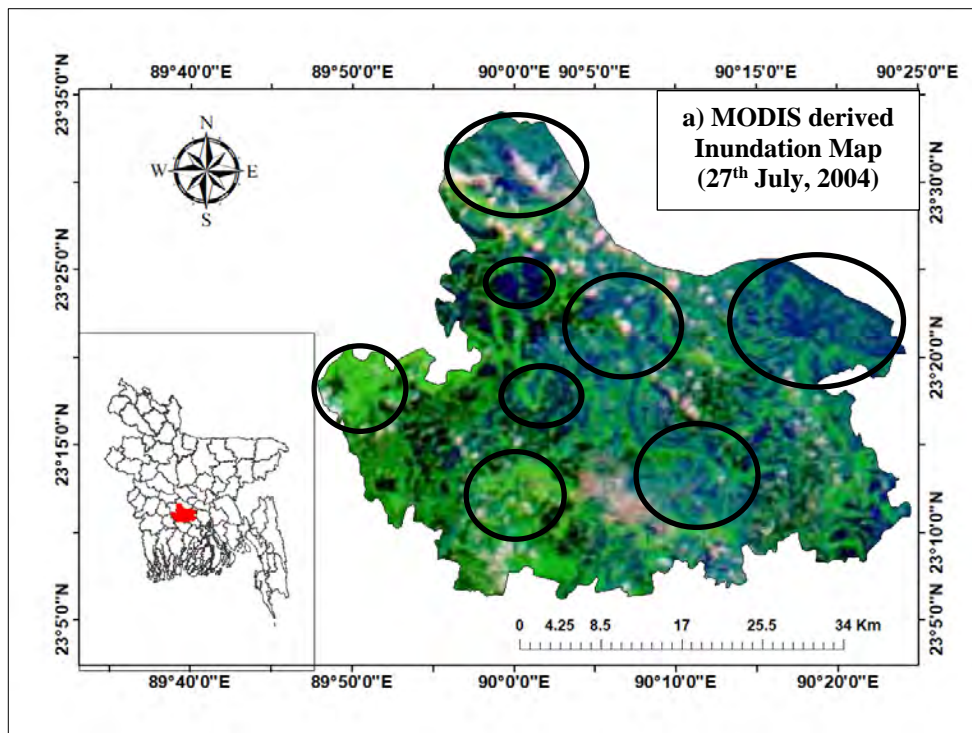


Figure 5.6: Qualitative comparison between a) MODIS derived inundation Map and b) model generated inundation map (during the flood)

simulated 2D flood inundation as well. The 2D flood inundation is usually validated comparing with the available satellite images (Tazin, 2018; Nishat, 2017). In this section, the qualitative comparison is done between the simulated model and observed available satellite image of MODIS. The Qualitative comparison has done for two situations- before flood condition and during flood condition. Figure 5.5 and Figure 5.6 show the comparison between MODIS derived flood inundation map and model generated flood inundation map for both before the flood and during flood conditions respectively.

Here, the green color shows the non-water zone whereas the blue part shows the flood water zone. Figure 5.5 shows that there is no flood in the MODIS inundation map and model generated inundation map on 1st July, 2004. From Figure 5.6 it is observed that the inundation between the MODIS inundation map and model generated inundation map are adequately alike on 27th July, 2004. Common places of the inundated area between observed flood map and model-simulated flood map have been marked by circles for easy visualization. Comparison between observed flood from satellite imagery and model result is found satisfactory.

5.3 Analysis of Historical Flood Events of Arial Khan River

5.3.1 Flood Inundation Maps of Historical Flood Events

After calibration and validation of the 1D-2D coupled model, it has been simulated for the historical flood events of 1988, 1998, 2004, 2007 and 2010. Later, they are used to prepare historical flood inundation maps. On this purpose, inundation depth from 0 to 0.3 is classified as Class 1 (F0), 0.3 to 0.9 m has been classified as class 2 (F1), 0.9 m to 1.8 m inundation depth has been classified as class 3 (F2), inundation depth from 1.8 m to 3.6 m has been classified as class 4 (F3) and inundation depth more than 3.6 m has been classified as class 5 (F4). This inundation classification is developed by the National Water Management Plan (NWMP).

The flood inundation maps of 1988, 1998, 2004, 2007 and 2010 are shown in Figure 5.7, 5.8, 5.9, 5.10 and 5.11 respectively. The summary of the flood affected area of the historical flood events is summarised in Table 5.1.

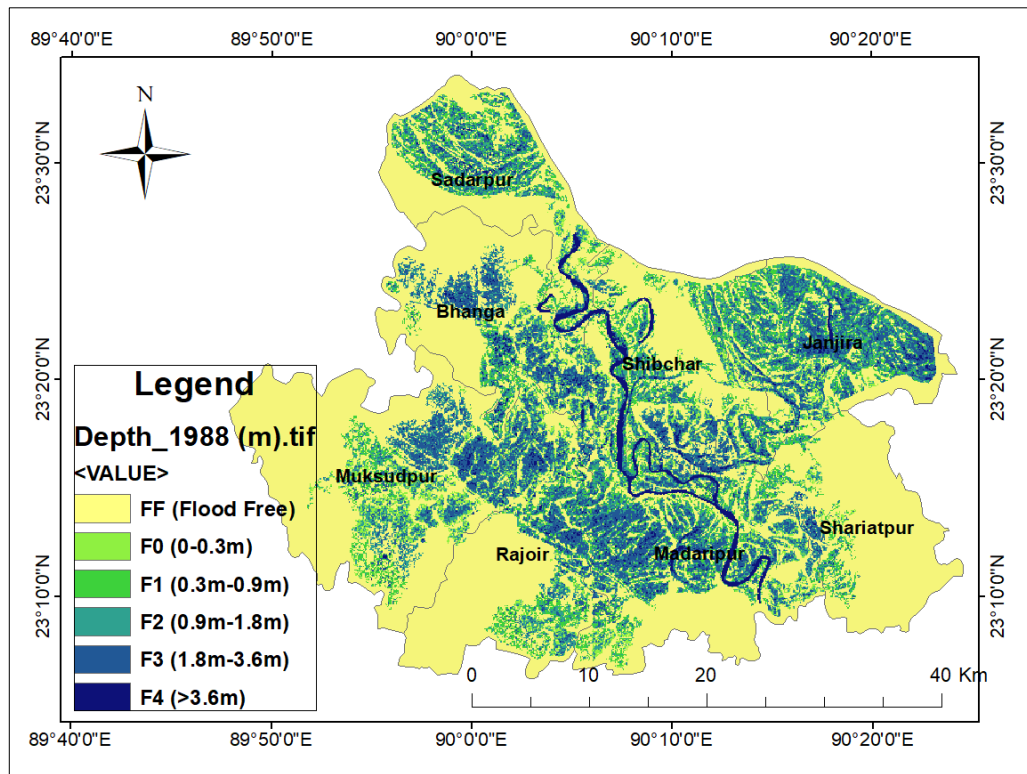


Figure 5.7: Flood inundation map of 1988 based on maximum flood depth

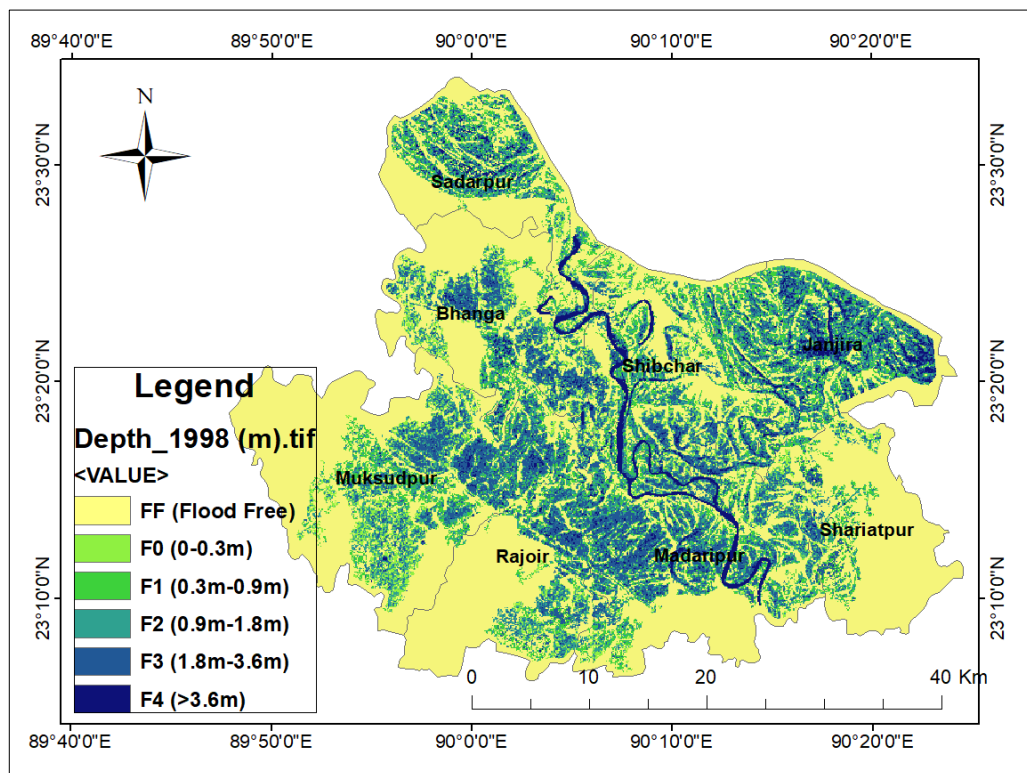


Figure 5.8: Flood inundation map of 1998 based on maximum flood depth

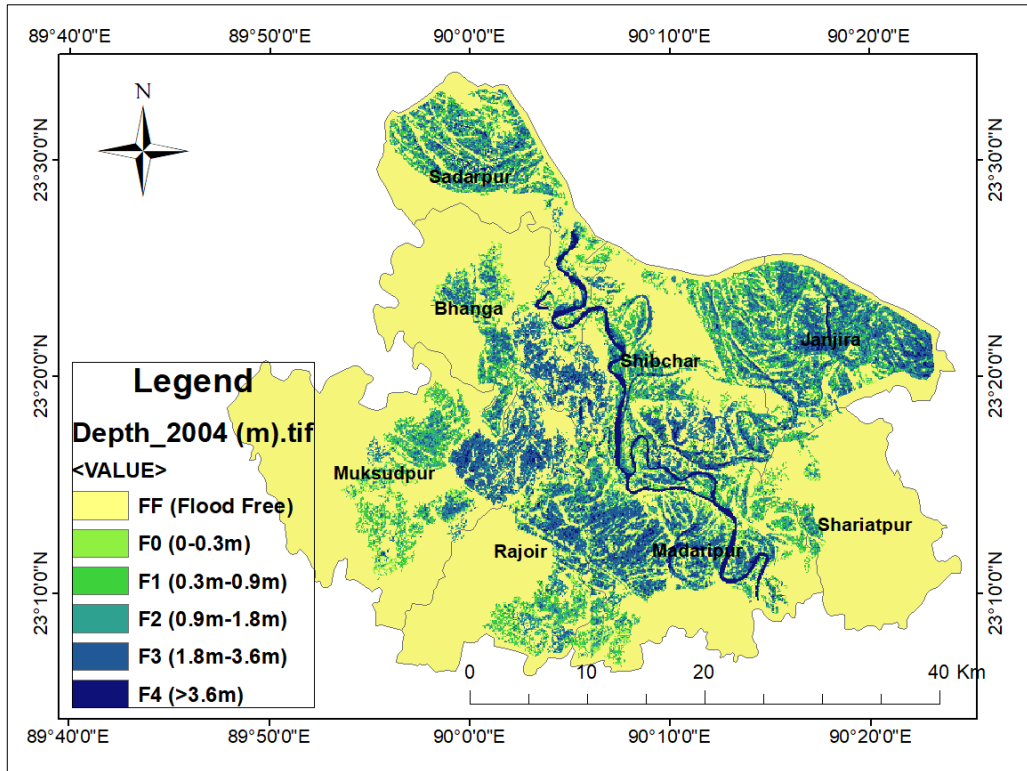


Figure 5.9: Flood inundation map of 2004 based on maximum flood depth

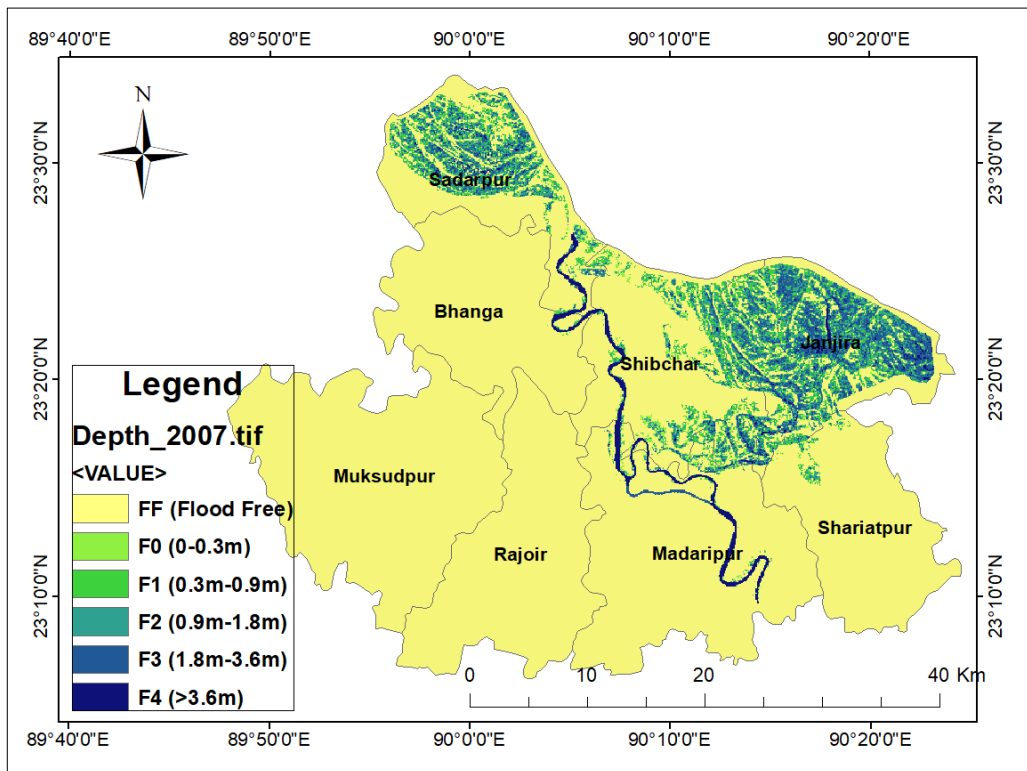


Figure 5.10: Flood inundation map of 2007 based on maximum flood depth

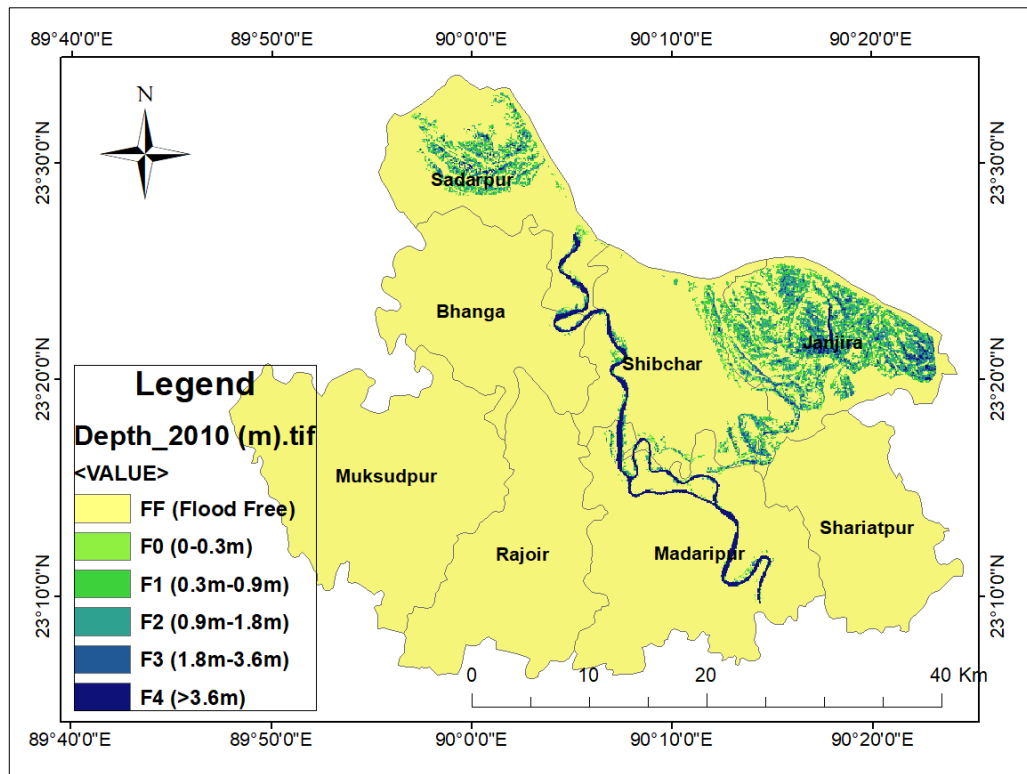


Figure 5.11: Flood inundation map of 2010 based on maximum flood depth

Table 5.1: Flood Affected Areas on the flood of 1998, 1998, 2004, 2007 and 2010

Year	Flood Affected Area (km ²)
1988	584
1998	661
2004	509
2007	212
2010	114

Table 5.1 shows that the flood affected area is the highest for the flood of 1998. The flood inundation area is found nearly 610 km². This result coincides with the real flood statistics of Bangladesh. The flood event of 1998 is considered as the biggest flood event of Bangladesh in the twentieth century. In 1998, over 75% of the total area of the country was flooded. Hence, the flood inundation area and flood depth of 1998 are found the maximum in our study area too. The flood event of 1988 and 2004 was also catastrophic where, 585 km² and 509 km² area were inundated. The flood also occurred in 2007 and 2010, which were not that much catastrophic. Hence, the flood affected area found very

low for these flood events 212 and 114 km² respectively. Upazila wise flood affected areas are also calculated and shown in Table 5.2.

Table 5.2: Upazilla-wise flood affected area for historical flood events

District	Upazila	Flood affected area (km ²)				
		1988	1998	2004	2007	2010
Faridpur	Bhanga	56.86	66.64	44.97	1.59	1.65
	Sadarpur	56.36	58.22	55.25	51.62	19.63
Gopalganj	Maksudpur	72.74	97.30	46.49	0.00	0.00
Madaripur	Madaripur	133.42	139.59	123.42	12.51	11.14
	Rajoir	70.36	74.16	58.78	0.00	0.00
	Shibchar	69.53	82.15	62.82	31.05	11.49
Shariatpur	Shariatpur	13.06	24.45	6.18	2.62	0.09
	Zanjira	111.35	113.49	111.51	112.54	69.93

5.4 Flood Hazard and Risk Assessment of Arial Khan River under Climate Change Scenarios

The future flow hydrographs at the offtake of Arial Khan is generated from the linear regression equation between Arial Khan and Padma. The downstream boundary discharge at Madaripur is fixed with the water level hydrograph of 1998 being the worst flood situation for Arial Khan River. The sea level rise has been incorporated increasing the base value by the future sea level projections of the RCP 2.6 and 8.5 scenarios provided by AR5 of IPCC (Stocker, et al., 2013). Finally, Arial Khan 1D-2D coupled model has been simulated for different time slices: baseline (1976-2005), 2020s (2006-2035), 2050s (2036-2065) and 2080s (2066-2095) of both RCP 2.6 and RCP 8.5. Then, hazard and risk maps are prepared based on those model simulations.

5.4.1 Flood Inundation Assessment for RCP 2.6 & RCP 8.5 Scenario

The flood inundation maps of different periods, base period, 2020s, 2050s and 2080s of RCP 2.6 and RCP 8.5 are shown in Figure 5.12, 5.13, 5.14, 5.15, 5.16, 5.17 and 5.18.

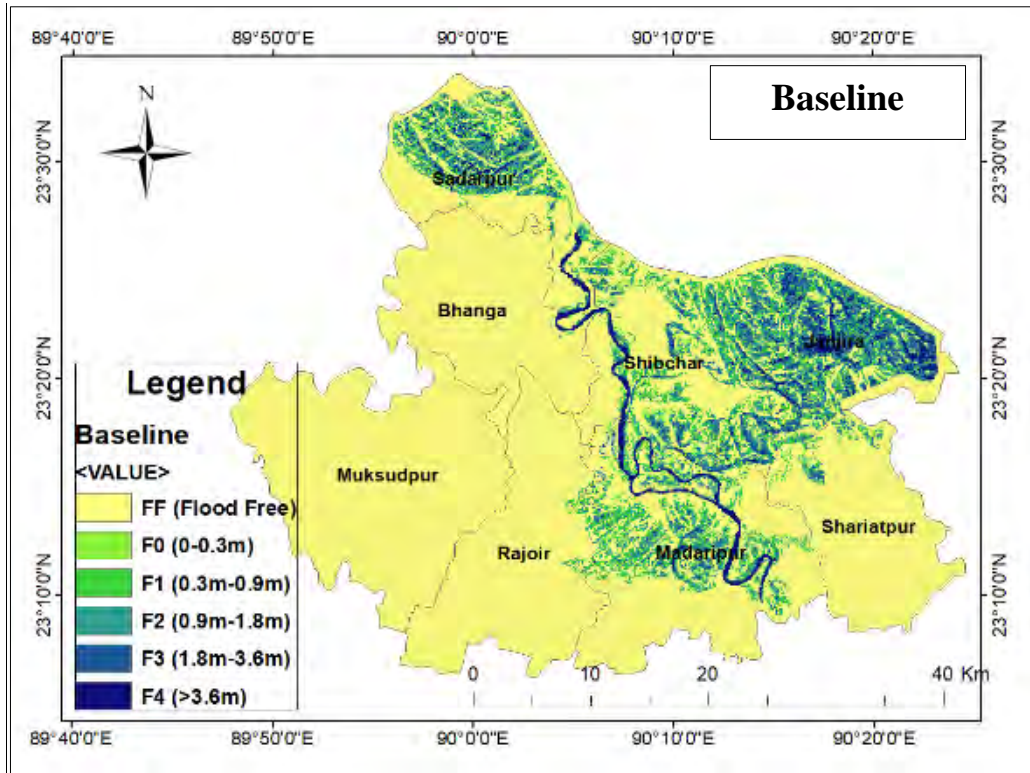


Figure 5.12: Flood inundation map for baseline

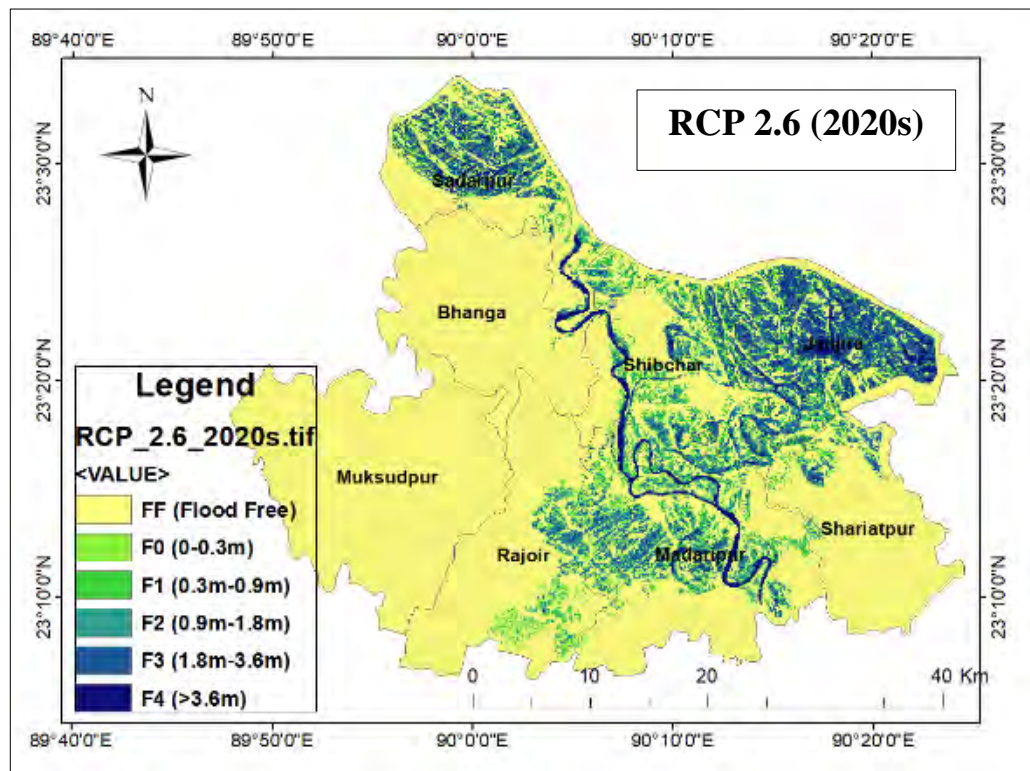


Figure 5.13: Flood inundation map for the 2020s of RCP 2.6

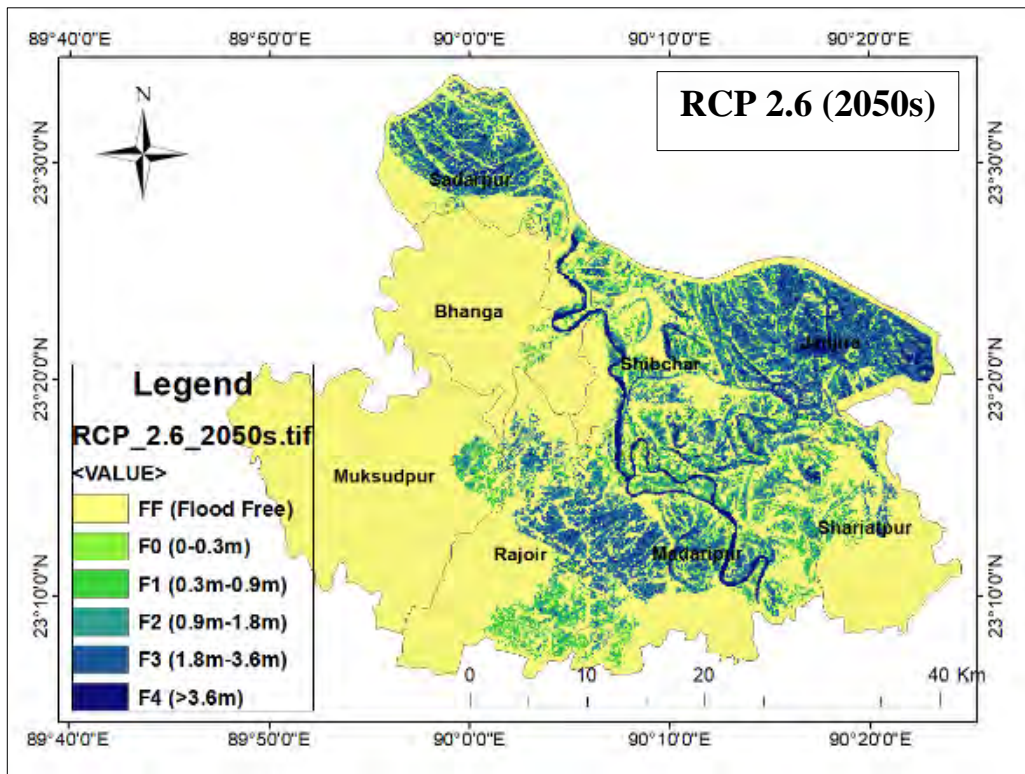


Figure 5.14: Flood inundation map for the 2050s of RCP 2.6

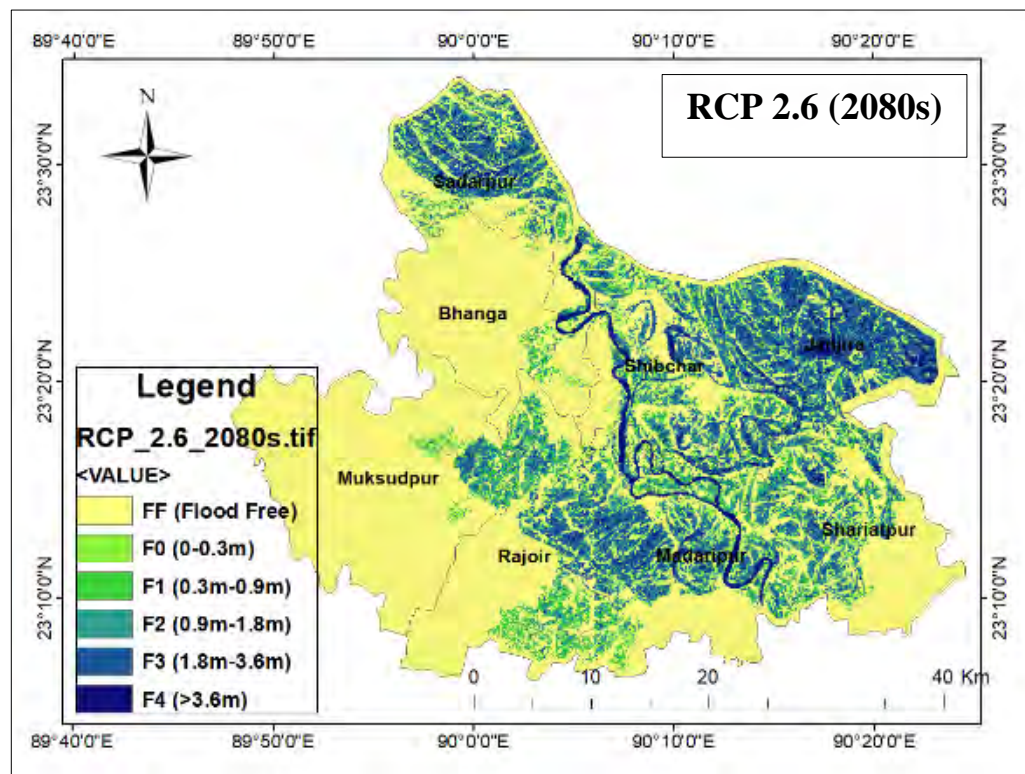


Figure 5.15: Flood inundation map for the 2080s of RCP 2.6

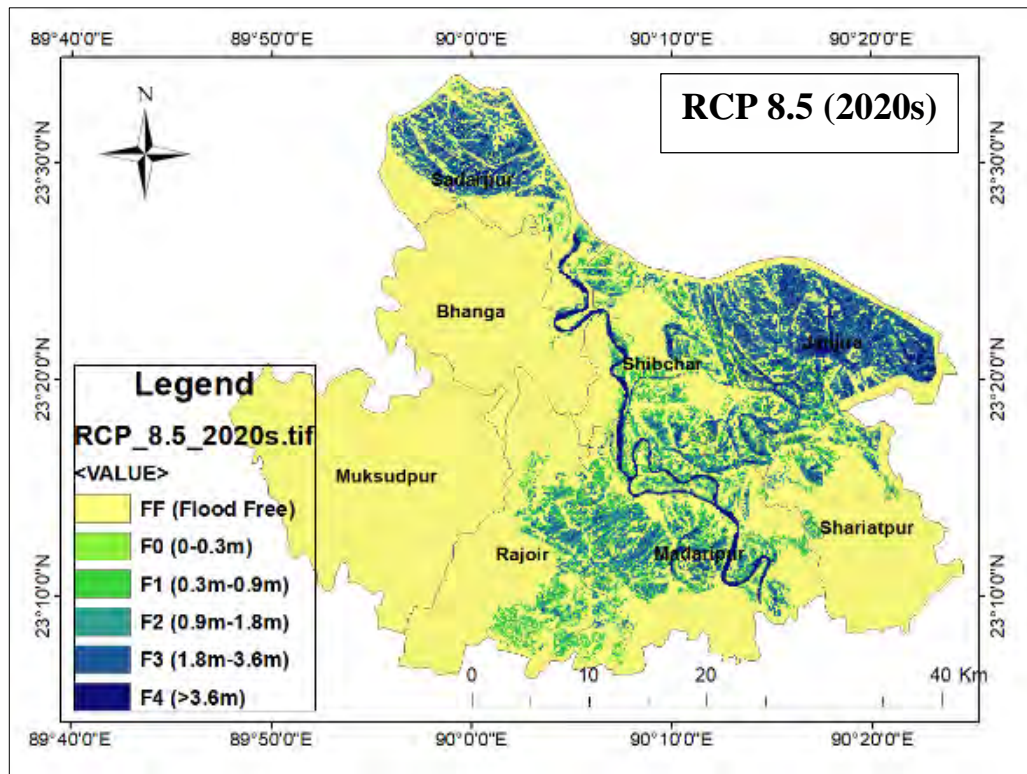


Figure 5.16: Flood inundation map for the 2020s of RCP 8.5

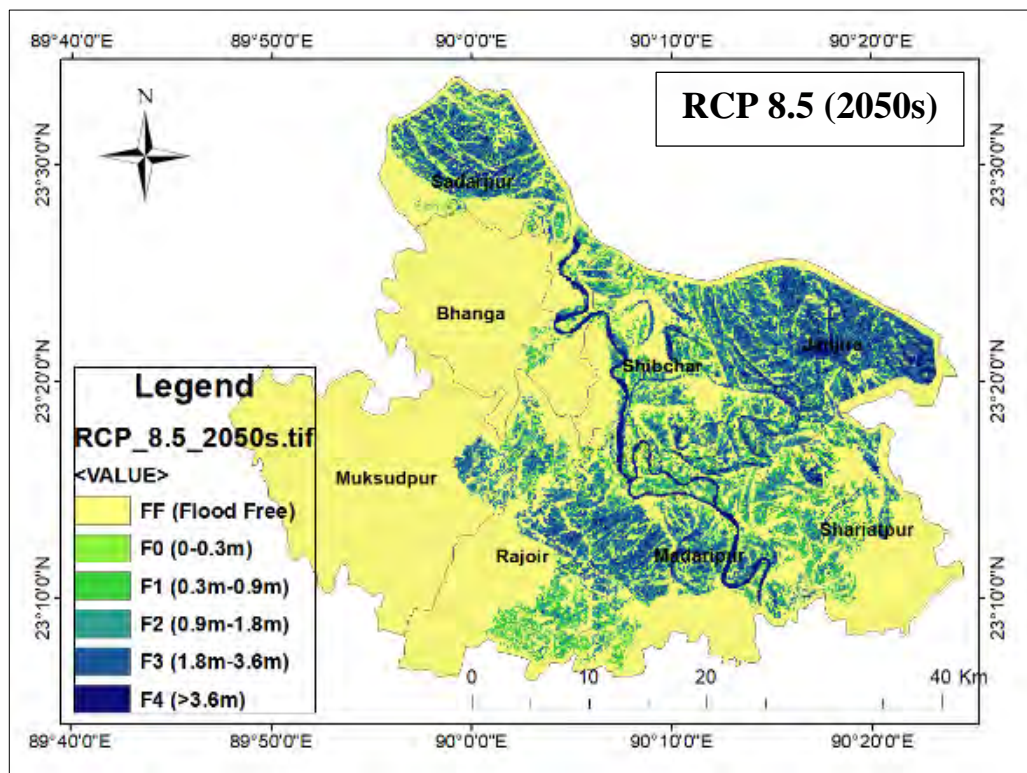


Figure 5.17: Flood inundation map for the 2050s of RCP 8.5

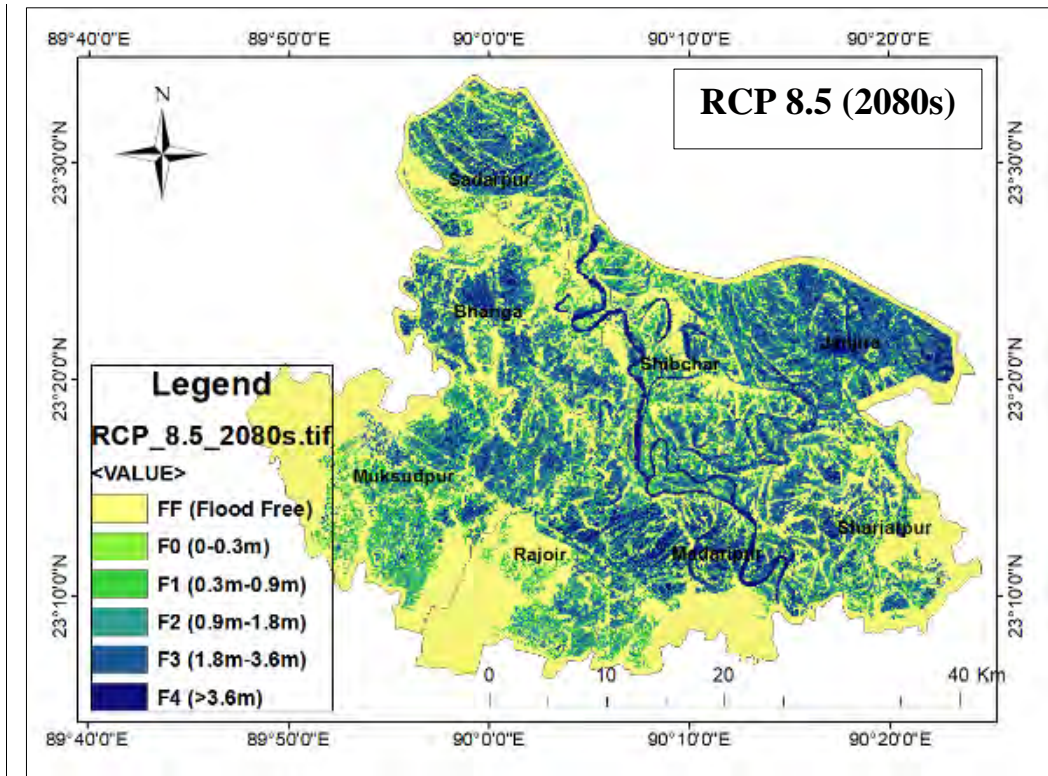


Figure 5.18: Flood inundation map for the 2080s of RCP 8.5

In these inundation maps, flood depths are classified in 5 classes: F0 (0-0.3m), F1 (0.3m-0.9m), F2 (0.9m-1.8m), F3 (1.8m-3.6m) and F4 (>3.6m) as classified by NWMP classification.

The Figures from baseline to 2080s of RCP 2.6 and 8.5 clearly show that, though there is an increasing trend of flood area from baseline to 2080s, both for RCP 2.6 and RCP 8.5. From baseline to 2050s, the difference between RCP 2.6 and RCP 8.5 are slight. However, the difference becomes very violent after the 2050s. The total flood affected area in the 2080s of RCP 2.6 is nearly 550 km² which are 30% of the study area. On the other hand, the total flood affected area in the 2080s of RCP 8.5 is almost 850 km² which are nearly 47% of the whole study area.

Table 5.3 shows the Upazilla-wise flood affected area for each of the periods of RCP scenarios. It shows that, at present condition, only 4 out of 8 Upazila are flooded. They are Sadarpur, Madaripur, Shibchar, and Zanjira. The flood in Bhanga, Rajoir and Shariatpur are very insignificant, and there is no flood in Maksudpur. However, the scenarios increased in magnitude and extent with time.

Table 5.3: Upazilla-wise flood affected area (km²) for RCP 2.6 and RCP 8.5 Scenarios

District Name	Upazila Name	Base Line	Flood Affected Area (km ²)					
			RCP 2.6			RCP 8.5		
			1976- 2005	2020s	2050s	2080s	2020s	2050s
Faridpur	Bhanga	1.91	1.99	4.26	7.85	1.98	4.89	103.13
	Sadarpur	53.51	54.75	75.43	80.03	54.61	77.00	86.16
Gopalganj	Maksudpur	0.00	0.00	7.44	16.78	0.00	7.62	107.95
Madaripur	Madaripur	59.74	79.62	109.27	128.46	84.31	119.08	149.76
	Rajoir	1.82	24.29	38.03	54.65	30.15	47.94	84.26
	Shibchar	49.52	54.67	69.32	78.48	54.75	74.43	102.03
Shariatpur	Shariatpur	5.71	10.96	25.79	45.79	11.05	32.65	60.16
	Zanjira	113.45	113.53	135.24	138.95	113.56	137.48	139.57
Total Area		285.67	339.81	464.77	550.99	350.40	501.10	833.01

The condition significantly exaggerates after the 2050s. The flood affected areas under Bhanga, Sadarpur, Maksudpur, Madaripur, Rajoir, Shichar, Shariatpur and Zanjira are 7.85, 80.03, 16.78, 128.46, 54.65, 78.48, 45.79 and 138.95 km² respectively for RCP 2.6 whereas the flood affected areas for RCP 8.5 are 103.13, 86.16, 107.95, 149.76, 84.26, 102.03, 60.16 and 139.57 km² respectively. So it can be interpreted that the flood affected area is going to increase significantly in the future due to climate change.

5.4.2 Flood Hazard Assessment for RCP 2.6 and RCP 8.5 Scenario

In this study, the flood depth is considered as the hazard parameter. Mean flood depths are calculated for each of the Upazilla of the study area. The mean flood depth varies from 0 to 2 for all the projections of RCP 2.6 and 8.5 (Table 5.4). For a systematic representation, they are normalized in a range of 1 to 100 using Equation (4-5) and tabulated in Table 5.5.

Table 5.4: Upazilla-wise mean flood depth (m) for RCP 2.6 and RCP 8.5 Scenarios

District Name	Upazila Name	Base	Mean Flood Depth (m)					
		Line	RCP 2.6			RCP 8.5		
		1976- 2005	2020s	2050s	2080s	2020s	2050s	2080s
Faridpur	Bhanga	0.06	0.07	0.08	0.12	0.07	0.09	1.14
	Sadarpur	0.78	0.85	0.95	1.09	0.86	0.98	1.31
Gopalganj	Maksudpur	0.00	0.00	0.04	0.08	0.00	0.05	0.64
Madaripur	Madaripur	0.56	0.69	0.93	1.04	0.76	0.96	1.42
	Rajoir	0.02	0.14	0.36	0.44	0.23	0.38	0.77
	Shibchar	0.58	0.67	0.80	0.91	0.68	0.83	1.27
Shariatpur	Shariatpur	0.06	0.12	0.31	0.51	0.14	0.39	0.80
	Zanjira	1.40	1.50	1.62	1.79	1.51	1.66	2.00

Table 5.5: Upazilla-wise normalized flood depth for RCP 2.6 and RCP 8.5 Scenarios

District Name	Upazila Name	Base Line	Normalized Mean Flood Depth					
		1976- 2005	RCP 2.6			RCP 8.5		
		1976- 2005	2020s	2050s	2080s	2020s	2050s	2080s
Faridpur	Bhanga	4.2	4.4	5.2	6.8	4.4	5.5	57.5
	Sadarpur	39.7	43.2	48.0	54.8	43.6	49.7	65.8
Gopalganj	Maksudpur	1.0	1.0	3.0	5.0	1.0	3.6	32.6
Madaripur	Madaripur	28.9	35.2	47.1	52.3	38.8	48.5	71.4
	Rajoir	1.8	8.0	19.1	22.6	12.4	20.0	39.3
	Shibchar	29.8	34.4	40.7	46.3	34.8	42.2	63.7
Shariatpur	Shariatpur	4.0	7.2	16.2	26.4	8.1	20.2	40.7
	Zanjira	70.2	75.3	81.2	89.8	75.9	83.4	100.0

For preparing zone-wise flood hazard maps, the study area is categorized into five hazard zones – 0 to 20, 20.01 to 40, 40.01 to 60, 60.01 to 80 and 80.01 to 100 named as Very Low, Low, Medium, High and Very High hazard zones. The spatio-temporal change of different hazard zones for RCP 2.6 and RCP 8.5 are shown in Figure 5.19, 5.20, 5.21, 5.22, 5.23, 5.24 and 5.25.

Figure 5.19 shows that at the base period, Bhanga, Maksudpur, Shariatpur, and Rajoir were in the very low hazard zone, Sadarpur, Shibchar, and Madaripur were in the low hazard zone, and Zanjira was in the high hazard zone. In the 2080s of RCP 2.6, Bhanga and Maksudpur are in the very low hazard zone, Rajoir and Shariatpur are in the low hazard zone, Sadarpur, Shibchar, and Madaripur are in the medium hazard zone, and Janjira is in the very high hazard zone (Figure 5.22). In the 2080s of RCP 8.5, Madaripur and Rojoir are in the low hazard zone, Bhanga and Shariatpur are in the medium hazard zone, Sadarpur, Shibchar, and Madaripur are in the high hazard zone, and Zanjira is in very High Hazard zone (Figure 5.25). These hazard maps indicate that each of the Upazilla has been degrading to 1 or 2 categories for the RCP 8.5 scenario. Hence, every Upazila has become more hazardous under the future climate change scenario.

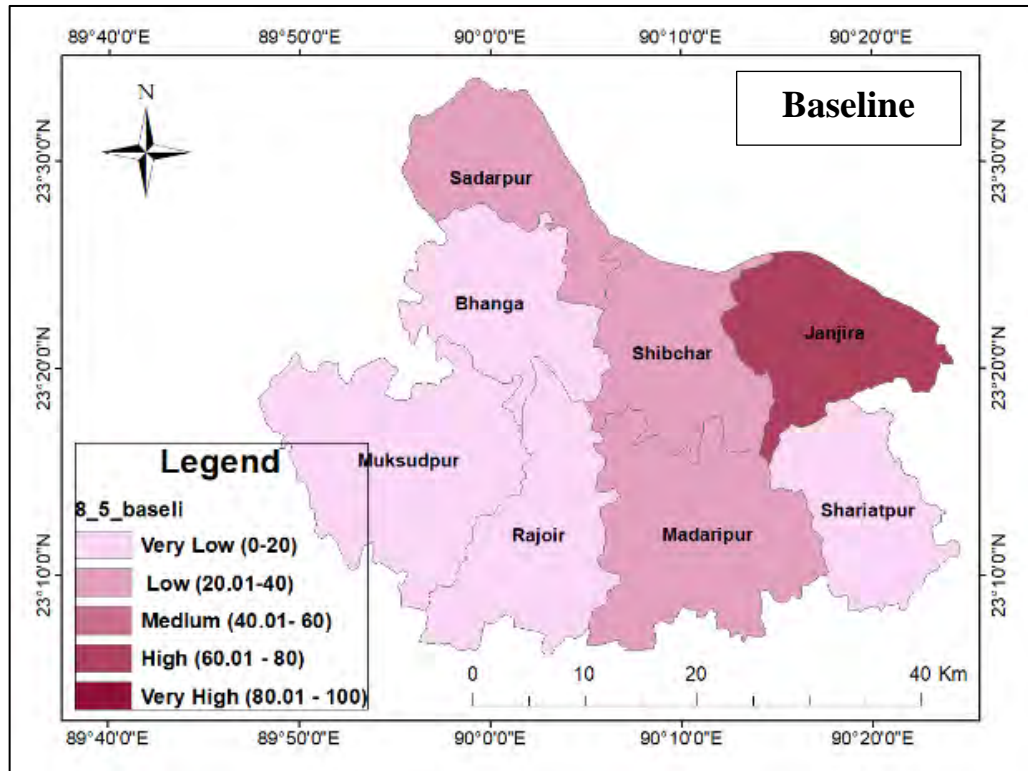


Figure 5.19: Flood hazard map for baseline

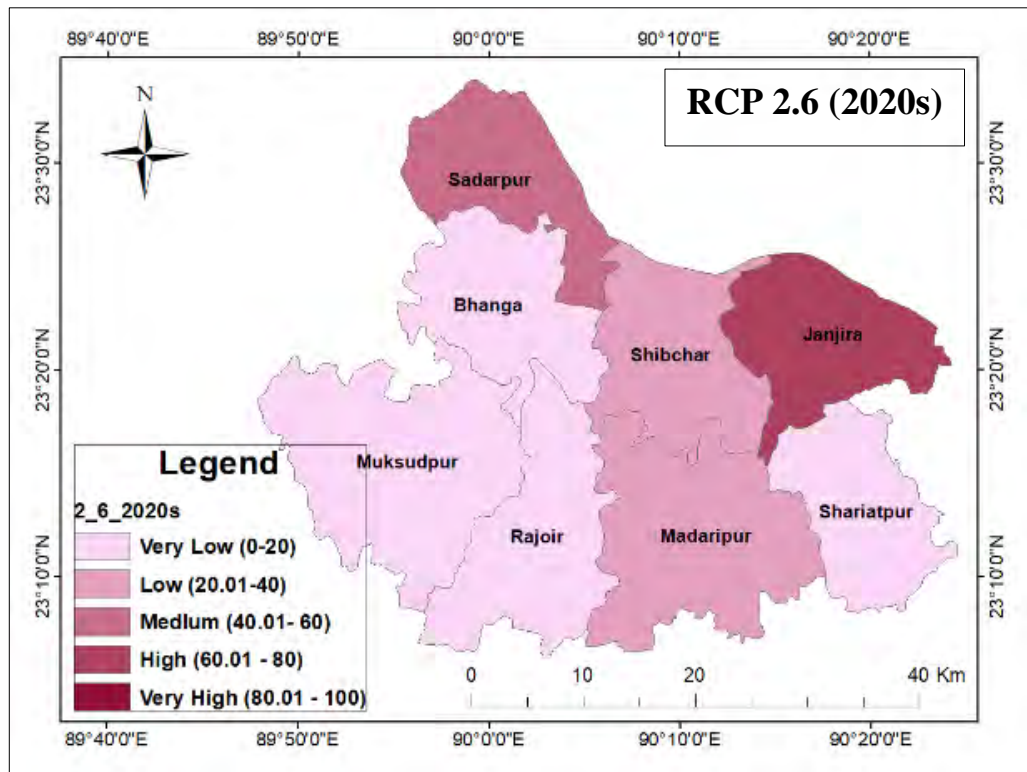


Figure 5.20: Flood hazard map for the 2020s of RCP 2.6

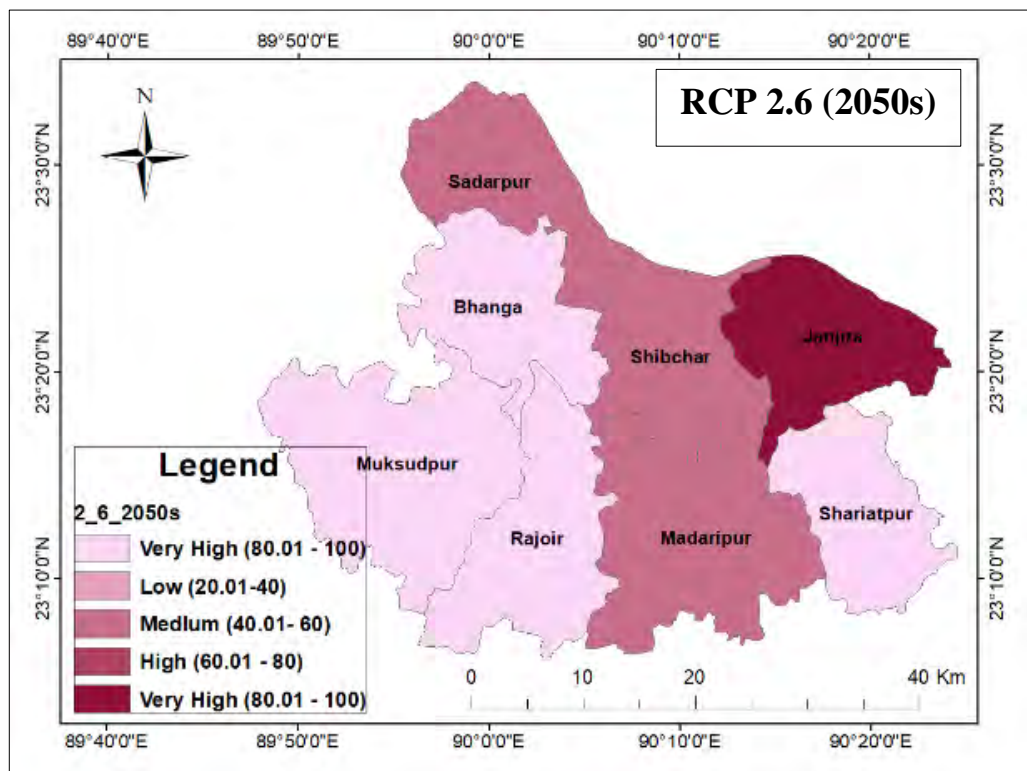


Figure 5.21: Flood hazard map for the 2050s of RCP 2.6

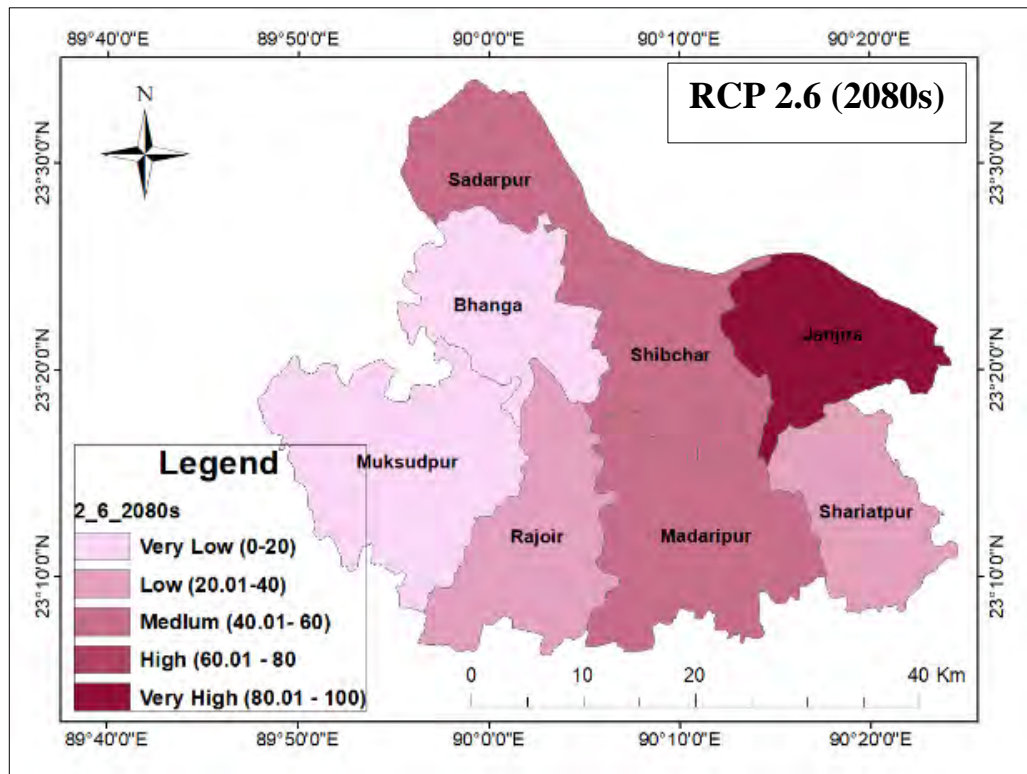


Figure 5.22: Flood hazard map for the 2080s of RCP 2.6

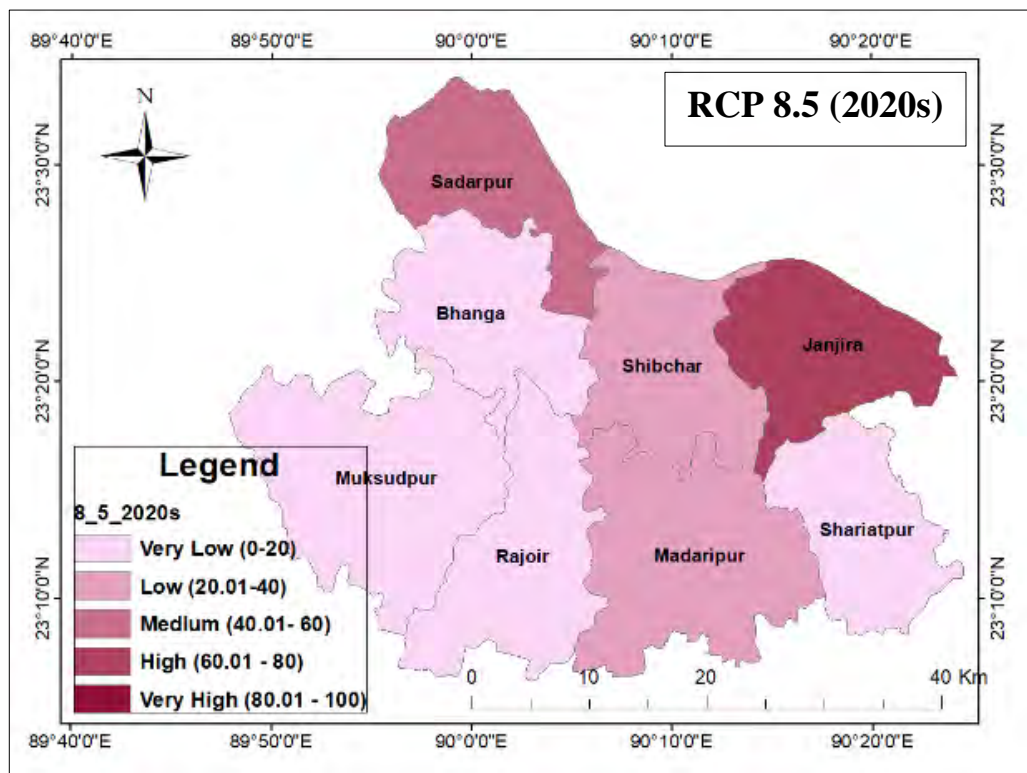


Figure 5.23: Flood hazard map for the 2020s of RCP 8.5

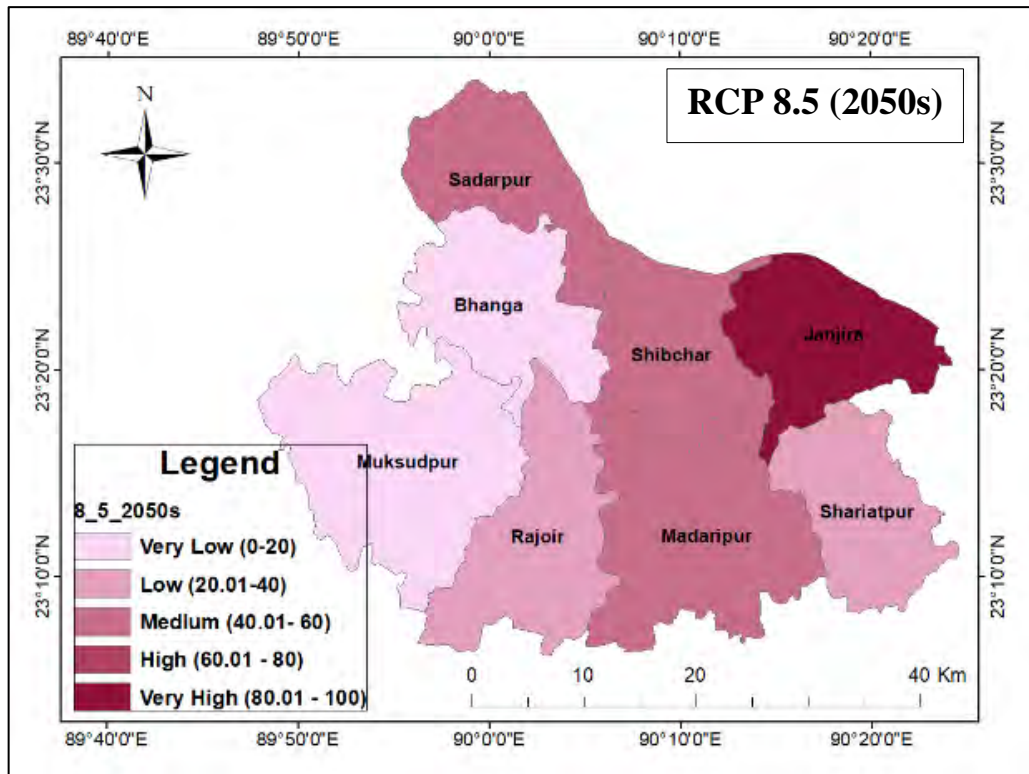


Figure 5.24: Flood hazard map for the 2050s of RCP 8.5

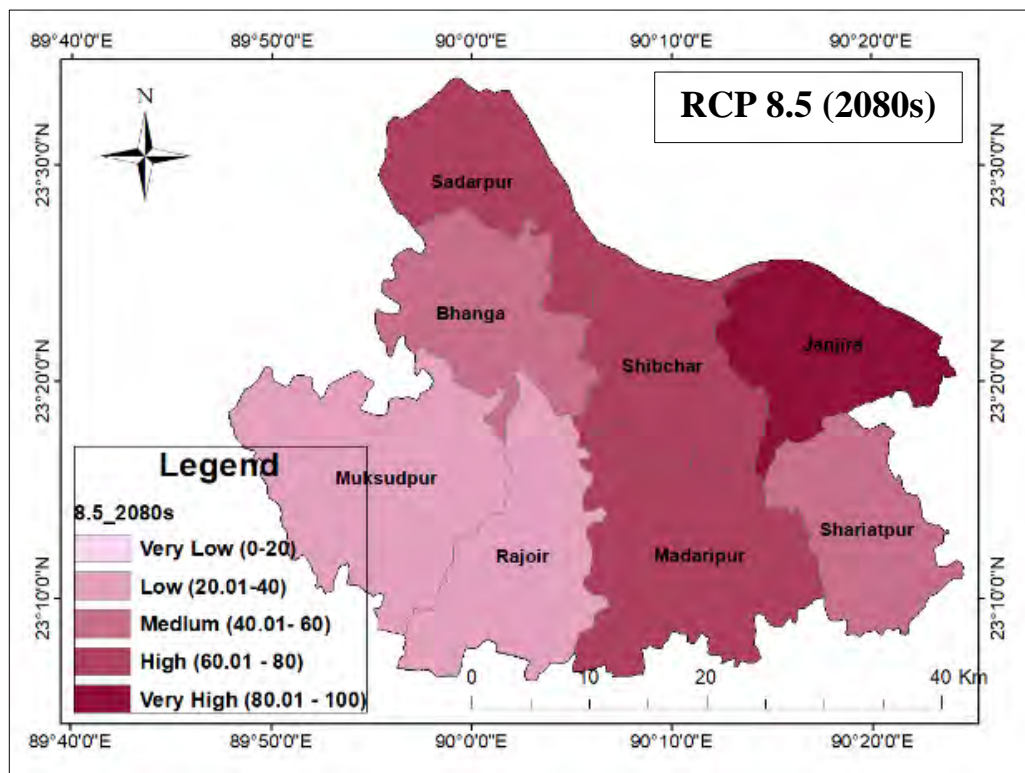


Figure 5.25: Flood hazard map for the 2080s of RCP 8.5

Table 5.6: Percentage of Area under different hazard zones for different projections
RCP 2.6 and RCP 8.5

Scenarios	Period	Percentage of Area				
		Very Low (0-20)	Low (20.01-40)	Medium (40.01-60)	High (60.01 - 80)	Very High (80.01 - 100)
Base Period	1976-2005	48	34	0	18	0
RCP 2.6	2020s	48	24	10	18	0
	2050s	48	0	34	0	18
	2080s	21	27	34	0	18
RCP 8.5	2020s	48	24	10	18	0
	2050s	21	27	34	0	18
	2080s	0	22	26	34	18

The percentage area under different hazard zones for both RCP 2.6 and 8.5 are summarized in Table 5.6. Table 5.6 shows that at base condition 48% area is in the very low hazard zone, 34% area is in the low hazard zone and 18% area is in the High hazard zone. At present condition, there is no area under a very high hazard zone. However, it has changed to 21% in the very low hazard zone, 27% in the low hazard zone, 34% in the medium hazard zone, 18% in the very hazard zone in the 2080s of scenario RCP 2.6.

If we go through the column of the 2080s of RCP 8.5, the scenarios are more alarming. In RCP 8.5, 22% area falls in the low hazard zone, 26% area falls in the medium hazard zone, 34% area is under high hazard zone, and 18% area is under very high hazard zone. So future, climate change will decrease the very low and low hazard zone drastically in the 2080s. On the other hand, high and very high hazard zone will increase due to climate change compared to the baseline in the near future.

5.4.3 Flood Exposure and Vulnerability Assessment

The Upazila-wise magnitudes of different indicators of exposure and vulnerability collected from the BBS Districts Statistics 2011 are tabulated in Table 5.7. Then, they are normalized in a range of 1 to 100 using Equation 4-5 and 4-6 (Table 5.8). The relative contribution of the indicators of exposure and vulnerability are for each of the Upazila are shown in Figure 5.26, 5.27 and 5.28 in the form of bar charts.

Table 5.7: Magnitude of Exposure and Vulnerability Indicators (Source: Population Census 2011 & Agricultural Census 2008)

District	Upazila	Exposure		Vulnerability											
		Populati on density (sq. km)	No. of househol d	Cropp ed land (acre)	Sensitivity (+ dependency)					Adaptive Capacity (- dependency)					
					Disable populati on (%)	Depend ent populati on ratio	Female to male ratio	Poverty rate (%)	Paka and Semi Paka house	Commun ication Infrastru cture	Producti vity of crop	Literacy Rate	Health center	Flood Shelte r	Growt h Centre
Faridpur	Bhanga	1203.07	57164	29001	1.41	41.89	106.69	17.00	29.65	481	167	47.0	11	4	4
	Sadarpur	712.80	40219	28517	1.41	43.11	107.72	20.50	27.73	490	166	43.2	4	3	4
Gopalgonj	Maksudpur	938.52	61807	45296	1.40	42.56	105.32	29.90	16.17	531	141	52.5	13	0	4
Madaripur	Madaripur	1221.15	74451	36627	0.97	41.86	101.81	17.50	22.76	819	163	51.1	14	0	15
	Rajoir	997.52	48764	30002	1.92	41.96	102.34	15.40	22.11	335	152	48.2	5	0	4
	Shibchar	955.88	69623	42988	1.30	42.91	103.33	20.20	24.27	7707	164	43.5	17	0	6
Shariatpur	Shariatpur	1200.82	45883	22441	1.29	42.42	101.88	31.60	19.76	486	147	51.2	12	0	4
	Zanjira	788.01	41715	23301	1.31	45.05	102.02	34.90	7.84	471	160	44.4	9	2	1

Table 5.8: Normalised Values of Exposure and Vulnerability Indicators

District	Upazila	Exposure			Vulnerability										
		Popula tion density	No. of hous ehold	Cropped land	Sensitivity (+ dependency)					Adaptive Capacity (- dependency)					
					Disable populati on	Depen dent popula tion ratio	Female to male ratio	Poverty rate	Paka and Semi Paka house	Commun ication Infrastru cture	Produc tivity of crop	Literacy Rate	Health center	Flood Shelter	Growth Centre
Faridpur	Bhanga	96	50	29	47	2	83	9	1	98	1	60	47	1	79
	Sadarpur	1	1	27	47	40	100	27	10	98	5	100	100	26	79
Gopalganj	Maksudpur	45	63	100	45	23	60	75	62	97	100	1	31	100	79
Madaripur	Madaripur	100	100	62	1	1	1	12	32	94	16	16	24	100	1
	Rajoir	56	26	34	100	4	10	1	35	100	58	47	92	100	79
	Shibchar	48	86	90	36	34	26	25	25	1	12	97	1	100	65
Shariatpur	Shariatpur	96	17	1	35	18	2	83	46	98	77	15	39	100	79
	Zanjira	16	5	5	37	100	4	100	100	98	28	87	62	51	100

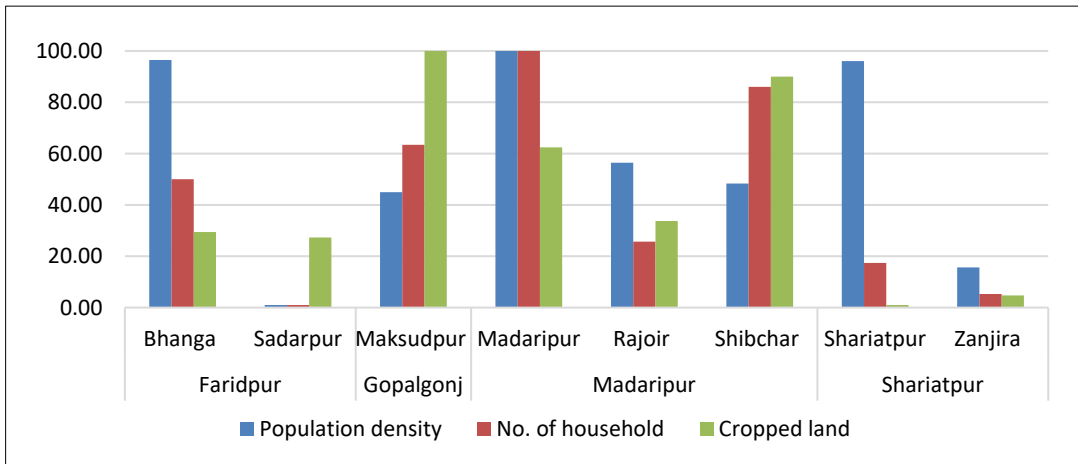


Figure 5.26: Relative contribution of exposure indicators in the study area

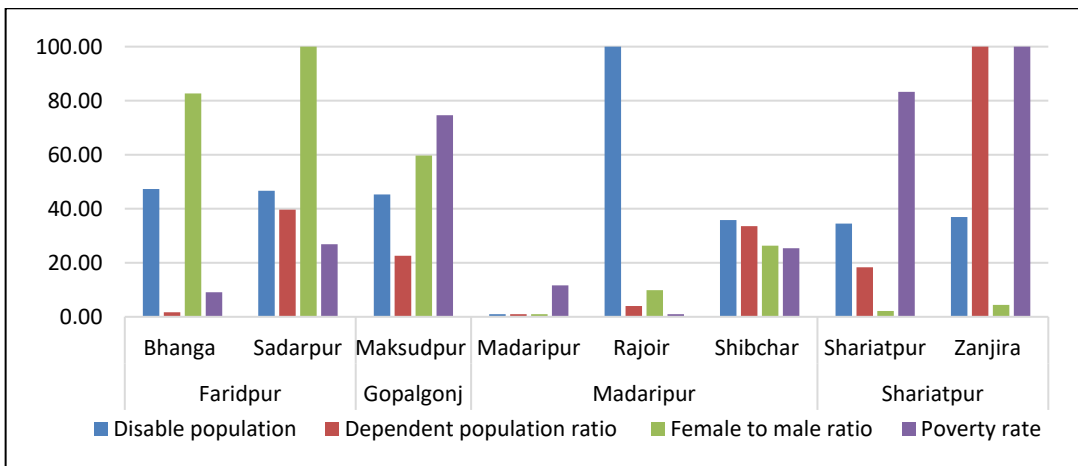


Figure 5.27: Relative contribution of vulnerability indicators (+ve dependency) in the study area

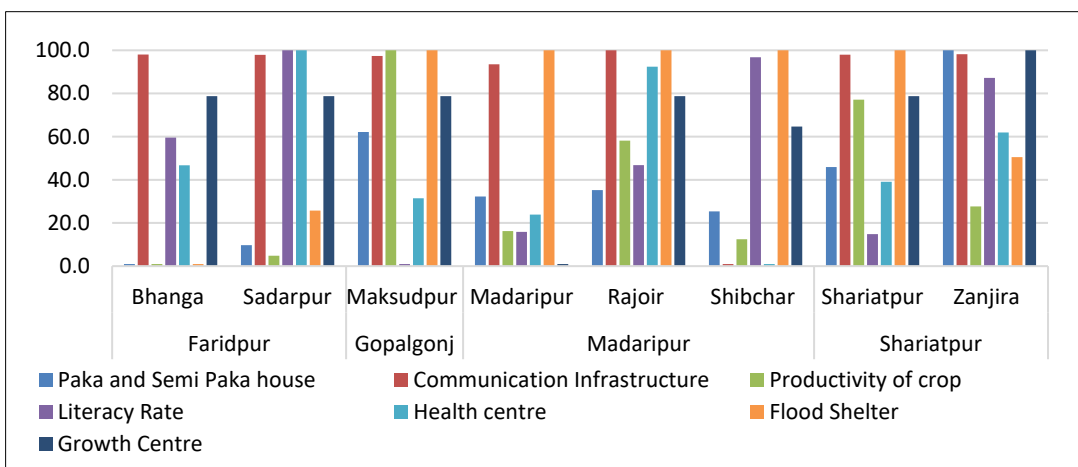


Figure 5.28: Relative contribution of vulnerability Indicators (-ve dependency) in the study area

Final exposure and vulnerability indices are prepared giving equal weight to each of the indicators. Then, the exposure is grouped into five categories, selecting an equal interval of exposure factor. The five categories are Very Low, Low, Medium, High and Very High exposure zones and the exposure factors are 0-20, 21.01-40, 40.01-60, 60.01-80 and 80.01-100, respectively. Similar categorization has been done for the vulnerability as well. Figure 5.29 and 5.30 show Upazila-wise exposure and vulnerability maps.

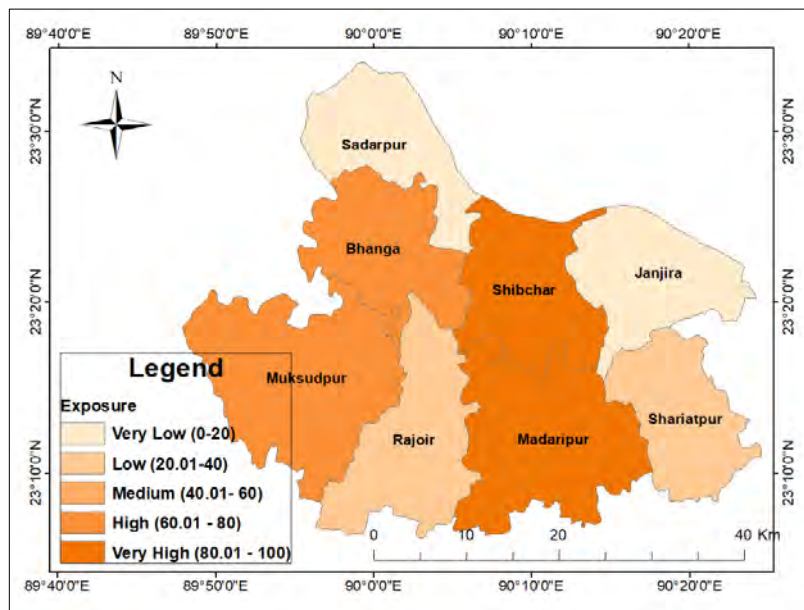


Figure 5.29: Exposure Map of the Study Area

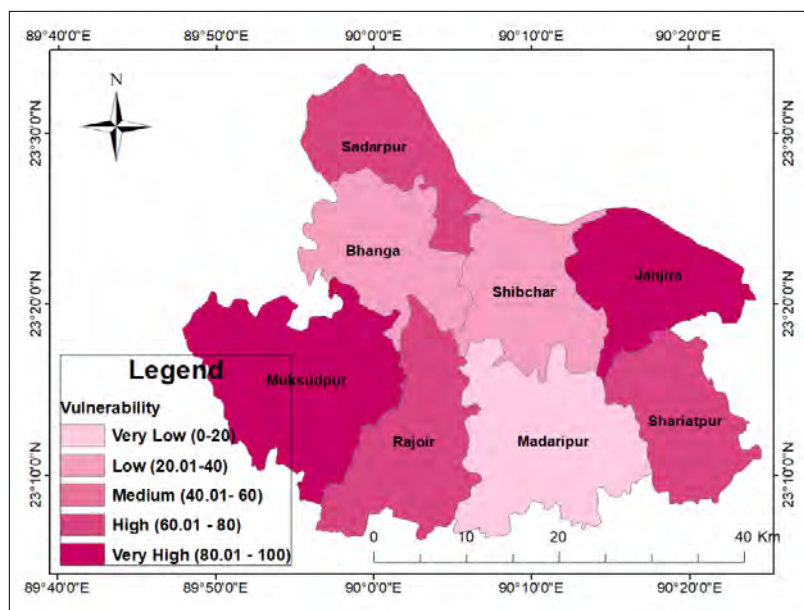


Figure 5.30: Vulnerability Map of the Study Area

Figure 5.29 shows that the numbers of land units under different categories are 2, 2, 0, 2 and 2 and the percentage areas are 28%, 27%, 0%, 21% and 24% for Very Low, Low, Medium, High and Very High exposure zones, respectively. Figure 5.29 further shows that the exposure is least in Zanjira and Sadarpur. The reason behind this is the low population density in these two Upazilas. As there are few populations in these areas, they are less exposed to any hazard. On the other hand, the population is high in Shibchar and Madaripur. Hence, they are more exposed to hazard.

Figure 5.30 shows the Upazila-wise vulnerability zones. The number of the land unit under different categories are 1, 2, 0, 3 and 2 and the percentage areas are 11, 22, 0, 37, 29 for Very Low, Low, Medium, High and Very High vulnerability zones, respectively. In the case of vulnerability, Madaripur is the least vulnerable among all the Upazilas. The reason behind its low vulnerability is that there are very less Disable and Dependent population. Besides, Female to male ratio and Poverty rate are also low. Contrary, the number of Paka and Semi Paka house, Communication Infrastructure, Crop Productivity, Literacy Rate, Health center, Flood Shelter and Growth Centre are also high. Though Zanjira falls into the very low exposed zone, it is the highest in vulnerability, because the percentage of dependable people and poverty rate are the highest in this area. At the same time, paka and semi-paka house, communication infrastructure and growth center number are very low.

5.4.4 Flood Risk Assessment for RCP 2.6 and RCP 8.5 Scenario

In this study, risk has been calculated as mentioned in AR5 of IPCC where, risk has been expressed as a function of hazard, exposure, and vulnerability. Hence, the flood hazard of each of the land unit has been multiplied with the exposure and vulnerability of each of the land unit calculated in Section 5.3.4, and finally, the risk of each of the land unit has been calculated using Equation (4-8). Here, the exposure and vulnerability values are used from the Population Census of 2011 and Agriculture Census of 2008, and they are kept constant in each of the periods of future scenarios too. Table 5.9 shows the risk values of each of the Upazilla. The risk values among the Upazilla were found to vary from 2894.82 to 202351.41 for all the projections of RCP 2.6 and RCP 8.5. For a systematic representation, they are normalized in a range of 1 to 100 using Equation (4-5). The normalized values are tabulated in Table 5.10.

Table 5.9: Upazilla-wise Risk for RCP 2.6 and RCP 8.5

District Name	Upazila Name	Base Line	Risk Values					
			RCP 2.6			RCP 8.5		
			1976-2005	2020s	2050s	2080s	2020s	2050s
Faridpur	Bhanga	7581	7893	9342	12294	7862	9861	103869
	Sadarpur	7096	7719	8567	9786	7792	8871	11764
Gopalganj	Maksudpur	6208	6208	18433	30821	6208	22213	202351
Madaripur	Madaripur	2895	3519	4711	5230	3880	4854	7143
	Rajoir	4864	21669	51936	61413	33786	54534	107034
	Shibchar	68413	79092	93512	106379	80121	96941	146458
Shariatpur	Shariatpur	9712	17289	38846	63508	19571	48616	97806
	Zanjira	7019	7527	8120	8984	7594	8345	10000

Table 5.10: Upazilla-wise normalized Risk for RCP 2.6 and RCP 8.5

District Name	Upazila Name	Base Line	Normalized Risk Values					
			RCP 2.6			RCP 8.5		
			1976-2005	2020s	2050s	2080s	2020s	2050s
Faridpur	Bhanga	3.3	3.5	4.2	5.7	3.5	4.5	51.1
	Sadarpur	3.1	3.4	3.8	4.4	3.4	4.0	5.4
Gopalganj	Maksudpur	2.6	2.6	8.7	14.9	2.6	10.6	100.0
Madaripur	Madaripur	1.0	1.3	1.9	2.2	1.5	2.0	3.1
	Rajoir	2.0	10.3	25.3	30.0	16.3	26.6	52.7
	Shibchar	33.5	38.8	46.0	52.4	39.3	47.7	72.3
Shariatpur	Shariatpur	4.4	8.1	18.8	31.1	9.3	23.7	48.1
	Zanjira	3.0	3.3	3.6	4.0	3.3	3.7	4.5

Similar to hazard, exposure and vulnerability, the study area is divided into five risk zones based on five equal intervals of Risk values from 0 to 20, 20.01 to 40, 40.01 to 60, 60 to 80.01 and 80.01 to 100 named as Very Low Risk, Low Risk, Medium Risk, High Risk and Very High Risk zone respectively. Figure 5.31, 5.32, 5.33, 5.34, 5.35, 5.36 and 5.37 show the spatio-temporal change of flood risk zones for each of the land units both for RCP 2.6 and 8.5 scenarios.

When the indices for flood hazard, vulnerability, and exposure are combined, several 'hotspots' of flood risk become evident across floodplains of Arial Khan River. For example, in the base period, Zanjira is in the high hazard zone area, but while the question of associated risk has come, it becomes a low risk zone. Because, though this Upazilla is profoundly affected by flood hazard, the exposure and vulnerability are very low. Hence, overall flood risk has decreased. A similar thing happened for the future too. Despite its high hazardous categorization, it becomes the very low hazard zone in the future projection of the 2080s for RCP 8.5.

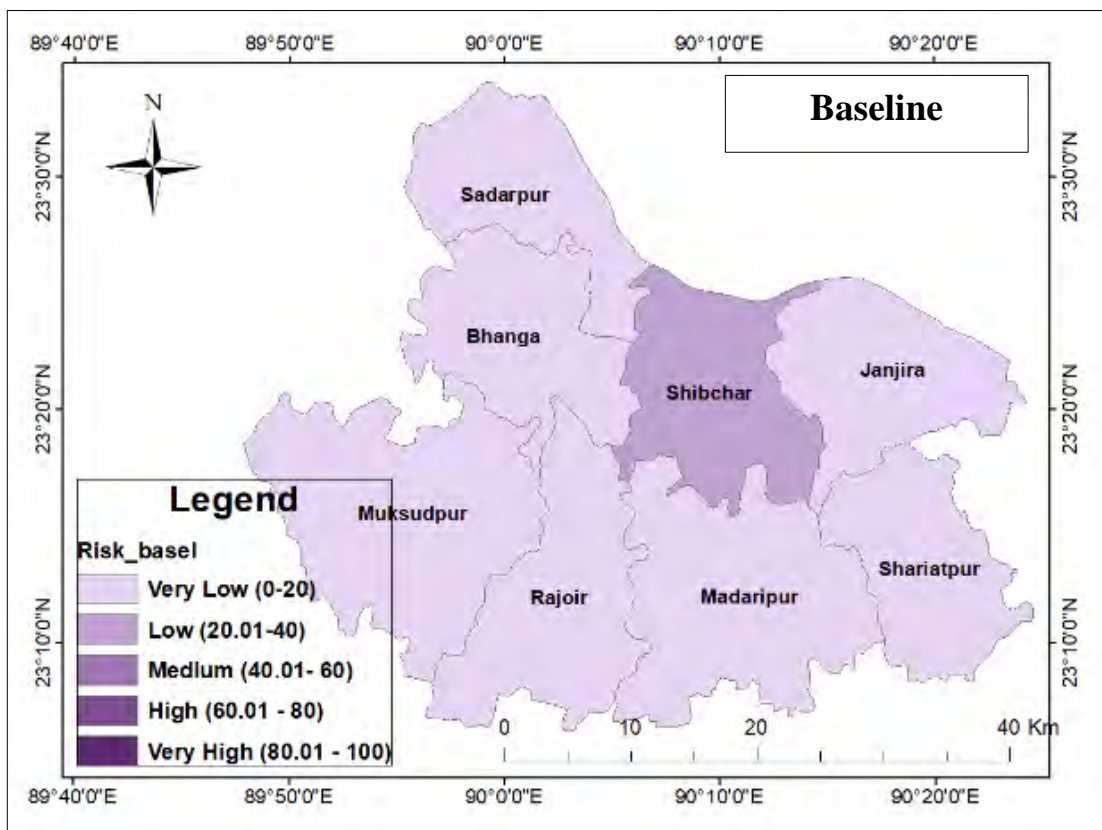


Figure 5.31: Flood risk map for the baseline

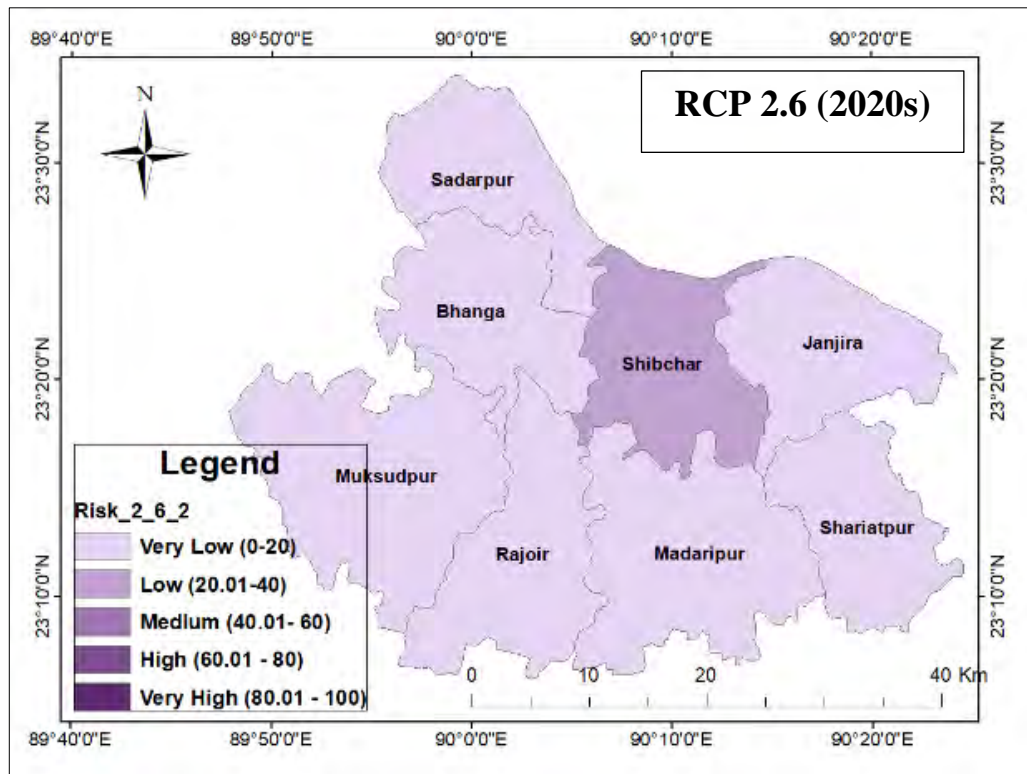


Figure 5.32: Flood risk map for the 2020s of RCP 2.6

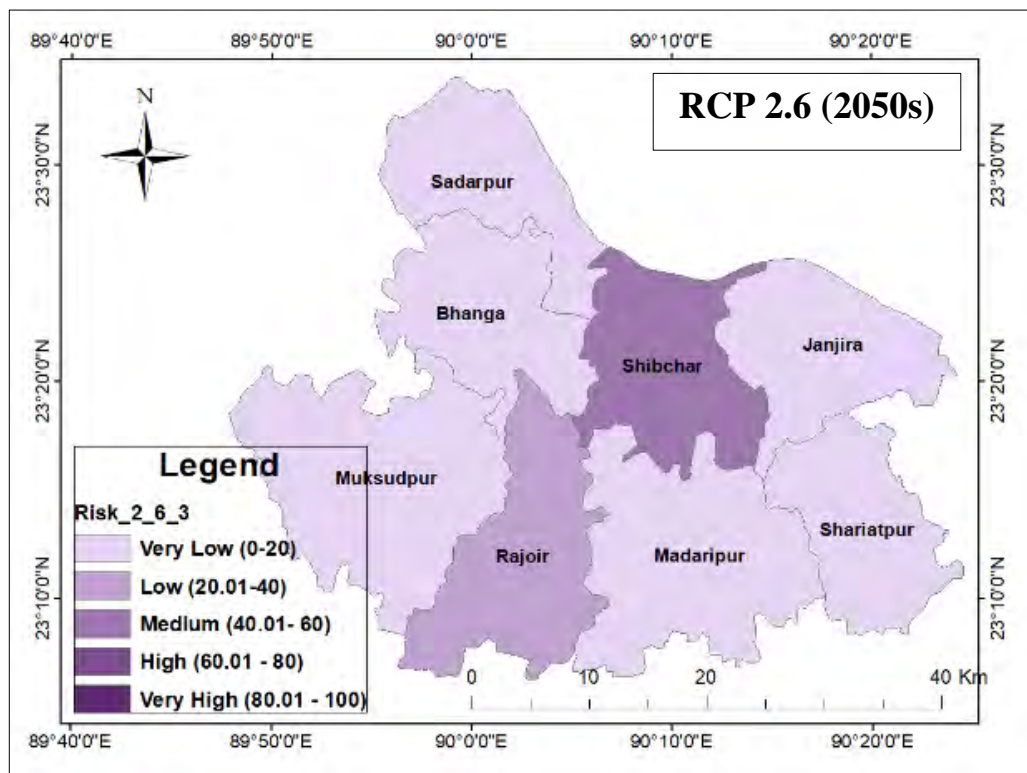


Figure 5.33: Flood risk map for the 2050s of RCP 2.6

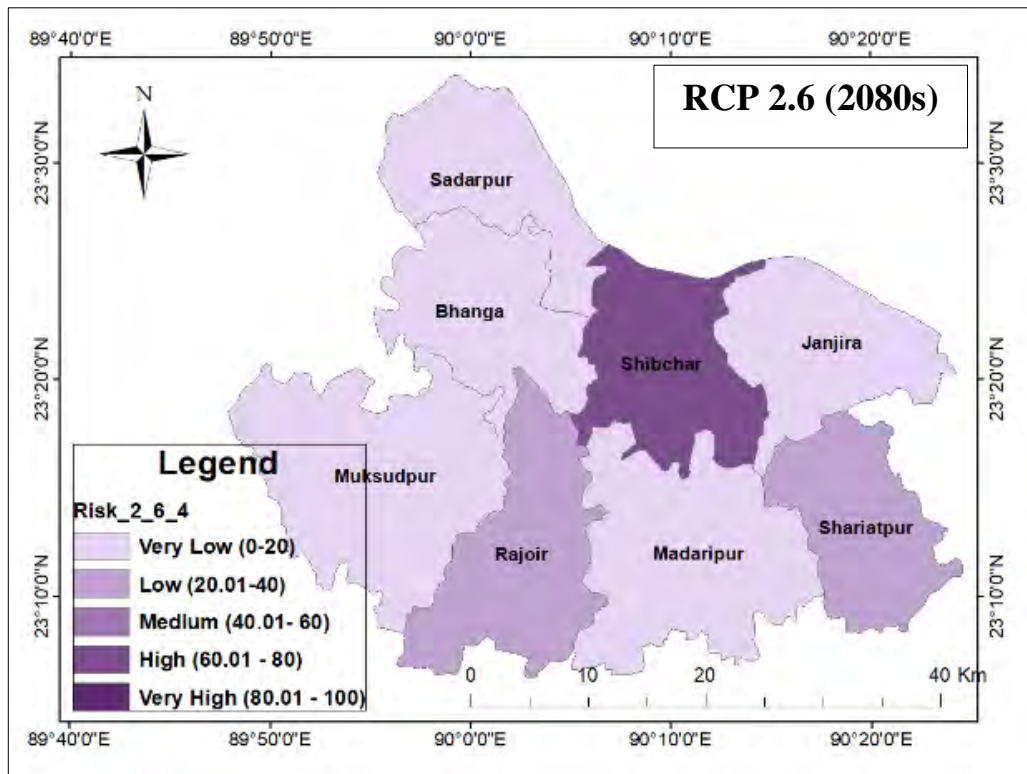


Figure 5.34: Flood risk map for the 2080s of RCP 2.6

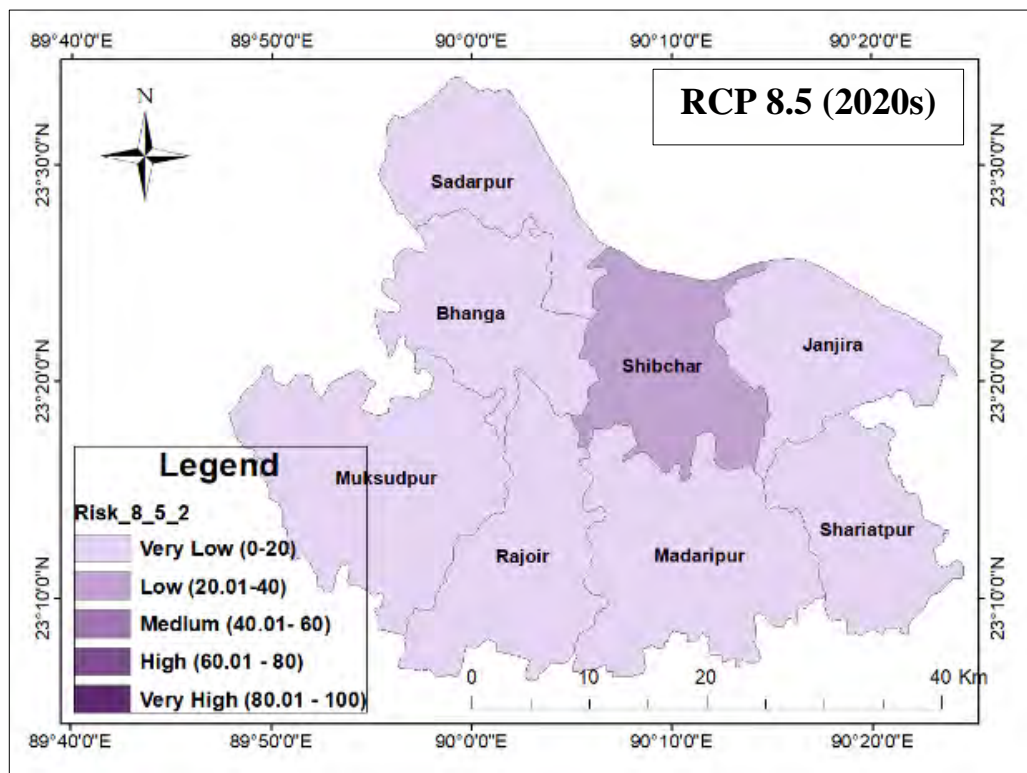


Figure 5.35: Flood risk map for the 2020s of RCP 8.5

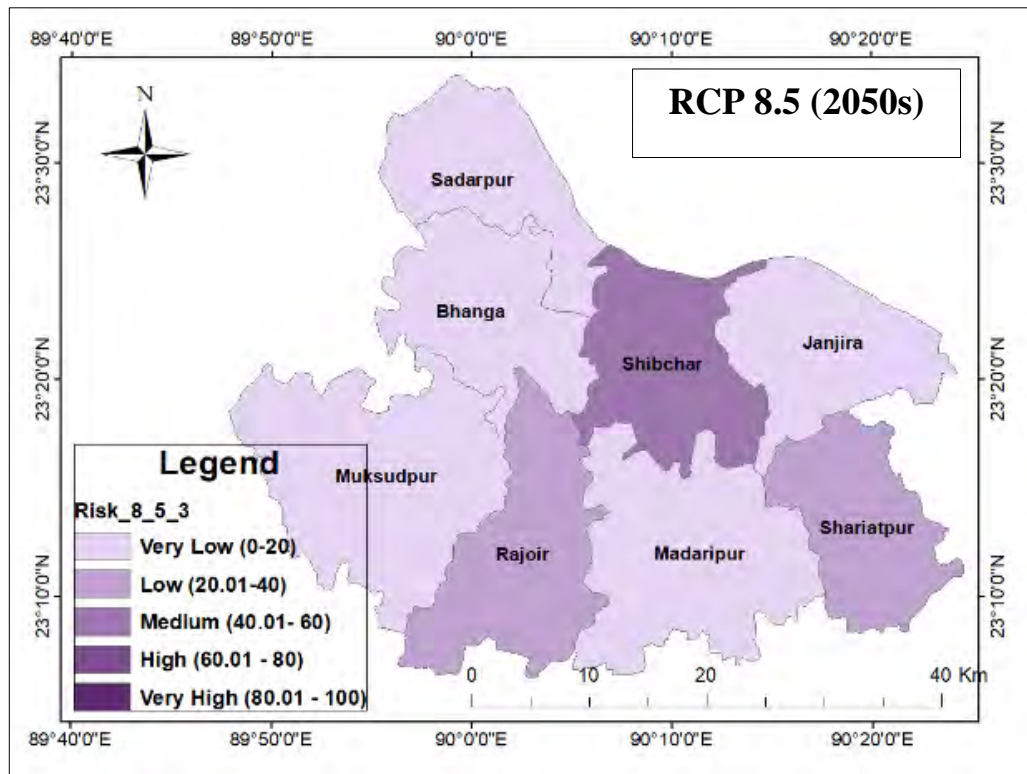


Figure 5.36: Flood risk map for the 2050s of RCP 8.5

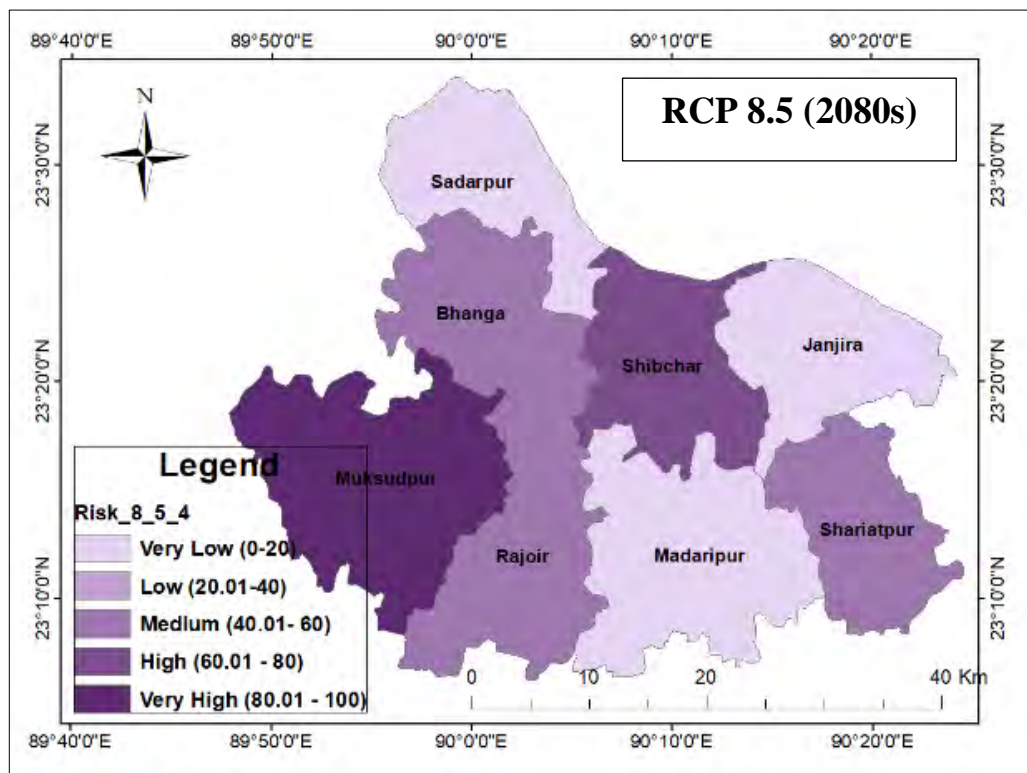


Figure 5.37: Flood risk map for the 2080s of RCP 8.5

The opposite situation happens for Madaripur. If only hazard factor is considered, it is in a low hazard zone, but it becomes the very high risk zone while vulnerability and exposure factors are considered with hazard factor. Because exposure and vulnerability, both factors were high for Madaripur. Like this, the hazard maps are changed manifold while they are converted to Risk maps. Hence, risk assessment is required together with hazard assessment to quantify the actual climate change impact and to incorporate any flood management plan or strategy.

Table 5.11: Percentage of area under different risk zones for different projections of RCP 2.6 and RCP 8.5

Scenarios	Period	Percentage of Area				
		Very Low (0-20)	Low (20.01-40)	Medium (40.01-60)	High (60.01 - 80)	Very High (80.01 - 100)
Base line	1976-2005	87	13	0	0	0
RCP 2.6	2020s	87	13	0	0	0
	2050s	76	11	13	0	0
	2080s	60	27	13	0	0
RCP 8.5	2020s	87	13	0	0	0
	2050s	60	27	13	0	0
	2080s	39	0	37	13	11

Table 5.11 shows that the percentage of area under different risk zones for different projections of RCP 2.6 and RCP 8.5. In the base period, 87% and 23% area are under the very low and low risk zone. It becomes 60% in the very low risk zone, 27% in low risk zone and 13% in medium risk zone in the 2080s of RCP 2.6 and it becomes 39%, 37%, 13% and 11% in very low, medium, high and very high hazard zone in RCP 8.5. Climate change will decrease the very low and low risk zone drastically in the year 2080. On the other hand, the high and very high risk will increase due to climate change compared to the base period. So, it can be interpreted that future climate change will have a terrible effect on the flood situation of Arial Khan River floodplain and the corresponding risk will increase to a large extent too.

5.5 Discussions

This study focuses on the fluvial flood hazard and risk assessment of Arial Khan River under future climate change scenarios. The assessment of inundation maps and hazard maps for different projections of RCP 2.6 and RCP 8.5 show that there is an increasing trend of the flood from baseline to 2080s, both for RCP 2.6 and RCP 8.5 scenarios. From baseline to 2020s, there is almost no difference between RCP 2.6 and RCP 8.5. The difference between the 2020s to 2050s is slight. However, this variation becomes very drastic after the 2050s. The inundation area and hazard increase manifolds in the 2080s of RCP 8.5 than that of RCP 2.6. Because atmospheric carbon-di-oxide concentration, global surface temperature, north hemisphere sea ice extent, sea level rise is almost similar to 2020. Little bit more difference is observed up to 2050. After that, the difference between RCP 2.6 and RCP 8.5 is very rapid and high. Simultaneously, according to IPCC, global surface temperature changes at the end of the 21st century is likely to exceed 1.5°C relative to 1850 to 1900 for all RCP scenarios except RCP 2.6. Moreover, it is likely to exceed 2°C for RCP 6.0 and RCP 8.5 and more likely than not to exceed 2°C for RCP 4.5. Furthermore, warming will continue beyond 2100 under all RCP scenarios except RCP 2.6. Hence, the inundation extent, flood affected area, and % of the area under the higher rank of hazard zone are found highest for the 2080s of the RCP 8.5 scenario. These results coincide with the results of different climate studies and IPCC reports, which validates the accuracy of this study and its acceptance in using these results outputs for the flood management plans along Arial Khan River floodplain as well.

However, one major limitation of the inundation and hazards maps prepared in this study might be the downstream water level boundary for future scenarios which is fixed using the water level hydrograph of 1998 and incorporating the future sea level projections (55-82 cm) of the RCP 2.6 and RCP 8.5 scenarios provided by IPCC (2014) directly without considering its actual magnitude at the downstream boundary due to climate change. This limitation could have been minimized simulating any hydrodynamic model covering the southern coastal part of Bangladesh (including Arial Khan River) extending up to the Bay of Bengal and incorporating future projections of flows in GBM basins and the sea level rise in BoB as upstream and downstream boundaries conditions respectively. A similar study is recently done by Mondal, et al. (2018) in which, it is found that the flood peaks might increase by 25-72 cm by the end of this century in the major rivers for RCP 8.5 scenario, depending on the river and the location on the river, due to increase in rainfall

in the upstream areas and rise in sea level in the Bay of Bengal. As we did not follow this approach and use the sea level rise projections directly at the downstream boundary, our inundation and hazard maps may overestimate flood a little bit.

In this study, the risk maps are prepared using the IPCC AR5 framework, where risk is calculated multiplying hazard, exposure, and vulnerability. The magnitude of flood hazard is found from the HEC-RAS 1D-2D coupled model for different projections of RCP 2.6 and 8.5. The magnitudes of vulnerability and exposure indicators are collected from the most recent data available in Bangladesh (Population Census of 2011 and Agricultural Census of 2008), and they are kept constant for assessing risk under future climate change impact. The incorporation of Shared Socio-economic Pathways (SSPs) would be the best way to calculate the actual risk scenarios in the future. The SSPs are part of a new framework that the climate change research community has adopted to facilitate the integrated analysis of future climate impacts, vulnerabilities, adaptation and mitigation. Information about the scenario process and the SSP framework are found in Moss, et al. (2010), Van Vuuren, et al. (2014), O'Neill, et al. (2014) and Kriegler, et al. (2014). In SSPs, population, GDP and urbanization data are provided on a global scale. Later, applying the global RCP–SSP–SPA scenario framework, country scale or sub-national scale or multi-scale or participatory scenario approach is quantified (Kebede, et al., 2018). However, the collection of these datasets is a rigorous process. Moreover, it is hard to get the future projections of each of the exposure and vulnerability indicators used in this study. Hence, SSPs has not been incorporated in this study. This might adulterate the risk maps to some extent. Another limitation in exposure and vulnerability estimation was assigning equal weightage to each of the exposure and vulnerability indicators. Proper weight to each of the indicators on the basis of literature reviews, stakeholder workshops and field visits according to the Principal Component Analysis (PCA) or Multi-Criteria Analysis (MCA) would enrich this study (Uddin, et al., 2019; Jahan, 2018). This is also avoided to make this study simple.

However, the risk maps prepared in this study gives an overall view of the probable flood risks for the floodplains of Arial Khan River in the future. It further shows that incorporation of vulnerability and exposure with hazard gives a completely different horizon to the overall assessment. It is observed that some medium hazard zones have a high risk of flood damage. There are many upazilas like Zanjira which are not hazardous

but fall in the very high risk zone due to its vulnerable socio-economic condition, or this may happen if the land units with important land use and infrastructure have more unprotected areas. The opposite scenario has been observed too. Madaripur is such an example. Despite being a low hazard zone, it is categorized as the high risk zone. Hence, for a proper flood management scheme or plan, hazard map or hazard zoning is not enough alone, it needs risk assessment as well. Examining both hazard and risk maps, decisions should be taken accordingly. A hazardous area may be risk-free incorporating and improving early forecasting and warning system only. On the other hand, a low hazardous area with high socio-economic vulnerable society needs more flood shelters, health care centers and employment opportunity rather than incorporating flood forecasting and warning system only. So, for a sustainable flood management plan, it is very important to consider the impact of climate change and study on hazard, exposure, vulnerability, and risk both separately and combinedly as well.

Despite some limitations stated above, this study takes a noble attempt to develop hazard and risk maps of Arial Khan River floodplain for RCP 2.6 and RCP 8.5 scenarios using IPCC AR risk frameworks which have not studied yet in Bangladesh. It is expected that the results found in this study will be useful for the concerned authorities in identifying the hazard and risk zones of Arial Khan River and thereby incorporating and planning a more suitable, economical and sustainable flood management strategies along the Arial Khan River. The hazard and risk maps of the 2020s can be incorporated in short term or mid-term plans. Additionally, the maps of the 2050s can be incorporated in any long term plan such as a 50-year plan. Most importantly, the maps of the 2080s can be complied with the recent Delta Plan 2100 prepared by Bangladesh Government. However, not only the planners, these maps can be useful for the residents in the floodplain who can use this information for self-preparedness. Also, it also provides considerable management implications for emergency preparedness, including aid and relief operations for high risk and very high risk areas in future flood events.

Besides, compared to the wide range of research conducted in other flood-prone countries, research work carried out in Bangladesh on future flood situation for different climate change scenarios is very limited. This study will undoubtedly inspire other researchers to work on the future flood situation considering climate change impact. Simultaneously, this study incorporates a methodology or guideline as well, to

incorporate the globalize climate scenarios of a large basin to a small local river and its floodplain using combined statistical, hydrological and hydrodynamic model.

CHAPTER 6

CONCLUSIONS AND RECOMMENDATIONS

6.1 Conclusions

Climate change and its impact is a major concern of the twenty-first century. It is already evident from many climate studies and literatures that climate change will significantly increase the flood intensity and frequency manifolds in future climate change impact. Additionally, the flood risk will increase too. In this study, an HEC-RAS 1D-2D coupled model of Arial Khan has been set up for assessing the flood hazard and risk of Arial Khan River floodplains for different projections of RCP 2.6 and 8.5.

A calibrated and validated SWAT model has been used to generate the future flow at hydrographs at Brahmaputra and Ganges for different projections of RCP scenarios. A 1D model of Ganges-Brahmaputra-Padma has been set up to generate the future flow of Padma for those RCP scenarios. Calibration and validation of this model have been performed for the year of 2016 and 2017 respectively, where Manning's roughness coefficient 'n' was the calibration parameter. This 1D model has been calibrated and validated at Mawa (SW 93.5L) station with respect to discharge. The result showed a good correlation between the observed and simulated water level data for Manning's roughness coefficient 'n' of 0.025-0.03. The value of the coefficient of determination, R^2 is 0.9168 and 0.8212 for calibration and validation respectively, and the value of NSE is 0.9138 and 0.7424 for calibration and validation respectively which were found in acceptable range.

Later, the upstream discharge at the offtake of Arial Khan has been calculated establishing a linear regression equation between the offtake of Arial Khan and Mawa of Padma. The performance of this equation has been assessed through R^2 and P value. The R^2 is found nearly 0.6 which is within the satisfactory range. The P value is found less than 0.001 which proves its statistical significance. After establishing that the equation performs reasonably well, it is used as the boundary condition of Arial Khan 1D-2D coupled model. The downstream water level boundary at Madaripur is fixed with the water level hydrograph of 1998 and incorporating the future sea level projections of the RCP 2.6 and 8.5 scenarios provided by IPCC (2014). Before simulating the 1D-2D coupled model of Arial Khan for different projections of RCP scenarios, it has been calibrated and validated

for Manning's roughness coefficient 'n' = 0.015-0.02 for the year of 2015 and 2017 respectively. The R^2 values are found 0.997 and 0.989 and NSE values are found 0.892 and 0.882 for calibration and validation respectively. After calibration and validation, MODIS satellite image on 1st July, 2004 and 27th July 2004 has been used for flood inundation comparison. Comparison between observed flood from satellite imagery and model result was satisfactory which leads this model for further flood analysis.

After calibration and validation, Arial Khan 1D-2D coupled model is simulated for the historical flood events of 1988, 1998, 2004, 2007 and 2010. The inundation area is found the maximum for the flood of 1998. Later, it is simulated for different time slices: baseline (1976-2005), 2020s (2006-2035), 2050s (2036-2065) and 2080s (2066-2095) of both RCP 2.6 and RCP 8.5.

The inundation maps of different projections of RCP 2.6 and RCP 8.5 show that there is an increasing trend of flood area from baseline to 2080s, both for RCP 2.6 and RCP 8.5. At the base period, the flood affected area is only 285 km², which is 15% of the study area. The total flood affected area in the 2080s of RCP 2.6 is nearly 550 km² which are 30% of the study area. On the other hand, the total flood affected area in the 2080s of RCP 8.5 is almost 850 km² which are nearly 47% of the whole study area. Additionally, the mean flood depth is found to be increased as well. Hence, while designing any hydraulic structures or measures, this increase in flood level needs to be incorporated as well.

The analysis of hazard maps shows that at the base condition, 48% area is in the very low hazard zone, 34% area is in the low hazard zone and 18% area is in the High hazard zone. However, it changed to 21% in the very low hazard zone, 27% in the low hazard zone, 34% in the medium hazard zone, 18% in the very hazard zone in the 2080s of scenario RCP 2.6. Furthermore, the situation gets worse and more alarming for the 2080s of RCP 8.5. In the 2080s of RCP 8.5, 22% area becomes low hazard zone, 26% area becomes medium hazard zone, 34% area is under high hazard zone, and 18% area is under very high hazard zone.

Later, the risk is calculated multiplying flood hazard of each of the land with the exposure and vulnerability of each of the land unit as mentioned in AR5 report of IPCC. Here, the

exposure and vulnerability values are used from the Population Census of 2011 and Agriculture Census of 2008, and they are kept constant in each of the periods.

Risk assessment shows that in the base period, 87% and 23% area under a very low and low risk zone. It becomes 60% in the very low risk zone, 27% in low risk zone and 13% in medium risk zone in the 2080s of RCP 2.6 and it becomes 39%, 37%, 13% and 11% in very low, medium, high and very high hazard zone in RCP 8.5. Climate change is going to decrease the very low and low risk zone and increase the high and very high risk zone in the future.

The overall assessment for different projections of RCP 2.6 and RCP 8.5 show that there is an increasing trend of the flood from baseline to 2080s, both for RCP 2.6 and RCP 8.5. From baseline to 2020s, there is no difference between RCP 2.6 and RCP 8.5. The difference is slight from the 2020s to 2050s, but this variation becomes very drastic after the 2050s. The inundation pattern, hazard and risk extent increase manifolds in the 2080s of RCP 8.5 than that of RCP 2.6. Because after the 2050s, the atmospheric carbon-dioxide concentration, global surface temperature, north hemisphere sea ice extent, sea level rise is going to be very rapid and violent in RCP 8.5 and it is going to be continued even after 2100. Hence, the inundation depth, flood affected area, % of the area under the higher rank of hazard zone and risk zone are found the highest for the 2080s of RCP 8.5.

Future analysis of hazard and risk maps further show that some medium hazard zones have a high risk of flood damage and vice versa. This happens when the land units with important land use and infrastructure have more unprotected areas, or the socio-economic vulnerability is high in those land units. Hence, for a proper flood management scheme or plan, both hazard and risk assessment are required.

The results found in this study provide useful information about the flood hazard and flood risk areas in the Arial Khan River floodplain. It is expected that the hazard and risk maps prepared in this study will be useful for the planners and policy makers in identifying the higher hazard and risk zones of Arial Khan River and thereby incorporating and planning a more suitable, economical and sustainable flood management strategies along the Arial Khan River.

6.2 Recommendations for Future Studies

In this study, flood hazard and risk assessment are conducted for Arial Khan River floodplain under the future climate change scenario of RCP 2.6 and RCP 8.5. For this purpose, an HEC-RAS 1D-2D coupled model of Arial Khan has been set up and later the climate change scenarios are incorporated as the boundary conditions. Later, future flood hazard and risk maps are prepared based on this model's simulations. Based on the results and the experience gained during the study, the following recommendations are made.

- This study has been done using 1D and 2D coupling. For the comparison purpose or better understanding, pure 2D analysis can be performed in the future, if fine resolution bathymetry of Arial Khan is found.
- Digital elevation model plays a vital role to enhance the capability of the model. It is recommended to use the high-resolution digital spatial database for real replication of topography for the better performance of the model.
- In this study, a linear regression equation is developed between the flow of the Padma River and Arial Khan River. Use of a non-linear relationship of flow may improve the result.
- Flood depth is used as the hazard parameter in this study. However, more hazard parameters such as flooding duration, velocity, and shear stress can be used for better prediction.
- Two RCP scenarios - the low emission scenario RCP 2.6 and high emission scenario RCP 8.5 have been considered in this study. For a full view of climate change impact, the other two RCP scenarios –RCP 4.5 and RCP 6 can be simulated in the future.

REFERENCES

- Abbaspour, K. et al., 2007. Modelling hydrology and water quality in the pre-alpine/alpine Thur watershed using SWAT. *Journal of Hydrology*, p. 413–430.
- Abera, Z., 2011. *Flood Mapping and Modeling on Fogera Flood Plain: A case study of Ribb River*. s.l.:M.Sc. thesis, Department of civil engineering, Addis Ababa University, Ethiopia.
- Adger, W. N. et al., 2002. Adaptation to climate change: Setting the Agenda for Development Policy and Research. *Progress in Development Studies*, 3(3), p. 179–195.
- Agard, J. & Schipper, L., 2015. IPCC WGII AR5 glossary. In: s.l.:s.n.
- Ahmed, A. U. & Alam, M., 1999. Development of climate change scenarios with general circulation models. In: *In Vulnerability and adaptation to climate change for Bangladesh*. s.l.:Springer, Dordrecht, pp. 13-20.
- Akter, J., Sarker, M. H. & Haque, P., 2013. *Morphological Processes And Effective River Erosion Management: A Case Study of The Arial Khan River In Bangladesh*. s.l., s.n.
- Ali, M. et al., 2018. Challenges for flood risk management in flood-prone Sirajganj region of Bangladesh. *Journal of Flood Risk Management*, p. e12450.
- Allen, S. et al., 2016. Glacial lake outburst flood risk in Himachal Pradesh, India: an integrative and anticipatory approach considering current and future threats. *Natural Hazards*, 84(3), pp. 1741-1763.
- Anh, T., Kha, D., Duc, D. & Son, N., 2016. Hydraulic modeling for flood vulnerability assessment, case study in river basins in North Central Vietnam. *Procedia Engineering, ELSEVIER*, Volume 65, pp. 23-30.
- Anik, M. & Khan, A., 2016. *Flood inundation mapping of Jamuna basin using HEC-RAS 1D/2D coupled model*. s.l.:B.Sc. Thesis. Department of Water Resources Engineering, Bangladesh University of Engineering and Technology.

- Arino, O. et al., 2008. GlobCover the most detailed portrait of Earth. *ESA Bulletin*, Volume 136, pp. 25-31.
- BBC News, 1998. *World: South Asia Bangladesh floods rise again*. [Online] Available at: http://news.bbc.co.uk/2/hi/south_asia/157254.stm [Accessed 8 January 2019].
- Beniston, M. et al., 2007. Future extreme events in European climate: an exploration of regional climate model projections. *Climatic Change*, 81(1), pp. 71-95.
- Birkmann, J., 2006. Measuring vulnerability to promote disaster-resilient societies: Conceptual frameworks and definitions. In: *Measuring Vulnerability to Natural Hazards: Towards Disaster Resilient Societies*. s.l.:s.n., p. 9–54.
- Birkmann, J., 2014. Data, indicators and criteria for measuring vulnerability: theoretical bases and requirements. In: *Measuring vulnerability to natural hazards: towards disaster resilient*. s.l.:United Nations University Press, Tokyo, pp. 55-57.
- Bonsal, B., Zhang, X., Vincent, L. & Hogg, W., 2001. Characteristics of daily and extreme temperatures over Canada. *Journal of Climate*, 14(9), pp. 1959-1976.
- Braun, M., Altan, H. & Beck, S., 2014. Using regression analysis to predict the future energy consumption of a supermarket in the UK. *Applied Energy*, Volume 130, pp. 305-313.
- Brunner, G., Piper, S., Jensen, M. & Chacon, B., 2015. *Combined 1D and 2D Hydraulic Modeling within HEC-RAS*. s.l., s.n., pp. 1432-1443.
- Brunner, G. W., 2016b. *Combined 1D and 2D Modeling with HEC-RAS*. s.l.: US Army Corps of Engineers, Institute for Water Resources, Hydrologic Engineering Center.
- Brunner, G. W., 2016. *HEC-RAS River Analysis System : Hydraulic Reference Manual*. s.l.:U.S. Army Corps of Engineers, Institute for Water Resources, Hydrologic Engineering Center, 609 Second Street, Davis, CA 95616.
- BWDB, 2011. *Bangladesh er Nod-Nodi*. s.l.:Bangladesh Water Development Board, Dhaka, Bangladesh.

- Cardona, O. D. et al., 2012. Determinants of risk: exposure and vulnerability. In: *Managing the Risks of Extreme Events and Disasters to Advance Climate Change Adaptation: A Special Report of Working Groups I and II of the Intergovernmental Panel on Climate Change (IPCC)*. s.l.:Cambridge, UK, and New York, NY, USA.
- CEGIS, 2010. Morphological Analysis of Padma River. In: *Padma Multipurpose Bridge Design Project. River Training Works, Updated Scheme Design Report*". s.l.:s.n.
- Chen, W., Cutter, S., Emrich, C. & Shi, P., 2013. Measuring social vulnerability to natural hazards in the Yangtze river delta region, China.. *Int J Disaster Risk Sci*, Volume 4, p. 169–181.
- Chowdhury, J. & Karim, M. F., 1997. *A risk based zoning of storm surge prone area of the Ganges tidal plain*. s.l., s.n., pp. 171-185.
- Cutter, S., Boruff, B. & Lynn, S. W., 2003. Social vulnerability to environmental hazards. *Social Science Quarterly*, Volume 84, pp. 242-261.
- Cutter, S. & Finch, C., 2008. Temporal and spatial changes in social vulnerability to natural hazards. *Proc Natl Acad Sci*, Volume 105, p. 2301–2306.
- Das, P. et al., 2018. Flood Inundation Mapping on Surma-Kusiyara Floodplain Using Hec-Ras 1d/2d Couple Model..
- DDM, 2016. *Risk Atlas : Multi-Hazards Risk and Vulnerability Assessment, Modeling and Mapping*. s.l.:s.n.
- Fahad, M. G. R. et al., 2018. Regional changes of precipitation and temperature over Bangladesh using bias-corrected multi-model ensemble projections considering high-emission pathways. *International Journal of Climatology*, 38(4), pp. 1634-1648.
- FAO, 1974. *FAO-UNESCO Soil Map of the World, 1:5,000,000*.. [Online].
- FFWC, 2005. *Annual Flood Report*, s.l.: Bangladesh Water Development Board.
- FFWC, 2011. *Annual Flood Report 2011*, Dhaka, Bangladesh: Bangladesh Water Development Board.

FFWC, 2012. *Annual Flood Report 2012*, Dhaka, Bangladesh: Bangladesh Water Development Board.

FFWC, 2013. *Annual Flood Report 2013*, Dhaka, Bangladesh: Bangladesh Water Development Board.

FFWC, 2014. *Annual Flood Report 2014*, Dhaka, Bangladesh: Bangladesh Water Development Board.

FFWC, 2015. *Annual Flood Report 2015*, Dhaka, Bangladesh: Bangladesh Water Development Board.

FFWC, 2016. *Annual Flood Report 2016*, Dhaka, Bangladesh: Bangladesh Water Development Board.

FFWC, 2017. *Annual Flood Report 2017*, s.l.: BWDB.

FFWC, 2019. *Flood Forecasting & Warning Center*. [Online] Available at: <http://www.ffwc.gov.bd/> [Accessed 8 January 2019].

Flood Archive, 2003. [Online] Available at: <http://www.dartmouth.edu/~floods/Archives/1987sum.htm> [Accessed 8 January 2019].

Giorgi, F. & Gutowski Jr, W., 2015. Regional dynamical downscaling and the CORDEX initiative. *Annual Review of Environment and Resources*, Volume 40, pp. 467-490.

González, C. et al., 2010. Climate change and risk of leishmaniasis in North America: predictions from ecological niche models of vector and reservoir species. *PLoS neglected tropical diseases*, 4(1), p. e585..

Hasan, M. A. & Islam, A. K. M. S., 2018. Evaluation of Microphysics and Cumulus Schemes of WRF for Forecasting of Heavy Monsoon Rainfall over the Southeastern Hilly Region of Bangladesh. *Pure and Applied Geophysics*, 175(12), p. 4537–4566.

HEC-GeoRAS, 2009. *GIS Tools for Support of HEC-RAS using Arc-GIS*. s.l.:s.n.

HEC-RAS, 2016. *HEC-RAS River Analysis System: 2D Modeling User's Manual*. 5 ed. s.l.:s.n.

Hicks, F. E. & Peacock, T., 2005. Suitability of HEC-RAS for flood forecasting. *Canadian Water Resources Journal*, 30(2), pp. 159-174.

Hossain, M., 2015. *Local level flood forecasting system using mathematical model incorporating WRF model predicted rainfall*. s.l.:MSc Thesis. Bangladesh University of Engineering and Technology (BUET). Dhaka -1000.

Hossain, M. S., 2013. *Flood Damage And Risk Assessment Model In The Haor Basin Of Bangladesh*. s.l.:M.Sc. Thesis, Institute of Water and Flood Management, BUET, Dhaka - 1000.

Hussain, S., 2012. *Study on flood pattern of Bangladesh using flood inundation maps generated from MODIS images..* s.l.:B.Sc. Thesis, Department of Water Resources Engineering, BUET, Dhaka -1000.

IPCC, 2001. Climate change 2001: synthesis report, a contribution of working groups I, II, and III to the Third Assessment Report of the intergovernmental panel on climate change. In: *The Third Assessment Report (TAR)*. s.l.:Cambridge: Cambridge University Press, 398.

IPCC, 2013. Summary for Policymakers. In: *In: Climate Change 2013: The Physical Science Basis. Contribution of Working Group I to the Fifth Assessment Report of the Intergovernmental Panel on Climate Change*. s.l.:s.n.

IPCC, 2014. *Climate Change 2014 Synthesis Report*. s.l.:s.n.

IPCC, 2014. *IPCC, 2014: Climate change 2014: Impacts, adaptation, and vulnerability. Part A: Global and sectoral aspects. Contribution of working group II to the fifth assessment report of the intergovernmental panel on climate change..* s.l.:s.n.

Islam, A., Bala, S. & Haque, M., 2010. Flood inundation map of Bangladesh using MODIS time-series images. *Journal of Flood Risk Management*, Volume 3, p. 210–222.

Islam, A. S., Bala, S. K. & Haque, M. A., 2010. Flood inundation map of Bangladesh using MODIS time-series images. *Journal of Flood Risk Management*, 3(3), pp. 210-222.

Islam, M. & Sado, K., 2000. Flood hazard assessment in Bangladesh using NOAA AVHRR data with geographical information system. *Journal of Hydrological Processes* , 14(3), p. 605–620.

IWM, 2014. *Policy Brief : Local Level Policy Hazard Maps for Flood, Storm Surge & Salinity*. s.l.:Ministry of Disaster Management and Relief.

Jahan, M., 2018. *Multi-Scale Assessment of Risks to Environmental Hazards in Coast Area of Bangladesh*. s.l.:M.Sc. Thesis. Institute of Water and Flood Management, BUET, Dhaka -1000.

Kabir, R. et al., 2017. *Socio-Economic Vulnerability Assessment due to Storm Surge Hazard in Bangladesh Coast*. s.l., 6th International Conference on Water & Flood Management (ICWFM-2017).

Kay, S. et al., 2015. Modelling the increased frequency of extreme sea levels in the Ganges–Brahmaputra–Meghna delta due to sea level rise and other effects of climate change. *Environmental Science: Processes & Impacts*, 17(7), pp. 1311-1322.

Kebede, A. et al., 2018. Applying the global RCP–SSP–SPA scenario framework at sub-national scale: A multi-scale and participatory scenario approach. *Science of The Total Environment*, Volume 635, pp. 659-672.

Kennedy, E., 1984. *Discharge ratings at gaging stations: Techniques of Water-Resources Investigations of the U.S. Geological Survey*. s.l.:US Government Printing Office, Washington.

Knebl, M., Yang, Z., Hutchison, K. & Maidment, D., 2005. Regional scale flood modeling using NEXRAD rainfall, GIS, and HEC-HMS/RAS: a case study for the San Antonio River Basin Summer 2002 storm event. *Journal of Environmental Management*, 75(4), pp. 325-336.

Koks, E., Jongman, B., Husby, T. & Botzen, W., 2015. Combining hazard, exposure and social vulnerability to provide lessons for flood risk management. *Environmental Science & Policy*, Volume 47, pp. 42-52.

Kriegler, E. et al., 2014. A new scenario framework for climate change research: the concept of shared climate policy assumptions. *Climatic Change*, 122(3), pp. 401- 414.

- Legates, D. & McCabe, G., 1999. Evaluating the use of “goodness-of-fit” Measures in hydrologic and hydroclimatic model validation. *Water Resources Research*, Volume 35, pp. 233-241.
- Lehner, B., Verdin, K. & Jarvis, A., 2008. New global hydrography derived from spaceborne elevation data. *Eos, Transactions American Geophysical Union*, 89(10), pp. 93-94.
- Mamun, M. Y., 2008. *A Study On Offtake Morphology And Conveyance Characteristics Of Arial Khan River*. s.l.:M.Sc. Thesis. Department of Water Resources Engineering, BUET, Dhaka.
- Masood, M. & Takeuchi, K., 2012. Assessment of flood hazard, vulnerability and risk of mid-eastern Dhaka using DEM and 1D hydrodynamic model. *Natural hazards*, 61(2), pp. 757-770.
- Masood, M., Yeh, P., Hanasaki, N. & Takeuchi, K., 2015. Model study of the impacts of future climate change on the hydrology of Ganges–Brahmaputra–Meghna basin.. *Hydrology and Earth System Sciences*, 19(2), pp. 747-770.
- Maurer, E. & Hidalgo, H., 2008. Utility of daily vs. monthly large-scale climate data: an intercomparison of two statistical downscaling methods.. *Hydrology and Earth System Sciences*, Volume 12, pp. 551-563.
- Meinshausen, M. et al., 2011. The RCP greenhouse gas concentrations and their extensions from 1765 to 2300. *Climate Change*, Volume 109, pp. 213-241.
- Mirza, M. M. Q., 2002. Global warming and changes in the probability of occurrence of floods in Bangladesh and implications. *Global environmental change*, 12(2), pp. 127-138.
- Mirza, M., Warrick, R. & Ericksen, N., 2003. The implications of climate change on floods of the Ganges, Brahmaputra and Meghna rivers in Bangladesh. *Climatic Change*, 57(3), pp. 287-318.
- Mohammed, K. et al., 2018. Future Floods in Bangladesh under 1.5°C, 2°C, and 4°C Global Warming Scenarios. *Journal of Hydrologic Engineering*, 23(12).

- Mohammed, K. et al., 2019. Assessment of changes in extreme flows of the Ganges-Brahmaputra-Meghna river system under high-end climate change. *Water International*. (under review).
- Mondal, S. et al., 2018. Assessing High-End Climate Change Impacts on Floods in Major Rivers of Bangladesh Using Multi-Model Simulations. *Global Science and Technology Journal*, 6(2), pp. 1-14.
- Moore, M., 2011. *Development of a high-resolution 1D/2D coupled flood simulation of Charles City, Iowa.* s.l.:MSc Thesis. University of Iowa, Iowa..
- Moriasi, D. et al., 2007. Model evaluation guidelines for systematic quantification of accuracy in watershed simulations. *Transactions of the ASABE*, 50(3), pp. 885-900.
- Moss, R. et al., 2010. The next generation of scenarios for climate change research and assessment. *Nature*, 463(7282), pp. 747-756.
- Nash, J. & Sutcliffe, J., 1970. River flow forecasting through conceptual models part I — A discussion of principles. *Journal of Hydrology* , 10(3), pp. 282-290.
- Nishat, A., 1998. A discussion on flood management in Bangladesh. Special Workshop on 1998 Flood, Nagorik Durjog-Mokabela Uddogh.
- Nishat, U., 2017. *Flood Inundation Mapping of Jamuna River Floodplain Using HEC-RAS 2D Model.* s.l.:B.Sc. Thesis. Department of Waer Resources Engineering, Bangladesh University of Engineering & Technology, Dhaka-1000.
- O'Neill, B. et al., 2014. A new scenario framework for climate change research: the concept of shared socioeconomic pathways. *Climatic Change*, 122(3), pp. 387- 400.
- O'Connor, J. E. & Costa, J. E., 2004. Spatial distribution of the largest rainfall-runoff floods from basins between 2.6 and 26,000 km² in the United States and Puerto Rico. *Water Resources Research*, 40(1).
- Oppenheime, M. et al., 2014. Emergent risks and key vulnerabilities Climate Change 2014: Impacts, Adaptation, and Vulnerability Part A: Global and Sectoral Aspects. . In: *Contribution of Working Group II to the Fifth Assessment Report of the*

Intergovernmental Panel on Climate Change . s.l.:Cambridge, United Kingdom: Cambridge University Press, p. 1039–99.

Parhi, P. K., Sankhua, R. N. & Roy, G. P., 2012. Calibration of Channel Roughness for Mahanadi River, (India) Using HEC-RAS Model. *Journal of Water Resource and Protection*, Issue 4, pp. 847-850.

Patel, D. et al., 2017. Assessment of flood inundation mapping of Surat city by coupled 1D/2D hydrodynamic modeling: a case application of the new HEC-RAS 5. *Natural Hazards*, 89(1), pp. 93-130.

Quiroga, V. M., Kure, S., Udo, K. & Mano, A., 2016. Application of 2D numerical simulation for the analysis of the February 2014 Bolivian Amazonia flood: Application of the new HEC-RAS version 5.. *Ribagua*, 3(1), pp. 25-33.

Reliefweb, 1998. *Bangladesh floods recede, but death toll rises*. [Online] Available at: <https://reliefweb.int/report/bangladesh/bangladesh-floods-recede-death-toll-rises>

[Accessed 8 January 2019].

Rouf, T., 2015. *Flood Inundation Map of Sirajgonj District Using Mathematical Model*. s.l.:M.Sc. Thesis, Department of Water Resources Engineering, BUET, Dhaka, Bangladesh.

Schneider, S. H. e. a., 2007. *Schneider, S. H. et al. (2007). Assessing key vulnerabilities and the risk from climate change Climate Change 2007: Impacts, Adaptation and Vulnerability..* s.l.:Cambridge, UK: Cambridge University Press.

Shaw, R., Mallick, F. & Islam, A., 2013. Disaster risk reduction approaches in Bangladesh. *Springer*.

Shrestha, S. & Lohpaisankrit, W., 2016. Flood hazard assessment under climate change scenarios in the Yang River Basin, Thailand. *International Journal of Sustainable Built Environment, ELSEVIER*.

Silva, G., Weerakoonb, S. & Herath, S., 2016. Event Based Flood Inundation Mapping Under the Impact of Climate Change: A Case Study in Lower Kelani River Basin, Sri Lanka. *Hydrology Current Research*, 7(1), pp. 1-6.

- Smith, P., 1995. Hydrologic data development system CRWR Online Report. *Department of Civil Engineering, University of Texas at Austin*, 95(1).
- Srinivas, K., Werner, M. & Wright, N., 2009. Comparing forecast skill of inundation models of differing complexity: The case of Upton upon Severn. In: *Flood Risk Management: Research and Practice – Samuels et al. (eds)*. s.l.:Taylor & Francis Group, London.
- Stocker, T. F. et al., 2013. *IPCC 2013: Climate Change 2013: The Physical Science Basis, Contribution of Working Group I to the Fifth Assessment Report of the Intergovernmental Panel on Climate Change*. s.l.:s.n.
- Stocker, T. et al., 2013. *IPCC, 2013: summary for policymakers in climate change 2013: the physical science basis, contribution of working group I to the fifth assessment report of the intergovernmental panel on climate change*. s.l.:s.n.
- Tazin, T., 2018. *Flood Hazard Mapping of Dharala Floodplain using HEC-RAS 1D/2D Coupled Model*. Dhaka: s.n.
- Timbadiya, P., Patel, P. & Porey, P., 2011. Calibration of HEC-RAS model on prediction of flood for lower Tapi River, India. *Journal of Water Resource and Protection*, 3(11), p. 805.
- Tingsanchali, T. & Karim, M. F., 2005. Flood hazard and risk analysis in the southwest region of Bangladesh. *Hydrological Processes*, 19(10), pp. 2055-2069.
- Tu, V. & Tingsanchali, T., 2010. *Flood hazard and risk assessment of Hoang Long River basin, Vietnam*. s.l., In Proceeding of International MIKE by DHI Conference.
- Uddin, M. et al., 2019. Mapping of climate vulnerability of the coastal region of Bangladesh using principal component analysis. *Applied Geography*, Volume 102, pp. 47-57.
- UN, 1991. *Mitigating Natural Disasters: Phenomena, Effects and Options: a Manual for Policy Makers and Planners*. s.l.:UN Publications, New York.
- USGS, 1998. *Geographic Information Systems. United States Geological Survey.*, s.l.: s.n.

Van Vuuren, D. et al., 2014. A new scenario framework for climate change research: scenario matrix architecture. *Climatic Change*, 122(3), pp. 373-386.

WARPO. R. P. O., 2004. *National Water Management Plan*, s.l.: s.n.

Weedon, G. et al., 2014. The WFDEI meteorological forcing data set: WATCH Forcing Data methodology applied to ERA-Interim reanalysis data. *Water Resources Research*, 50(9), p. 7505–7514.

Whitehead, P. et al., 2015. Impacts of climate change and socio-economic scenarios on flow and water quality of the Ganges, Brahmaputra and Meghna (GBM) river systems: low flow and flood statistics. *Environmental Science: Processes & Impacts*, 17(6), pp. 1057-1069.

Winkley, B., Lesleighter, E. & Coon, J., 1994. Instability Problems of the Arial Khan River, Bangladesh. In: *he Variability of Large Alluvial Rivers*. s.l.:ASCE Press, New York, pp. 269-284.

WMO, 2003. Integrated Flood Management Case Study in Bangladesh: Flood Management.. *The Associated Programme on Flood Management*, pp. 5-6.

Yang, J., Townsend, R. D. & Daneshfar, B., 2006. Applying the HEC-RAS model and GIS techniques in river network floodplain delineation. *Canadian Journal of Civil Engineering*, 33(1), pp. 19-28.